First Quarter
1994

AFRRI Reports

Armed Forces Radiobiology Research Institute

8901 Wisconsin Avenue • Bethesda, Maryland 20889-5603

REPORT DOCUMENTATION PAGE

Public reporting burden for this collection of information is estimated to average 1 hour per response, including the time for reviewing instructions, searching existing data sources, gathering and maintaining the data needed, and completing and reviewing the collection of information. Send comments regarding this burden estimate or any other aspect of this collection of information, including suggestions for reducing this burden, to Washington Headquarters Services, Directorate for Information Operations and Reports, 1215 Jefferson Davis Highway, Suite 1204, Arlington, VA 22202-4302, and to the Office of Management and Budget, Paperwork Reduction Project (0704-0188), Washington, DC 20503

1. AGENCY USE ONLY *(Leave blank)*	2. REPORT DATE June 1994	3. REPORT TYPE AND DATES COVERED Reprints

4. TITLE AND SUBTITLE

AFRRI Reports, First Quarter 1994

5. FUNDING NUMBERS

PE: NWED QAXM

6. AUTHOR(S)

7. PERFORMING ORGANIZATION NAME(S) AND ADDRESS(ES)

Armed Forces Radiobiology Research Institute
8901 Wisconsin Avenue
Bethesda, MD 20889-5603

8. PERFORMING ORGANIZATION REPORT NUMBER

SR94-1 - SR94-8

9. SPONSORING/MONITORING AGENCY NAME(S) AND ADDRESS(ES)

Uniformed Services University of the Health Sciences
4301 Jones Bridge Road
Bethesda, MD 20814-4799

10. SPONSORING/MONITORING AGENCY REPORT NUMBER

11. SUPPLEMENTARY NOTES

12a. DISTRIBUTION/AVAILABILITY STATEMENT

Approved for public release; distribution unlimited.

12b. DISTRIBUTION CODE

13. ABSTRACT *(Maximum 200 words)*

This volume contains AFRRI Scientific Reports SR94-1 through SR94-8 for January-March 1994.

14. SUBJECT TERMS

15. NUMBER OF PAGES
67

16. PRICE CODE

17. SECURITY CLASSIFICATION OF REPORT UNCLASSIFIED	18. SECURITY CLASSIFICATION OF THIS PAGE UNCLASSIFIED	19. SECURITY CLASSIFICATION OF ABSTRACT UNCLASSIFIED	20. LIMITATION OF ABSTRACT UL

CONTENTS

Scientific Reports

SR94-1: Brook I, Tom SP, Ledney GD. Quinolone and glycopeptide therapy for infection in mouse following exposure to mixed-field neutron-γ-photon radiation.

SR94-2: Joseph JA, Hunt WA, Rabin BM, Dalton TK, Harris AH. Deficits in the sensitivity of striatal muscarinic receptors induced by ^{56}Fe heavy-particle irradiation: Further "age–radiation" parallels.

SR94-3: Keyser DO, Pellmar TC. Synaptic transmission in the hippocampus: Critical role for glial cells.

SR94-4: Patchen ML, Fischer R, MacVittie TJ, Seiler F, Williams DE. Single and combination cytokine therapies for treatment of radiation-induced hematopoietic injury: Effects of *c-kit* ligand and interleukin-3.

SR94-5: Patchen ML, Fischer R, Schmauder-Chock EA, Williams DE. Mast cell growth factor enhances multilineage hematopoietic recovery in vivo following radiation-induced aplasia.

SR94-6: Rokita H, Neta R, Sipe JD. Increased fibrinogen synthesis in mice during the acute phase response: Cooperative interaction of interleukin 1, interleukin 6, and interleukin 1 receptor antagonist.

SR94-7: Schmauder-Chock EA, Chock SP, Patchen ML. Ultrastructural localization of tumour necrosis factor-alpha.

SR94-8: Strassmann G, Fong M, Windsor S, Neta R. The role of interleukin-6 in lipopolysaccharide-induced weight loss, hypoglycemia and fibrinogen production, in vivo.

Quinolone and glycopeptide therapy for infection in mouse following exposure to mixed-field neutron-γ-photon radiation

I. BROOK*†, S. P. TOM and G. D. LEDNEY

Abstract. The effects of increased doses of mixed-field neutron-γ-photon irradiation on bacterial translocation and subsequent sepsis, and the influence of antimicrobial therapy on these events, were studied in the C3H/HeN mouse. Animals were given 4·25, 4·50, 4·75, 5·00 and 5·25 Gy of mixed-field $[n/(n+\gamma)=0·7]$ radiation. The mortality rate of mice and recovery of bacteria were directly related to the radiation dose. *Enterobacteriaceae* were mostly isolated from the livers of mice exposed to 5·00 and 5·25 Gy, and aerobic Gram-positive cocci were recovered from those exposed to 4·50 and 4·75 Gy. Oral therapy with L-ofloxacin reduced mortality of all groups of animals except those given 4·25 and 4·50 Gy. This reduction was associated with a decrease in the number of the recovered *Enterobacteriaceae*. However, the number of Gram-positive cocci was unaffected. Addition of i.m. glycopeptide therapy failed to prevent Gram-positive coccal infection, due to the development of glycopeptide-resistant *Enterococcus faecalis*. These data demonstrate a relationship between the doses of mixed-field radiation and the rates of infection due to *Enterobacteriaceae*. While L-ofloxacin therapy reduces the infection rate, prolongs survival and prevents mortality, the addition of a glycopeptide can enhance systemic infection by resistant bacteria in the irradiated host.

1. Introduction

Ionizing radiation increases a recipient's susceptibility to systemic infection due to endogenous and exogenous organisms (Kaplan *et al.* 1965, Brook *et al.* 1986). Most endogenous infections in γ-photon-irradiated animals originate in the bacterial flora of the gastrointestinal tract (Brook *et al.* 1986). Following irradiation, some members of that bacterial flora translocate to the liver and spleen, and they can be associated with fatal septicemia (Brook *et al.* 1986, Brook *et al.* 1988). The predominant organisms that can be recovered from septic animals are *Enterobacteriaceae* and *Streptococcus* spp. Preventing translocation of these bacteria and providing therapy of the subsequent sepsis can reduce mortality in experimental infection (Brook *et al.* 1990). However, antimicrobial agents that inhibit the anaerobic gastrointestinal flora can also enhance bacterial translocation and increase the mortality rate (Brook *et al.* 1988).

Previous studies (Brook and Ledney 1990, 1991, Brook *et al.* 1990) demonstrated the ability of quinolone therapy to reduce bacterial translocation and subsequent sepsis due to *Enterobacteriaceae* in the γ-photon-irradiated mouse. However, bacterial sepsis was documented in over one-quarter of the mice due to quinolone resistant *Streptococcus* spp. (Brook and Ledney 1991). The addition of an antimicrobial agent such as penicillin, which is effective against the *Streptococcus* spp., reduced the infection due to quinolone resistant *Streptococcus* spp. and increased the survival rate (Brook and Ledney 1991). Because of the growing resistance of *Streptococcus* spp. to penicillin and the occurrence of other Gram-positive pathogens such as *Staphylococcus* spp., evaluating the efficacy of a more potent antimicrobial agent was desired. Most of the past research relating to infection following irradiation was done in γ-photon-irradiated animals, and limited work was done on the bacterial aetiology and therapy of sepsis following neutron irradiation (Hammond *et al.* 1955).

Exposure to neutron radiation can occur accidentally or following therapeutic use of radiation. Although infection can occur following γ-photon as well as neutron irradiation, infection following neutron irradiation may have unique features due to the greater effect that neutrons have upon the intestinal epithelial cell lining than do γ-photons (Ledney *et al.* 1991). This study was designed to investigate the effect of increased doses of mixed-field neutron-γ-photon irradiation on bacterial translocation and subsequent sepsis and the mortality rate in mice using therapy with L-ofloxacin (a quinolone) and vancomycin or teicoplaning (glycopeptides).

2. Materials and methods

2.1. *Animals*

Female C3H/HeN mice (approximately 12 weeks old) were obtained from the National Cancer Insti-

*Author for correspondence: Itzhak Brook, MD, Naval Medical Research Institute, Bethesda, MD 20889, USA.
†Wound Infection Management Program, Experimental Hematology Department, Armed Forces Radiobiology Research Institute, Bethesda, MD, USA.

tute animal breeding facility (Frederick, MD, USA). All animals were kept in quarantine for about 2 weeks before transfer to a room with a 12-h light–dark cycle. Representative samples were examined to ensure the absence of specific bacteria and common murine diseases. Animals were maintained in a facility accredited by the American Association for Accreditation of Laboratory Animal Care in microisolator cages on hardwood chip bedding, and were provided commercial rodent chow and acidified water (pH 2·2) that was changed to tap water 48 h before irradiation. All experimental procedures were done in compliance with National Research Council guidelines and approved by an Institutional Animal Care and Use Committee.

2.2. *Mixed-field irradiation*

Mixed-field irradiation was performed using the AFRRI TRIGA Mark-F reactor. This reactor is a movable-core pool-type facility with maximum operational steady-state power of 1 MW. The reactor was operated at 45 kW. The neutron to total dose of neutrons and γ-photons ($[n/(n+\gamma)]$ dose ratio of 0·7) was achieved by irradiating mice through a 5-cm lead shield, 255 cm from the tank wall and 120 cm above the exposure room floor (Ledney *et al.* 1991). The mean energy for neutrons and γ-photons in experiments was approximately 0·8 MeV (Zeman and Ferlic 1984). Thus, mice received radiation doses with a spectrum of energies that contained a mixture of neutrons ($n = 70\%$) and γ-photons ($\gamma = 30\%$). All irradiations were performed at a total dose rate of 38 cGy/min. The total dose-rate varied $< 2\%$ over the entire radiation field. Mice were irradiated in aerated aluminum tubes that rotated at 1·5 rpm.

2.3. *Antimicrobial agents*

Standard powder formulation of antimicrobials were used for *in vitro* susceptibility studies. The antimicrobials were administered orally (L-ofloxacin), or i.m. (glycopeptides) in a volume of 0·1 ml sterile saline. The daily doses of the antimicrobial agents were 50 mg/kg for vancomycin (Eli Lilly Ind., Indianapolis, IN, USA) and 50 mg/kg for teicoplanin (Dow Pharmaceuticals, Cincinnati, OH, USA) given every 12 h and 20 mg/kg for oral L-ofloxacin (Ortho Pharmaceuticals Corp., Raritan, NJ, USA) given once a day. Control animals received 0·1 ml sterile saline i.m. once a day.

Serum concentrations of all antimicrobials were measured by the agar diffusion assay (Reeves *et al.* 1987) with *Bacillus subtilis*, ATCC strain number 6633 (American Type Culture Collection, Rockville, USA). Measurements were made in non-irradiated mice on day 5 of therapy at 1 and 11·5 h after glycopeptide administration and 23·5 h after L-ofloxacin administration. The method could not detect antimicrobial concentrations $< 0·2 \mu g/ml$.

2.4. *Microbiological methods*

Animals were killed by cervical dislocation. Specimens of livers and ilea were processed semiquantitatively for the presence of bacteria. No other organs were processed, and no blood samples were obtained because previous studies showed that liver cultures correlated best with sepsis (Brook *et al.* 1986). About 500 mg liver tissue and about 1 cm of ileum were aseptically removed and homogenized immediately. The specimens were swabbed onto media supportive of aerobic and anaerobic bacteria.

The media used for facultative and aerobic organisms were sheep blood and MacConkey agars. Aerobic plates were incubated in air and 5% carbon dioxide. Prereduced anaerobic sheep blood agar medium was used for anaerobic bacteria. Plates were incubated in anaerobic GasPak jars (BBL, Cockeysville, MD, USA) opened after 48 and 96 h of incubation, and observed for 7 days. All media were incubated at 37°C. Isolates were identified by standard criteria (Lennette *et al.* 1985, Sutter *et al.* 1985). Susceptibility testing was done using the Kirby–Bauer method (Lennette *et al.* 1985).

2.5. *Experimental design*

Antimicrobial treatments were initiated 72 h after irradiation and administered for 21 days. Animals were observed for survival for 60 days. Terminally-ill mice were killed during the experiment. The effect of increasing doses of mixed-field irradiation on translocation and mortality rate and the effect of L-ofloxacin therapy were studied in the first set of experiments. Increased doses of radiation were administered to each group: 4·25, 4·50, 4·75, 5·00 and 5·25 Gy. An additional group that was not irradiated served as a control. Six groups of 40 mice each were included in this experiment ($n = 240$). Each group was divided into two groups of 20: one group was observed for 60 days for survival, and the second group was used for cultures of liver and ileum. (Tables 1 and 2).

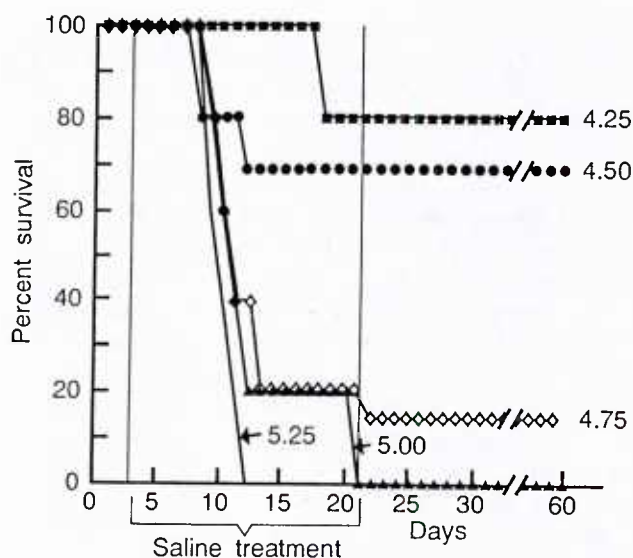In the second and third experiments, the effects of

Figure 1. Effects of various doses (Gy) of mixed field irradiation on survival of the saline-treated (control) C3H/HeN mouse.

quinolone and glycopeptide therapies were studied in mice exposed to 4·75 Gy. This dose was chosen because L-ofloxacin therapy had the best efficacy on survival. A total of 88 mice were included in the second experiment and 72 in the third experiment. Each experiment consisted of four equally divided sets of mice consisting of three antimicrobial therapy groups and a saline-treated control group. The therapy groups were as follows; one group received
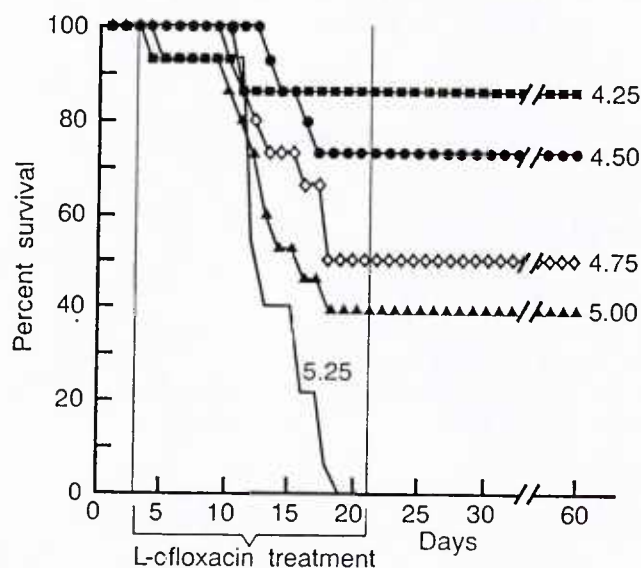

Figure 2. Effect of various doses (Gy) of mixed field irradiation on survival of the L-ofloxacin-treated C3H/HeN mouse.

L-ofloxacin, one a glycopeptide (vancomycin or teicoplanin), and one both L-ofloxacin and a glycopeptide. Each group consisted of 10 mice used for cultures of livers (five mice each on days 12 and 14 after irradiation) while the rest were used to monitor mortality. When fewer than five animals survived in a group, all were studied that day.

In the second experiment (Table 3) one group received oral L-ofloxacin, one teicoplanin, one the combination of the two, and one saline. In the third experiment (Table 4), one group received L-ofloxacin, one vancomycin, one the combination of the two, and one saline.

2.6. Statistical analysis

Statistical analysis was done using the Mantel–Cox test (Lee 1980).

3. Results

3.1. Mortality

In the first experiments (Figures 1 and 2), mortality rate was directly related to the dose of irradiation. In saline-treated mice, all mice exposed to 5·0 and 5·25 Gy, 85% of those exposed to 4·75 Gy, 30% exposed to 4·50 Gy, and 20% exposed to 4·25 Gy expired within 21 days. Therapy with L-ofloxacin did not change the ultimate survival of those exposed to 5·25 Gy although their mean survival time improved from 8·2 to 14·2 days. However, in those exposed to 5·00 Gy, 40% survived ($p < 0.05$), and in those exposed to 4·75 Gy, 50% survived ($p < 0.05$). There was no improvement in survival rate in those exposed to 4·50 and 4·25 Gy.

In the second and third sets of experiments, mortality was 20 and 40% in L-ofloxacin treated mice (Figures 3 and 4), as compared with 75 and 80% in saline-treated mice ($p < 0.05$). Mortality rate in those treated with either of the glycopeptides alone or a glycopeptide combined with L-ofloxacin was greater than controls ($p < 0.05$) or those treated with L-ofloxacin alone ($p 0.001$).

3.2. Isolation of bacteria

In the first experiment no bacteria were isolated from the livers of non-irradiated mice (data not shown) or those exposed to 4·25 Gy (Table 1).

Most of the organisms were recovered from mice irradiated with 5·00 and 5·25 Gy. Fifty-three differ-
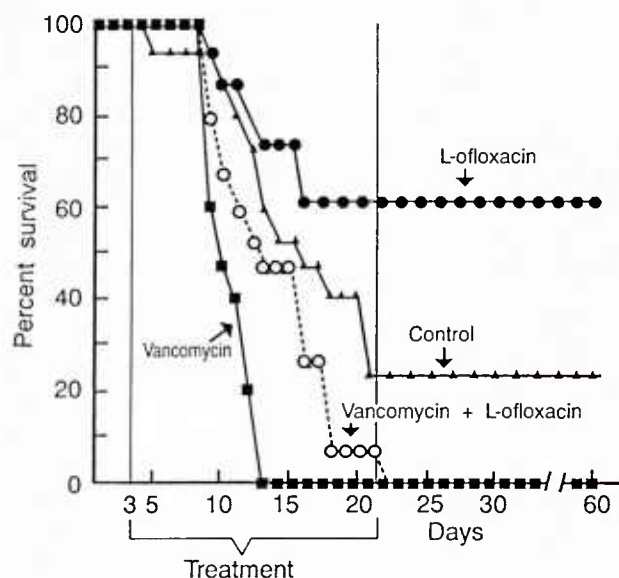
Figure 3. Survival of the 4·75 Gy mixed-field-irradiated C3H/HeN mouse treated with L-ofloxacin and vancomycin.

ent isolates were recovered from all mice: 21 (40%) from those exposed to 5·25 Gy; 18 (34%) from those exposed to 5·00 Gy; 11 (21%) from those exposed to 4·75 Gy; and 3 (6%) from those exposed to 4·50 Gy. The total number of recovered organisms increased from six organisms on day 8, to 15, 16 and 16 organisms on days 10, 12 and 14, respectively.

The predominant bacteria were *Escherichia coli* (21 isolates), alpha hemolytic *Streptococcus* (6), and *Enterobacter aerogenes* and *Acinetobacter* spp. (5 each). Most *Enterobacteriaceae* were recovered in mice exposed to 5·00 and 5·25 Gy and most *Staphylococcus* spp. were

recovered in those exposed to 4·50 and 4·75 Gy. Three strains of anaerobic cocci were also isolated. In one instance anaerobic cocci were the only isolate recovered from a liver abscess on day 8 after irradiation from a mouse given 5·00 Gy.

A significant reduction in the number of the isolated *Enterobacteriaceae* was noted in the livers of mice treated with L-ofloxacin (Table 2). Of the 19 isolates recovered from these animals, only two were *E. coli* and the others were Gram-positive bacteria.

The number of isolates recovered from the livers studied in the second experiment were 26 *Enterobacteriaceae* spp. (including 14 *E. coli*, five *Klebsiella pneumoniae*, four *Acinetobacter* spp. and three *E. aerogenes*) and 22 Gram-positive aerobic bacteria (including six *E. faecalis* and five *Staphylococcus aureus*) (Table 3).

In the third experiment the isolates were 24 *Enterobacteriaceae* spp., 23 Gram-positive aerobic bacteria (including 15 gamma-hemolytic streptococcus, five *E. faecalis* and four *S. aureus*) (Table 4). More *Enterobacteriaceae* were isolated in both sets of experiments in mice receiving the glycopeptides than in those receiving L-ofloxacin ($p < 0·05$). *E. faecalis* was isolated only in mice treated with glycopeptide alone or combined with L-ofloxacin.

Organisms similar to those isolated in the liver were also recovered in the ileum as predominant bacteria. *Enterobacteriaceae* were absent in the colon of mice treated with L-ofloxacin, while the number of strict anaerobes was unchanged. In contrast, the number of *Enterobacteriaceae* was unchanged in mice treated with a glycopeptide, but the number of strict anaerobes decreased to a minimum, and the number of *Streptococcus* spp. increased.
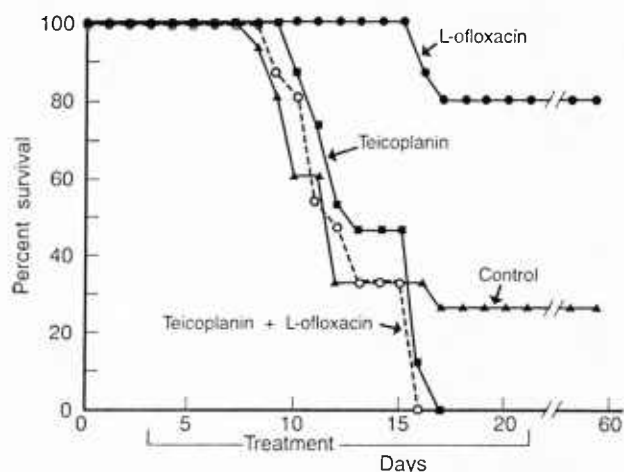

Figure 4. Survival of the 4·75 Gy mixed-field-irradiated C3H/HeN mouse treated with L-ofloxacin and teicoplanin.

3.3. *Antimicrobial serum concentrations*

Antimicrobial serum concentrations were obtained in five animals in each antimicrobial group on day 5 of therapy in unirradiated mice. The antimicrobial concentrations (mean ± SD) for L-ofloxacin at 1 and 23·5 h after injection were 2·4 ± 0·5 and 0·5 ± 0·2 µg/ml; for vancomycin at 1 and 11·5 h, 57·9 ± 6·4 and 12·5 ± 3·1 µg/ml; and for teicoplanin 49·6 ± 4·3 and 10·2 ± 2·3 µg/ml.

3.4. *Antimicrobial susceptibility*

All *E. faecalis* isolates were resistant to L-ofloxacin, teicoplanin and vancomycin as determined by the Kirby–Bauer method (Reeves *et al.* 1987).

Table 1. Bacteria recovered from livers of saline-treated mice irradiated with different doses (five mice per group were studied each day[a])

Irradiation dose (Gy):	Days after irradiation — 8					10					12					14					Total number of organisms
	4·25	4·50	4·75	5·00	5·25	4·25	4·50	4·75	5·00	5·25	4·25	4·50	4·75	5·00	5·25	4·25	4·50	4·75	5·00	5·25	
Aerobic bacteria																					
Escherichia coli				2			1	3	2			1	3	4					3	2	21
Klebsiella pneumoniae					1			1												1	3
Enterobacter aerogenes									1	1			1							2	5
Acinetobacter spp.				1						1					1				1	1	5
Staphylococcus epidermidis									1						1		1				3
Staphylococcus aureus									1						1			1	1		4
Alpha hem. streptococcus					1					1					2			2			6
Enterococcus faecalis										1					2						3
Anaerobic bacteria																					
Peptostreptococcus spp.					1					1									1		3
Total	0	0	0	3	3	0	1	4	5	5	0	1	4	4	7	0	1	3	6	6	53

[a] Only three mice were studied on day 14.

4. Discussion

These data demonstrate a relationship between the dose of mixed-field radiation to which the animals were exposed and the number and type of bacteria recovered. *Enterobacteriaceae* were more often isolated from mice exposed to 5·00 and 5·25 Gy, as compared with lower sublethal dosages, while aerobic Gram-positive cocci were mostly recovered from mice exposed to 4·50 and 4·75 Gy. These data are similar to those observed in γ-photon-irradiated mice (Brook *et al.* 1986) amd suggest common effects of neutron and γ-photon irradiation on the host gut flora and defenses. However, since the animals received a mixture of neutrons and γ-photons in this study, it is difficult to separate the effects of each type of radiation. The beneficial effect of quinolone therapy on survival of mice exposed to a higher dose of irradiation may be related to its activity against *Enterobacteriaceae*. These organisms were mostly recovered from livers of untreated animals and were eliminated from mice treated with quinolone. However, infection due to quinolone-resistant Gram-positive aerobic bacteria still occurred, and probably contributed to the mortality of those exposed to a high dose of radiation. The effect of quinolone

Table 2. Bacteria recovered from livers of L-ofloxacin-treated mice irradiated with different doses (5 mice per group were studied each day)

Irradiation dose (Gy):	Days after irradiation — 10					12					14					Total number of organisms
	4·25	4·50	4·75	5·00	5·25	4·25	4·50	4·75	5·00	5·25	4·25	4·50	4·75	5·00	5·25	
Aerobic bacteria																
Escherichia coli									1						1	2
Staphyloccus aureus			1										1			2
Staphyloccus epidermidis			1				1					1	1			4
Alpha hem. streptococcus		1	1				2	1		1		1				7
Streptococcus faecalis				1										1		2
Anaerobic bacteria																
Peptostreptococcus spp.					1									1		2
Total	0	1	3	1	1	0	3	1	1	1	0	2	2	2	1	19

Table 3. Recovery of organisms from livers of C3H/HeN mice irradiated with 4·75 Gy and treated with oral L-ofloxacin and i.m. teicoplanin

Organism	Therapy	Days after irradiation[a]		Total
		12	14	
Enterobacteriaceae spp	L-Ofloxacin	1/10	0/8	1/18
	Teicoplanin	6/7	3/5	9/12
	L-Ofloxacin and teicoplanin	4/8	2/3	6/11
	Saline	6/10	4/6	10/16
Aerobic Gram-positive bacteria	L-Ofloxacin	4/10	2/8	6/18
	Teicoplanin	5/7	2/5	7/12[b]
	L-Ofloxacin and teicoplanin	2/8	1/3	3/11[c]
	Saline	4/10	2/6	6/16

[a] Number of animals with bacteria/number of animals studied.
[b] *Enterococcus faecalis* resistant to teicoplanin (4 of 7).
[c] *Enterococcus faecalis* resistant to teicoplanin (2 of 3).

therapy is similar to the one observed in γ-photon-irradiated mice (Brook *et al.* 1990, Brook and Ledney 1990).

The addition of parenteral glycopeptide therapy, which was provided to improve the survival of the animals by suppressing the emerging Gram-positive coccal organisms in the gut, was surprisingly deleterious. Instead of reducing streptococcal and staphylococcal infection, mortality rate was enhanced and was associated with the emergence of a resistant *Enterococcus*. The observation of the deleterious effect of i.m. glycopeptide may be due to the excretion of the agent through the bile into the gastrointestinal tract (Geraci 1977) where it can reduce the number of strict anaerobic bacteria (Kennedy and Volz 1985a,b) while selecting a resistant *Enterococcus*.

The reduction in the number of anaerobic bacteria in the gut flora may promote the proliferation

of fungal species as well as antimicrobial-resistant bacteria. The findings of this study suggest that oral glycopeptide therapy can select an *E. faecalis*, resistant to both glycopeptides and quinolones. An increased frequency of recovery of these organisms was also reported in immunocompromized patients treated with vancomycin (Judeja *et al.* 1983, Green *et al.* 1991). Although quinolone therapy reduced the number of *Enterobacteriaceae* in the gut, the emergence of new pathogens was detrimental to the host. The emergence of a glycopeptide-resistant *E. faecalis* is an alarming observation, and if this phenomenon occurs in patients it will undoubtedly be of grave clinical consequence and should discourage overuse of glycopeptide therapy.

Vancomycin therapy was found to suppress the number of enteric bacilli population levels in mice and to promote *Candida albicans* fungemia (Kennedy

Table 4. Recovery of organisms from livers of C3H/HeN mice irradiated with 4·75 Gy and treated with oral L-ofloxacin and oral vancomycin

Organism	Therapy	Days after irradiation[a]		Total
		12	14	
Enterobacteriaceae spp.	L-Ofloxacin	0/10	0/8	0/18
	Vancomycin	7/10	4/7	11/17
	L-Ofloxacin and vancomycin	2/10	0/3	2/13
	Saline	6/10	5/9	11/19
Aerobic Gram-positive bacteria	L-Ofloxacin	2/10	4/8	6/18
	Vancomycin	3/10	2/7	5/17[c]
	L-Ofloxacin and vancomycin	4/10	3/3	7/13[c]
	Saline	3/10	2/9	5/19

[a] Number of animals with bacteria/number of animals studied.
[b] *Enterococcus faecalis* resistant to vancomycin (3 of 5).
[c] *Enterococcus faecalis* resistant to vancomycin (2 of 7).

and Volz 1985a,b, Green *et al.* 1991). Administration of vancomycin to patients with acute lymphocytic leukaemia promoted proliferation of *Candida* organisms in the gastrointestinal tract and increased the risk of candidemia (Ricket *et al.* 1991).

Although parenteral glycopeptide therapy has an important role and has been used for over two decades in the management of febrile neutropenic patients (Hathorn *et al.* 1987), this present study highlights the risk associated with administration of glycopeptide therapy alone or in combination with a quinolone in an effort tô prevent or abort bacterial infection following mixed-field irradiation. An increased risk of secondary bacterial infection was recently observed in patients receiving oral vancomycin therapy (Winston *et al.* 1990). Further studies are warranted to elucidate the mechanisms of emergence of bacterial resistance in response to such therapy. This animal model of failure of glycopeptide therapy in an immunocompromized host may be useful in understanding and overcoming the problem.

Acknowledgement

References

Brook, I., Elliott, T. B. and Ledney, G. D., 1990, Quinolone therapy of *Klebsiella pneumoniae* sepsis following irradiation: comparison of pefloxacin, ciprofloxacin, and ofloxacin. *Radiation Research*, **122**, 215–217.

Brook, I. and Ledney, G. D., 1990, Oral ofloxacin therapy of *Pseudomonas aeruginosa* sepsis in mice after irradiation. *Antimicrobial Agents and Chemotherapy*, **34**, 1387–1389.

Brook, I. and Ledney, G. D., 1991, Ofloxacin and penicillin G combination therapy in the prevention of bacterial translocation and animal mortality after irradiation. *Antimicrobial Agents and Chemotherapy*, **35**, 1685–1687.

Brook, I., Walker, R. I. and MacVittie, T. J., 1986, Effect of radiation dose on the recovery of aerobic and anaerobic bacteria from mice. *Canadian Journal of Microbiology*, **32**, 719–722.

Brook, I., Walker, R. I. and MacVittie, T. J., 1988, Effect of

antimicrobial therapy on bowel flora and bacterial infection in irradiated mice. *International Journal of Radiation Biology*, **53**, 709–716.

Geraci, J. E., 1977, Vancomycin. *Mayo Clinic Proceedings*, **52**, 631–634.

Green, M., Barbadora, K. and Michaels, M., 1991, Recovery of vancomycin-resistant Gram-positive cocci from pediatric liver transplant recipients. *Journal of Clinical Microbiology*, **29**, 2503–2506.

Hammond, C. W., Vogel, H. H. Jr., Clark, J. W., Cooper, D. B. and Miller, C. P., 1955, The effect of streptomycin therapy on mice irradiated with fast neutrons. *Radiation Research*, **115**, 354–360.

Hathorn, J. W., Rubin, M. and Pizzo, P. A., 1987, Empirical antibiotic therapy in the febrile neutropenic cancer patient: clinical efficacy and impact of monotherapy. *Antimicrobial Agents and Chemotherapy*, **31**, 971–977.

Judeja, L., Kantanjian, H. and Bolivar, R., 1983, *Streptococcus bovis* septicemia and meningitis associated with chronic radiation enterocolitis. *Southern Medical Journal*, **76**, 1588–1589.

Kaplan, H. W., Speck, R. S. and Jawetz, F., 1965, Impairment of antimicrobial defenses following total body irradiation of mice. *Journal of Clinical Medicine*, **40**, 682–691.

Kennedy, M. J. and Volz, P. A., 1985a, Effect of various antibiotics on gastrointestinal colonization and dissemination by *Candida albicans*. *Journal of Medical Veterinary Mycology*, **23**, 265–273.

Kennedy, M. J. and Volz, P. A., 1985b, Ecology of *Candida albicans* gut colonization. Inhibition of *Candida* adhesion colonization, and dissemination from the gastrointestinal tract by bacterial antagonism. *Infection and Immunity*, **49**, 654–663.

Ledney, G. D., Madonna, G. S., Elliott, T. B., Moore, M. M. and Jackson, W. E. III, 1991, Therapy of infections in mice irradiated in mixed neutron/photon fields and inflicted with wound trauma: a review of current work. *Radiation Research*, **128**, S18–28.

Lee, T. E., 1980, *Statistical Method for Survival Data Analysis* (Belmont, CA, Lifetime Learning), pp. 127–129.

Lennette, E. H., Balows, A., Hausler, W. and Shadomy, J. H., 1985, *Manual of Clinical Microbiology*, 4th Edn (Washington, DC, American Society for Microbiology).

Reeves, D. S., Phillips, I., Williams, J. V. and Wise, R., 1987, *Laboratory Methods in Antimicrobial Chemotherapy* (London, Churchill Livingstone).

Ricket, H. M., Andremont, A., Tancrede, C., Pico, J. L. and Jarvis, W. R., 1991, Risk factors for candidemia in patients with acute lymphocytic leukemia. *Reviews in Infectious Diseases*, **13**, 211–215.

Sutter, V. L., Citron, E. M., Edelstein, M. A. C. and Finegold, S. M., 1985, *Wadsworth Anaerobic Bacteriology Manual*, 4th Edn (Belmont, CA, Star).

Winston, D. J., Winston, G. H., Buckner, D. A., Gale, R., and Champlin, R. C., 1990, Ofloxacin versus vancomycin/polymyxin for prevention of infection in granulocytopenic patients. *American Journal of Medicine*, **88**, 36–42.

Zeman, G. H. and Ferlic, K. P., 1984, Paired Ion Chamber Constants for Fission Gamma-Neutron Fields. Technical Report TR84-8. Armed Forces Radiobiology Research Institute, Bethesda, MD. National Technical Information Services, Springfield, VA, AD A155069.

Deficits in the Sensitivity of Striatal Muscarinic Receptors Induced by ^{56}Fe Heavy-Particle Irradiation: Further "Age–Radiation" Parallels

J. A. Joseph,[1] W. A. Hunt,[2] B. M. Rabin,[3] T. K. Dalton, and Alan H. Harris

Behavioral Sciences Department, Armed Forces Radiobiology Research Institute, Bethesda, Maryland 20889–5603

Joseph, J. A., Hunt, W. A., Rabin, B. M., Dalton, T. K., and Harris, A. H. Deficits in the Sensitivity of Striatal Muscarinic Receptors Induced by ^{56}Fe Heavy-Particle Irradiation: Further "Age–Radiation" Parallels. *Radiat. Res.* 135, 257–261 (1993).

We had previously shown that there was a loss of sensitivity of muscarinic receptors (mAChR) to stimulation by cholinergic agonists (as assessed by examining oxotremorine enhancement of K^+-evoked release of dopamine from neostriatal slices) in animals that had been exposed to energetic particles (^{56}Fe, 600 McV/n), an important component of cosmic rays. This loss of mAChR sensitivity was postulated to be the result of radiation-induced alterations in phosphoinositide-mediated signal transduction. The present experiments were undertaken as a first step toward determining the locus of these radiation-induced deficits in signal transduction by examining K^+ enhancement of release of dopamine in ^{56}Fe-exposed animals (0, 0.1, and 1.0 Gy) with agents [A23187, a potent Ca^{2+} ionophore, or 1,4,5-inositol trisphosphate (IP_3)] that "bypass" the mAChR–G protein interface and by comparing the response to oxotremorine-enhanced K^+-evoked release of dopamine. Results showed that although oxotremorine-enhanced K^+-evoked release of dopamine was reduced significantly in the radiation groups, no radiation effects were seen when A23187 or IP_3 was used to enhance K^+-evoked release of dopamine. Since similar findings have been observed in aging, the results are discussed in terms of the parallels between aging and radiation effects in signal transduction that might exist in the neostriatum. © 1993 Academic Press, Inc.

INTRODUCTION

Among the myriad of problems that must be solved if astronauts are to travel to distant planets in our solar system, such as Mars, are those dealing with the effects of long-term exposure to space radiation, such as cosmic rays [for reviews, see Refs. (*1–5*)]. Such considerations will become especially important because shielding against heavy particles such as ^{56}Fe, an important component of cosmic rays, is presently very difficult. In attempts to elucidate these effects, our research has focused on the consequences of whole-body exposure to ^{56}Fe particles (600 MeV/n) on motor behavioral performance and related neurochemical parameters of the corpus striatum in rats. This structure has been shown to mediate a variety of motor behavioral functions such as coordination and muscle strength [for reviews, see Refs. (*6–8*)].

In our initial experiment (*9*), motor behavior was assessed in various groups of rats at 12 h to 14 days after ^{56}Fe-particle irradiation by examining the length of time that a rat could remain suspended by its forepaws from a wire. Biochemical assessments of striatal function were carried out immediately after the behavioral tests and up to 180 days after irradiation by determining the sensitivity of muscarinic acetylcholine receptors (mAChR)[4] to stimulation by muscarinic agonists. This latter assessment was made by examining the oxotremorine (OXO)-enhanced K^+-evoked release of dopamine (DA) from perifused striatal slices obtained from these animals. The results indicated that profound decrements occurred in both indices. The effects on K^+-evoked release of DA were evident as early as 12 h after irradiation and were seen as long as 180 days after irradiation.

Thus, there were deficits in the sensitivity of mAChR to agonist stimulation. However, the locus of these deficits within putative mAChR-initiating phosphoinositide (PI)-mediated signal transduction pathways remained unresolved by these studies. The mAChR are linked to G proteins, which are heterotrimers composed of $\alpha\beta\Gamma$ subunits. After stimulation of mAChR (specifically the PI-linked M_1 and M_3 subtypes) in the presence of Mg^{2+}, there is an exchange of GTP for GDP on the α subunit (*10*). The activated α_{GTP} subunit dissociates from the $\beta\Gamma$ subunits and interacts with effector molecules of phospholipase C, which catalyzes the cleavage of phosphatidylinositol 4,5-bisphos-

---

[1] Present address: Laboratory of Cellular and Molecular Biology, Gerontology Research Center/NIA, 4940 Eastern Ave., Baltimore, MD 21224.
[2] Present address. Division of Basic Research, National Institute on Alcohol Abuse and Alcoholism, Rockville, MD 20857.
[3] Present address, Department of Psychology, University of Maryland, Baltimore County, Catonsville, MD 21228.

[4] Abbreviations used: DA, dopamine; HPLC, high-performance liquid chromatography; IP_3, 1,4,5,-inositol trisphosphate; mAChR, muscarinic acetylcholine receptors; OXO, oxotremorine; PI, phosphoinositide.

phosphate (PIP_2). One product resulting from this reaction is 1,4,5-inositol trisphosphate (IP_3), one of the second messengers of this system (*11, 12*). An intrinsic low-K_M GTPase activity of the a subunit hydrolyzes GTP to GDP, releasing inorganic phosphate (P_i) and α_{GDP}, and reassociates with $\beta\Gamma$, ending the activation cycle (*13, 14*). IP_3 acts to evoke the quantal (*15*) release of Ca^{2+} from internal stores to carry the impulse further or impinge upon an effector. It is clear that alterations induced by exposure to ^{56}Fe particles at any point in this signal transduction pathway could affect the responsiveness of mAChR to agonist stimulation, resulting in reduced Ca^{2+} mobilization, alterations in neuronal processing, and ultimately, reduced behavioral performance.

As a first step toward making these analyses, the present experiment was carried out to determine if the locus of the deficit in mAChR-initiating PI-mediated signal transduction after exposure to ^{56}Fe particles occurred after the receptor–G protein complex in the biochemical pathway of signal transduction. For that reason we chose to examine K^+-evoked release of DA in striatal tissue from rats exposed to ^{56}Fe particles by "bypassing" this complex and stimulating signal transduction at later points in the pathway. In this regard, K^+-evoked release of DA was assessed after application of IP_3 or A23187 [a potent Ca^{2+} ionophore (*16*)] to perifused striatal slices from irradiated and control animals.

MATERIALS AND METHODS

Animals

Male Sprague–Dawley Crl:CD(SD)BR rats (Charles River Laboratories, Kingston, NY) weighing 200–300 g were used in these experiments. The rats were housed at an AAALAC-accredited vivarium at the Lawrence Berkeley Laboratory (LBL), Berkeley, CA. The rats were maintained in polycarbonate cages that contained autoclaved hardwood contact bedding (Beta Chip, Northeastern Products Corp., Warrensburg, NY). They were given food and water *ad libitum*. The animal holding rooms were kept at $21 \pm 1°C$ with $50 \pm 10\%$ humidity.

Radiation and Dosimetry

Rats were exposed to whole-body irradiation with high-energy ^{56}Fe particles (600 MeV/n) produced by the BEVALAC at LBL. In each experiment one rat was irradiated at a time. This energy provided a Bragg curve with the plateau region extending 8 cm in water. Since the diameter of the rat (including the plastic restrainer) was 7 cm, the animals were within this plateau region of the curve. Entrance dose measurements were made by the staff of the BEVALAC facility using parallel-plate ionization chambers with Mylar windows and N_2 gas flow positioned in the beam line (*17, 18*). The rats were irradiated in well-ventilated plastic holders. Rats were given one of three doses (0.0, 0.1, or 1.0 Gy) at a dose rate that averaged 1 Gy/min. The specified doses were received by all organs.

Perifusion Procedure

At 2–3 days after irradiation the animals were killed by decapitation; their brains were removed quickly, and the striata were dissected rapidly on ice. The tissue was then treated as described previously (*9, 16, 19, 20*). Briefly, cross-cut striatal slices (300 μm) were prepared from each animal using a McIlwain tissue chopper (Westbury, NY); slices from each animal

in the individual experimental and control groups were pooled and were placed into small glass vials that contained a modified Krebs-Ringer basal release medium containing 21 mM $NaHCO_3$, 3.4 mM glucose, 1.3 mM NaH_2PO_4, 1 mM EGTA, 0.93 mM $MgCl_2$, 127 mM NaCl, and 2.5 mM KCl (pH 7.4). The medium had been bubbled for 30 min with 95% O_2/5% CO_2. Slices from each vial were washed twice in this medium and aliquots were placed into the chambers of a perifusion apparatus. After being placed in the chambers of the perifusion apparatus, the tissue was allowed to equilibrate for 30 min while being perifused continuously with basal release medium at a rate of 124 μl/min. Gillson peristaltic pumps (Middleton, WI) controlled the flow rate of the medium. After the equilibration period, a 5-min baseline fraction was collected on ice. The tissue was then exposed to a HiKCl (release) medium that contained 30 mM KCl, 1.26 mM $CaCl_2$, and 57 mM NaCl, as well as the other components described above (pH 7.4). The tissue from each control or radiation group, depending upon the particular experiment, was treated with one of the agents (delivered in the release medium) under study. These included: (a) 100 μM of A23187 (Behring Diagnostics, La Jolla, CA), (b) 20 μM IP_3 (Sigma, St. Louis, MO) (c) 500 μM OXO, or (d) HiKCl alone. Five-minute fractions continued to be collected on ice for 30 min. The fractions were collected into tubes containing 0.3 ml of cold 0.4 M perchloric acid, 0.05% sodium metabisulfite, and 0.10% EDTA. These samples were then stored at $-80°C$ for later analysis of DA using high-performance liquid chromatography (HPLC) coupled to electrochemical detection.

The HPLC system consisted of a Varian Model 5000 ternary chromatograph, a Varian 401 data system, a Varian Model 8055 autosampler, and a Valco air-actuated injector with a 50-ml loop (all from Varian Associates, Sunnyvale, CA). The effluent was monitored with a Bioanalytical Systems LC-4B amperometric detector using a glassy carbon electrode. The detector potential was set at 0.72 V as an $Ag/AgCl_2$ reference electrode with a sensitivity of 10 nA/V. The mobile phase consisted of a filtered, degassed 100 mM KH_2PO_4 buffer containing 3 mM 1-heptanesulfonic acid, 100 μM EDTA, and 8% (V/V) acetonitrile (pH 3.6.) The components were eluted off a Waters 10 μm particle, μBondapak C_{18} reverse-phase column (30 $\times$ 0.39 cm; flow rate, 1 ml/min) maintained at 30°C. Results were calculated relative to known previous standards that were analyzed on the HPLC under similar conditions. Data were expressed as pmol/mg protein as analyzed using the procedure of Lowry *et al.* (*21*).

Data Analysis

Data from the perifusion experiments were analyzed by first computing difference scores by subtracting the peak amount (pmol/mg protein) of DA released to the release medium alone from that released under each of the other conditions (i.e., OXO, A23187, IP_3; see Results). These difference scores were then analyzed by analyses of variance and post-hoc t tests.

RESULTS

Release of DA to HiKCl Alone

An examination of the release of DA to HiKCl indicated that there were significant differences among the groups [$F(2,52) = 6.25$, $P < 0.005$]. Subsequent post-hoc t tests revealed that the 1.0-Gy group had significantly higher release of DA than either the 0.1-Gy or control groups [$t(53)$ 1.0 Gy vs 0.1 Gy = 3.62, $P < 0.001$; 1.0 Gy vs control = 2.59, $P < 0.02$]. The release of DA in the 0.1-Gy group did not differ significantly from that in the control group (0.1 Gy vs control $t < 1$, $P > 0.05$). For this reason subsequent analyses of the degree of enhancement by OXO, IP_3, or A23187 were carried out by analyzing the differences be-
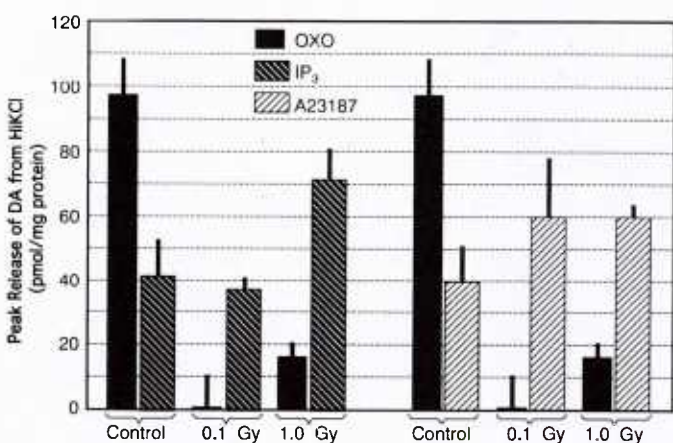
FIG. 1. Effects of exposure to 0.1 or 1.0 Gy of ^{56}Fe particles on the release of dopamine (DA) stimulated by oxotremorine (OXO), 1,4,5-inositol triphosphate (IP$_3$), or A23187.

tween HiKCl and the respective pharmacological treatment.

Enhancement of Release of DA by Oxotremorine, IP$_3$, or A23187

Comparisons of A23187 and oxotremorine. As shown in Fig. 1, there were differences among the groups in the ability of A23187 or OXO to enhance the release of DA from striatal tissue. Analysis of variance revealed these differences to be significant [F test for radiation condition × OXO-A23187 (2,32) = 15.85, $P < 0.001$]. Subsequent Duncan's post tests ($df = 32$) showed that OXO-enhanced K$^+$-evoked release of DA was significantly greater in the nonirradiated group than that by either the 0.1-Gy ($P < 0.001$) or 1.0-Gy ($P < 0.001$) irradiated groups, and that the irradiated groups did not differ from each other ($P > 0.05$). There were no differences among the various groups in the A23187 enhancement of K$^+$-evoked release of DA (all P values > 0.05, Duncan's tests). However, as can be seen from Fig. 1, A23187 produced significantly less enhancement of K$^+$-evoked release of DA than OXO in the control group (Duncan's test, $P < 0.05$). Because it was possible that the failure to find any group differences in the enhancement of K$^+$-evoked release of DA by A23187 was the result of reductions in the responses of the tissue from the controls, we also examined the differences between the effect of OXO and A23187 on K$^+$-evoked release of DA within each irradiated group. Duncan's tests revealed significant differences in both groups (0.1 Gy A23187 vs 0.1 Gy OXO, $P < 0.01$; 1.0 Gy A23187 vs 1.0 Gy OXO, $P < 0.05$), indicating that A23187 was significantly more efficacious than OXO in enhancing K$^+$-evoked release of DA in these irradiated groups.

Comparisons of IP$_3$ and oxotremorine. Similar results were seen with respect to IP$_3$ and OXO. As shown in Fig. 1,

IP$_3$ was more effective in enhancing K$^+$-evoked release of DA than OXO in the irradiated groups [F test for radiation condition × OXO-IP$_3$ (2,27) = 9.21, $P < 0.001$]. There were no differences among the various groups in IP$_3$-enhanced K$^+$-evoked release of DA (Duncan's tests, all $Ps > 0.05$), while as shown above, enhancement of K$^+$-evoked release of DA was seen only in the control (nonirradiated) groups. However, as with A23187, enhancement of K$^+$-evoked release of DA by IP$_3$ was actually less than that seen with OXO in the control group (Duncan's test, $P < 0.5$; $df = 27$). Thus we also examined the differences between IP$_3$ and OXO in the irradiated groups. Comparisons between IP$_3$ and OXO within each irradiated group indicated that there was a significant difference between enhancement of K$^+$-evoked release of DA by OXO and IP$_3$ in the 1.0-Gy group, indicating that IP$_3$ was effective in enhancing the release of DA in this group (see Fig. 1), but this effect was not seen in the 0.1-Gy group. Thus these findings indicated that both IP$_3$ and A23187 were more effective than OXO in enhancing K$^+$-evoked release of DA in the 1.0-Gy group, while the reverse was true for the control group.

DISCUSSION

The present results showed that once the initial "steps" in the signal transduction sequence were "bypassed," and Ca^{2+} was mobilized directly by the addition of A23187, enhancement of K$^+$-evoked release of DA was significantly greater in both irradiated groups (0.1 and 1.0 Gy) than it was in OXO groups. Similar results were seen with respect to the enhancement of K$^+$-evoked release of DA by IP$_3$. However, in this case statistically significant effects of IP$_3$ were seen only in the 1.0-Gy group. The 0.1-Gy group showed a trend toward an increase, but it was not significant.

While both A23187 and IP$_3$ appeared to have greater effects than OXO in the irradiated groups, they were less effective than OXO in the controls. While we cannot explain the loss of effectiveness of these compounds in the controls, these data suggest that the signal transduction initiated by mAChR in the irradiated rats is primarily intact below the ligand–mAChR–G protein interface. Preliminary results from ongoing experiments undertaken to determine the locus of the radiation-induced deficits in mAChR signal transduction support this hypothesis. They have revealed that this decrement occurs early in the process and probably involves alterations in the signal transduction process, possibly in the mAChR or its respective G protein. There are three critical areas that may be important. First, there may be radiation-induced neuronal loss which includes reductions in mAChR concentrations. It is known that exposure to ^{56}Fe at these doses can produce profound neuronal loss in the substantia nigras (Joseph et al., in preparation). There is also some evidence in aged animals which suggests

that the degree of OXO-enhanced K^+-evoked release of DA is dependent on the number of striatal mAChR (22). If this is also true after irradiation, then this would also contribute to the reductions in OXO-enhanced K^+-evoked release of DA.

A second area that may contribute to these reductions probably involves radiation-induced deficits mAChR–G protein coupling (the first step in signal transduction). At least two indices of receptor–G protein coupling appear to be altered in the striata of irradiated rats: (a) the ability of the receptor to uncouple from its respective G protein (Joseph et al., in preparation) and enter a low-affinity state upon stimulation, and (b) the ability of muscarinic agonists to stimulate low-K_M GTPase activity.[5]

Third, it is also possible that the free radicals produced during heavy-particle irradiation may induce neuronal membrane structural and functional alterations that may involve changes in lipid content, increases in membrane rigidity, or protein crosslinking (23). These membrane changes probably occur through free radical-induced lipid peroxidation.

We are presently carrying out experiments on putative effects of free radicals on membranes. However, until they are completed some evidence can be extrapolated from the findings in animals where damage from free radicals has taken its toll on central nervous system function. Extensive research has indicated that senescent organisms represent one such group (24–26). It has been postulated for a number of years that the accumulated effects of free radicals produced during normal metabolism are responsible for the alterations in the structure and function of membranes seen in senescence (23).

Thus, when these same parameters [i.e., motor behavior (6, 7) and enhancement of K^+-evoked release of DA by OXO (20)] were examined in middle-aged (12 months) and aged (24 months) rats, similar deficits were observed. These experiments indicated that there were declines in motor behavior and OXO-enhanced K^+-evoked release of DA that were similar to those found in irradiated animals. Subsequent experiments have shown that: (a) A23187 or IP_3 applied to striatal slices obtained from senescent rats yielded results similar to those seen here, (b) carbachol-stimulated low-K_M GTPase activity is reduced in striatal tissue obtained from aged animals (27), and (c) the ability of mAChR to uncouple from or remain coupled to its respective G protein is altered during aging (28).

Taken together, these results suggest that the deficits induced by exposure to ^{56}Fe particles or those that occur during aging may involve alterations in membrane integrity through lipid peroxidation. These changes, in turn, can alter the responsiveness, integrity, and transduction in a variety of systems. In the present case it could mean that radiation-induced alterations in the membrane may alter mAChR–G protein coupling/uncoupling, resulting in decreased receptor sensitivity.

These experiments provide further evidence for the "age–radiation parallel" hypothesis (29–32). However, there are at least two other important implications of these findings: (a) Since many of the astronauts are middle-aged or approaching middle age, these particles will be impinging upon nervous systems that are already showing the deleterious effects of age. Thus there may be immediate or delayed (as the individual continues to age) effects upon motor or cognitive performance. (b) Since oxidative damage may also be responsible for the deficits seen in aging, as well as in diseases such as tardive dyskinesia (33), Parkinson's disease (34), and Alzheimer's disease,[6] continued efforts to use radiation and aging models in concert should provide useful information on the role of lipid peroxidation induced by free radicals in central neuronal function.

REFERENCES

1. NCRP, Guidance on Radiation Received in Space Activities. Report No. 98, National Council on Radiation Protection and Measurements, Bethesda, MD, 1989.

2. S. B. Curtis, Lethal and potentially lethal lesions induced by radiation—A unified repair model. Radiat. Res. 106, 252–270 (1986).

3. S. Curtis and M. C. Wilkinson, Study of Radiation Hazards to Man on Extended Mission. Report Cr-1037, NASA, Washington, DC, 1968.

4. E. G. Stassinopoulos, The earth's trapped and transient space radiation environment. In Terrestrial Space Radiation and Its Biological Effects (P. D. McCormack, C. E. Swenberg, and H. Bucker, Eds.), pp. 5–35. Plenum, New York, 1988.

5. P. Todd, Unique biological aspects of radiation hazards—an overview. Adv. Space Res. 3, 187–194 (1983).

6. J. A. Joseph and G. S. Roth, Altered striatal dopaminergic and cho-

linergic reciprocal inhibitory control and motor behavioral decrements in senescence. *Ann. N.Y. Acad. Sci.* **521**, 110–122 (1988).

7. J. A. Joseph and G. S. Roth, Upregulation of striatal dopamine receptors and improvement of motor performance in senescence. *Ann. N.Y. Acad. Sci.* **515**, 355–366 (1988).

8. J. A. Joseph, G. S. Roth, and R. Strong, The striatum, a microcosm for the examination of age-related alterations in the CNS: A selected review. In *Review of Biological Research in Aging* (M. Rothstein, Ed.), pp. 181–199. Wiley/Liss, New York, 1990.

9. J. A. Joseph, W. A. Hunt, B. M. Rabin, and T. K. Dalton, Possible "accelerated striatal aging" induced by [56]Fe heavy particle irradiation: Implications for manned space flights. *Radiat. Res.* **130**, 88–93 (1992).

10. M. I. Simon, M. P. Strathmann, and N. Gautam, Diversity of G proteins in signal transduction. *Science* **252**, 802–808 (1991).

11. S. K. Fisher and B. W. Agranoff, Receptor activation and inositol lipid hydrolysis in neural tissues. *J. Neurochem.* **258**, 7358–7363 (1987).

12. M. J. Berridge and R. F. Irvine, Inositol phosphates and cell signalling. *Nature* **341**, 197–205 (1989).

13. S. Ghodsi-Hovsepian, W. S. Messer, and W. Hoss, Differential coupling between muscarinic receptors and G-proteins in regions of the rat brain. *Biochem. Pharmacol.* **39**, 1385–1391 (1990).

14. W. Hoss, P. H. Franklin, and S. Ghodsi-Hovsepian, Characterization of low K_M GTPase activity in rat brain: Comparison of opioid and muscarinic receptor stimulation. *J. Pharm. Sci.* **77**, 353–358 (1988).

15. L. Missiaen, C. W. Taylor, and M. J. Berridge, Spontaneous calcium release from inositol trisphosphate-sensitive calcium stores. *Nature* **352**, 242–244 (1991).

16. J. A. Joseph, T. K. Dalton, G. S. Roth, and W. A. Hunt, Alterations in muscarinic control of striatal dopamine autoreceptors in senescence: A deficit at the ligand-muscarinic receptor interface? *Brain Res.* **454**, 149–155 (1988).

17. J. T. Lyman and J. Howard, Dosimetry and instrumentation for helium and heavy ions. *Int. J. Radiat. Oncol. Biol. Phys.* **3**, 81–85 (1977).

18. A. R. Smith, L. D. Stephens, and R. H. Thomas, Dosimetry for radiobiological experiments using energetic heavy ions. *Health Phys.* **34**, 387 (1978).

19. J. A. Joseph, M. A. Kowatch, T. Maki, and G. S. Roth, Selective cross activation/inhibition of second messenger systems and the reduction of age-related deficits in the muscarinic control of dopamine release from perifused rat striata. *Brain Res.* **537**, 40–48 (1991).

20. J. A. Joseph, T. K. Dalton, and W. A. Hunt, Age-related decrements in the muscarinic enhancement of K+-evoked release of endogenous striatal dopamine: An indicator of altered cholinergic-dopaminergic reciprocal inhibitory control in senescence. *Brain Res.* **454**, 140–148 (1988).

21. O. H. Lowry, N. J. Rosebrough, A. L. Farr, and R. J. Randall, Protein measurement with Folin phenol reagent. *J. Biol. Chem.* **193**, 265–275 (1951).

22. K. Yamagami, J. A. Joseph, and G. S. Roth, Muscarinic receptor concentrations and dopamine release in aged rat striata. *Neurobiol. Aging* **13**, 51–56 (1991).

23. F. Schroeder, Role of membrane asymmetry in aging. *Neurobiol. Aging* **5**, 323–333 (1984).

24. D. Harman, The aging process. *Proc. Natl. Acad. Sci. USA* **78**, 7124–7128 (1981).

25. B. Halliwell, Oxidants and human disease: Some new concepts. *FASEB J.* **1**, 358–364 (1987).

26. B. Halliwell and J. M. C. Gutteridge, *Free Radicals in Biology and Medicine.* Clarendon Press, Oxford, 1989.

27. K. Yamagami, J. A. Joseph, and G. S. Roth, Decrement of muscarinic receptor-stimulated low K_m GTPase activity in striata and hippocampus from aged rat. *Brain Res.* **576**, 327–331 (1992).

28. R. M. Anson, R. Cutler, J. A. Joseph, K. Yamagami, and G. S. Roth, The effects of aging on muscarinic receptor/G protein coupling in the rat hippocampus and striatum. *Brain Res.* **598**, 302–306 (1992).

29. A. C. Upton, Ionizing radiation and aging. *Gerontologia* **4**, 162–176 (1959).

30. E. J. Ainsworth, R. J. M. Fry, P. C. Brennan, S. P. Stearner, J. H. Rust, and F. S. Williamson, Life shortening, neoplasia and systematic injuries in mice after single or fractionated doses of neutron or gamma radiation. In *Biological and Environmental Effects of Low-Level Radiation,* Vol II, pp. 77–92. International Atomic Energy Agency, Vienna, 1976.

31. R. C. Adelman, Loss of adaptive mechanisms during aging. *Fed. Proc.* **38**, 1968–1971 (1979).

32. A. K. De, S. Chipalkatti, and A. S. Aiyar, Effects of chronic irradiation on age-related biochemical changes in mice. *Radiat. Res.* **95**, 637–645 (1983).

33. J. L. Cadet, J. B. Lohr, and D. V. Jeste, Free radicals and tardive dyskinesia. *Trends Neurosci.* **9**, 107–108 (1986).

34. J. D. Adams and I. Odunze, Oxygen free radicals and Parkinson's disease. *Free Radical Biol. Med.* **10**, 161–191 (1991).

Synaptic Transmission in the Hippocampus: Critical Role for Glial Cells

DAVID O. KEYSER AND TERRY C. PELLMAR

Physiology Department, Armed Forces Radiobiology Research Institute, Bethesda, Maryland 20889-5603

ABSTRACT   The importance of glial cells in controlling the neuronal microenvironment has been increasingly recognized. We now demonstrate that glial cells play an integral role in hippocampal synaptic transmission by using the glial-specific metabolic blocker fluoroacetate (FAC) to selectively inhibit glial cell function. FAC inhibits evoked intracellular postsynaptic potentials (PSPs; $IC_{50} = 39$ μM) as well as population PSPs ($IC_{50} = 65$ μM) in field CA1 of the guinea pig hippocampal slice. Spontaneous synaptic transmission is concurrently decreased. These effects are time and dose dependent. ATP concentrations in glial but not neuronal elements are also significantly reduced with FAC treatment. Simultaneous application of the metabolic substrate isocitrate with FAC prevents both the reduction in glial ATP concentrations and the decrease in evoked PSPs. Given that isocitrate is selectively taken up by glia, these data further support a glial specific metabolic action of FAC. Additionally, FAC has no postsynaptic effects as peak responses to iontophoretically applied glutamate are unchanged. However, the decay of both iontophoretic and evoked PSPs are prolonged following FAC treatment suggesting inhibition of glutamate uptake may contribute to the FAC-induced depression of synaptic potentials. These results show, for the first time, that glial cells are critical for maintenance of synaptic transmission and suggest a role for glial cells in the modulation of synaptic efficacy. © 1994 Wiley-Liss, Inc.

INTRODUCTION

Glial cells, long thought to be simply support cells in the CNS, have recently been identified as a more dynamic class of cells whose functions are quite varied (Barres, 1991; Cornell-Bell et al., 1990a; Cornell-Bell and Finkbeiner, 1991; Finkbeiner, 1992; Kollegger et al., 1991; Martin, 1992). Glial cells are known to influence ionic balance and to take-up and metabolize certain neurotransmitters such as glutamate, the putative excitatory neurotransmitter in the hippocampus (Erecinska, 1990; Erecinska et al., 1986; Paulsen and Fonnum, 1989; Schousboe et al., 1977; Walz, 1989). Glial-neuronal interactions begin early in development (Hatten, 1990; Hatten and Mason, 1990) and glial cells play an active role in neuronal maturation and migration (Krysotek and Seeds, 1981; Moonen et al., 1982). Recent evidence suggests that glial cells express a variety of neurotransmitter and hormonal receptors (Hansson,

1989; Murphy and Pearce, 1987; von Blankenfeld and Kettenmann, 1991) and respond to receptor activation via classic ionotropic and second messenger pathways (Hansson, 1989; Murphy and Pearce, 1987; von Blankenfeld and Kettenmann, 1991), as well as with morphological alterations (Cornell-Bell et al., 1990b; Noble et al., 1992; Wenzel et al., 1991). These findings indicate that communications between glia and neurons persist in the mature CNS and suggest that glial-neuronal coupling plays a role in synaptic transmission.

While glial modulation of synaptic interactions has been a topic of investigation for several years, a requirement for glia in the maintenance of these interactions has not been thoroughly explored. We now present evi-

dence to suggest, for the first time, that glial cells play a critical role in the maintenance of synaptic transmission.

MATERIALS AND METHODS

Male Hartley guinea pigs were anesthetized with isoflurane and euthanized via cervical dislocation. The brain was rapidly removed, hemisected, and placed in ice-cold artificial cerebrospinal fluid (ACSF) containing (in mM): 124 NaCl, 3 KCl, 2.4 $CaCl_2$, 1.3 $MgSO_4$, 1.24 KH_2PO_4, 10 glucose, and 26 $NaHCO_3$, pH 7.4. The hippocampus was dissected from cerebral hemispheres, and slices (450 μm) were made using a McIlwain tissue chopper. Slices were allowed to incubate in oxygenated ACSF at room temperature for at least 1.5 h prior to use. Slices were transferred to a submerged slice recording chamber (Zbicz design) and continuously perfused with oxygenated ACSF and maintained at 30 ± 1°C. All drugs used were dissolved in ACSF and perfused at a rate of 1–2 ml/min.

The pyramidal cell layer of CA1 was visually identified under a dissecting microscope and neurons were impaled with glass microelectrodes (20–40 MΩ) filled with 2 M KCl or 2 M K-Acetate as previously described (Pellmar, 1987). Acceptable neurons had resting membrane potentials of −60 mV or greater with input resistances above 30 MΩ. Data were collected using a Dagan 8100 under current clamp mode using the switching circuitry.

Postsynaptic potentials (PSPs) were evoked with a concentric bipolar stainless steel stimulating electrode placed in stratum radiatum of the hippocampal slice. Holding current (50–200 pA) was often passed to hyperpolarize cells (−70 to −80 mV) so that 5–15 mV PSPs could be reliably elicited without evoking action potentials. At these membrane potentials, inhibitory PSPs are very close to their reversal potential and minimally contribute to the PSPs recorded with 2 M potassium acetate-filled electrodes. In experiments using 2 M KCl-filled electrodes, the chloride equilibrium potential (and consequently the inhibitory PSP reversal potential) is shifted and the recorded PSP is a mix of excitatory and inhibitory potentials. Results were similar under both recording conditions.

Glutamate was applied by iontophoresis. A glass iontophoretic microelectrode was filled with 0.5 mM glutamate and positioned in stratum radiatum in close proximity to the impaled neuron. Currents between 10–100 nA (5–50 ms duration) were used to eject glutamate. Bias currents up to 20 nA were applied to prevent leakage. Once responses to glutamate were established, transmitter was iontophoretically applied at 1 min intervals in all experiments.

For ATP measurements, whole hippocampal slices were incubated in 50 ml of control oxygenated ACSF for 30 min at 29–31°C. Drugs were added directly to control ACSF and slices incubated an additional 30 min. Slices were then removed and placed in 1 ml of 0.1% NaOH in control ACSF and rapidly frozen in liquid nitrogen. C6 glioma cells and synaptosomes were handled in similar fashion except that the incubation volume was reduced to 2 ml. ATP was measured with the Bioluminescent Somatic Cell Assay Kit for ATP (Sigma Chemical Co., St. Louis, MO). Slices were rapidly thawed, homogenized, and kept on ice. Light emissions were measured on a Picolite Luminometer System (model 6500). ATP standards were measured at the beginning and end of each set. Protein for each group was measured using the Bio-Rad Protein Assay (Bio-Rad, Richmond, CA). All measurements were taken in triplicate, averaged and expressed as nmol ATP/mg protein. For analysis data were expressed as the percent change from the paired control. Each single sample reflects either a) three hippocampal slices, b) one 75 sq cm flask of confluent C6 glial cells, or c) synaptosomes harvested from one hippocampus.

C6 cells, a rat glial tumor cell line, were obtained from American Type Culture Collection (Rockville, MD). Cells were grown in 75 cm^2 flasks (Corning) and maintained at 37°C in a humidified Lunaire incubator (Model BIO 613G, Williamsport, PA) oxygenated with 95% O_2, 5% CO_2. Culture media was composed of (in %) 41.25 Ham's F-10, 41.25 DMEM, 15.0 horse serum, 2.5 fetal bovine serum, and supplemented with 2.96 mg/100 ml penicillin G (GIBCO, Grand Island, NY). Fresh media was added at 24 h after plating and every other day thereafter. Cells were subcultured at 5–7 days at a ratio of 1:3. All C6 cells used in these experiments were from passages 37–46. Preparation for experimental use consisted of detachment with 0.25% trypsinized media, centrifugation at 300g for 15 min, and resuspension of the pellet in 2 ml of control ACSF. Cell preparations were used immediately.

Synaptosomes (P2 fraction) were prepared by selective centrifugation as previously described (Dodd et al., 1981; Gilman et al., 1986). Hippocampal slices were prepared as described above. The hippocampal CA1 field was dissected and placed in 10 volumes of ice-cold 0.32 M sucrose buffered with Tris-HCL, pH 7.4. The tissue was then minced and dispersed using a motor-driven homogenizer. Centrifugation was carried out at 3°C in a Sorvall Superspeed RC2-B centrifuge. The initial homogenate was centrifuged at 3,000g for 10 min to yield a crude nuclear pellet and a low-speed supernatant. The supernatant was transferred and centrifuged at 13,000g for 30 min to yield a synaptosomal pellet (P2 fraction). The supernatant was discarded and the pellet resuspended in 2 ml of control ACSF. The preparation was kept on ice and used within an hour after final centrifugation.

RESULTS

The glial specific metabolic inhibitor fluoroacetate (FAC) decreased synaptic potentials in pyramidal cells in field CA1 of hippocampal slices. At a concentration of 100 μM, FAC gradually depressed evoked PSPs
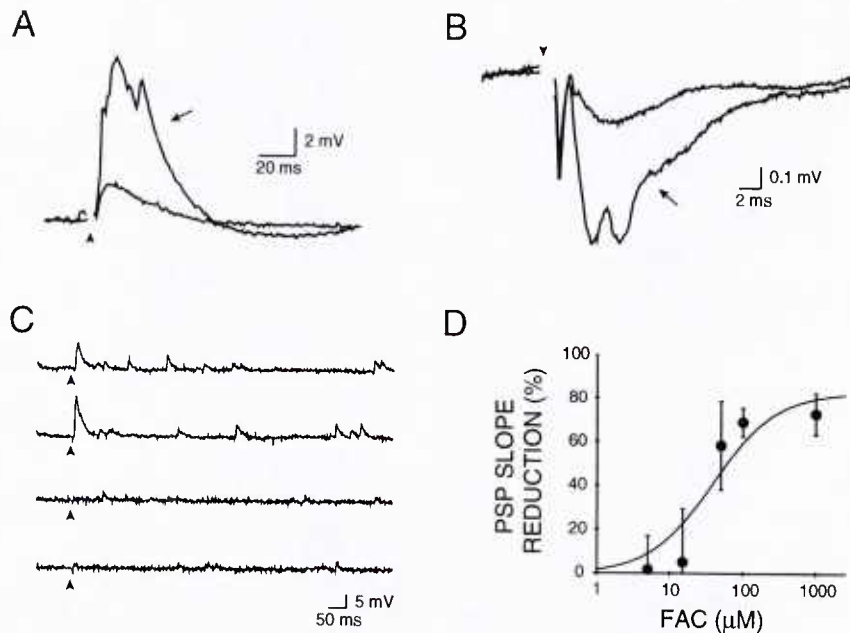
A

B

C

D

Fig. 1. Fluoroacetate inhibits evoked and spontaneous hippocampal neurotransmission through a block in glial metabolism. A: Intracellularly recorded PSPs are inhibited by FAC. Traces are the average of five consecutive PSPs recorded in control ACSF (arrow) and 30 min following application of 100 μM FAC. On this and subsequent traces stimulation artifact has been eliminated for clarity (solid arrow head). Membrane potential = −74 mV. B: FAC reduces field PSPs recorded in CA1 stratum radiatum. Traces are the average of 5 consecutive field PSPs recorded in control (arrow) and 30 min following FAC (100 μM) application. C: Spontaneous as well as evoked PSPs are inhibited by FAC. The top two traces, recorded consecutively, show evoked PSPs and spontaneous PSP activity in control ACSF. The bottom two traces depict the depression of the evoked PSP and the decrease in spontaneous PSP frequency. Membrane potential = −70 mV. D: FAC inhibits PSPs in a dose-dependent manner. Percent reduction in PSP slope, intracellular recording, is plotted against increasing concentrations of fluoroacetate. IC_{50} = 39.0 ± 11.4 μM. Data points are the mean of 4–8 separate experiments ± S.E.M. recorded 30 min following fluoroacetate application and expressed as a percent of control measurements in ACSF. The curve represents the function $y = b * x/(x + a)$ computer fit to the data points where a = the IC_{50} and b = the maximal effect.

(68.9 ± 6.6% decrease; N = 8) with a latency to onset approximately 15–20 min following FAC application. Figure 1A illustrates averaged intracellular recordings of typical evoked PSPs observed in control ACSF (arrow) and following a 30 min application of FAC in a hippocampal slice preparation. Membrane potential (CON = −74.2 ± 1.1 mV; FAC = −73.2 ± 1.2 mV) and membrane resistance (CON = 36.5 ± 3.5 MΩ; FAC = 38.0 ± 3.1 mΩ) of the neurons were not affected. FAC produced a similar decrease in extracellular field potentials recorded in stratum radiatum of field CA1 (Fig. 1B). Intracellularly recorded, spontaneous synaptic activity was attenuated concomitantly with the decline of the evoked PSP (Fig. 1C). The evoked PSP continued to decline through a 30 min wash with control ACSF. Spontaneous synaptic activity frequently recovered, but only partially. FAC (100 μM) was effective in all slice preparations tested (15/15 slices).

The dose-response relationship (Fig. 1D) revealed a sharp concentration dependence of FAC with little alteration in the evoked PSP at 5 μM and maximal depression at 100 μM (IC_{50} = 39.0 ± 11.4 μM). A similar dose-response relationship was observed for recorded field PSPs (IC_{50} = 65.0 ± 11.1 μM; data not shown).

To test the contribution of glial metabolism to the mechanism of FAC-induced PSP depression we pretreated slices with isocitrate (ISO), a metabolic substrate preferentially taken up by glia. ISO was added to control ACSF at a concentration of 1 or 3 mM; 10 mM glucose was present. Since both concentrations of ISO had identical effects, the data have been pooled. ISO had no direct effect on evoked PSPs yet inhibited FAC-induced PSP depression (Fig. 2). In fact, in the presence of ISO, FAC caused a small net increase in PSP slope (43.2 ± 19.4%, N = 6). ISO added to ACSF without glucose was not able to support slice electrophysiology. Glutamine (1 mM), a substrate that is both converted to α-ketoglutarate for entry into the tricarboxylic acid cycle (TCA) cycle and taken up by presynaptic nerve terminals for the production of glutamate, also attenuated FAC-induced PSP depression (8.6 ± 1.8% decrease; N = 3).

The specificity of FAC for glial metabolism was evaluated by measuring ATP concentrations in preparations of glial and neuronal elements. To measure ATP concentration, whole hippocampal slices were incubated in either control ACSF, ACSF plus 1 mM FAC or ACSF plus 1 mM FAC and 3 mM ISO for 30 min at 29–31°C. The metabolic inhibitor was effective in decreasing ATP levels in the slice preparation (Fig. 3). FAC depleted ATP concentration by 35% compared to control slices (P < 0.05). ISO prevented the metabolic effects of FAC just as it had the electrophysiological effects of FAC. Slices incubated in the presence of FAC and ISO showed
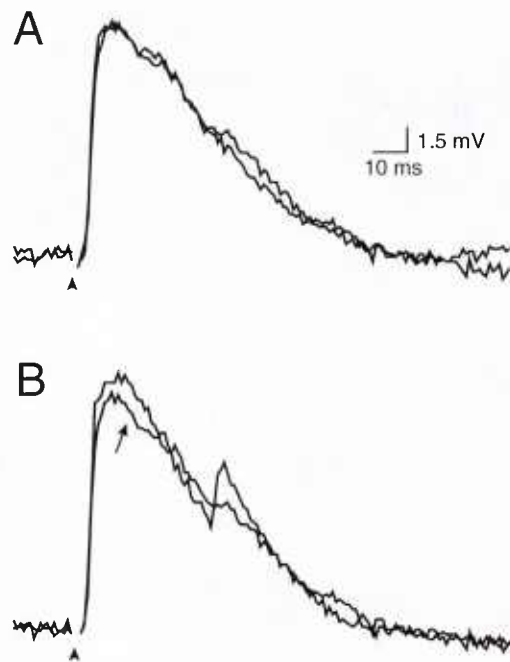
A

1.5 mV

10 ms

B

Fig. 2. Isocitrate pretreatment prevents FAC-induced PSP depression. A: Representative trace from a cell recorded in control ACSF superimposed on a trace recorded following a 30 min application of isocitrate (3 mM). No change is detected. B: Trace recorded following a 30 min application of FAC + ISO (FAC = 100 µM) superimposed on the same control + isocitrate trace shown in A. (arrow). No depression of the PSP is observed. Membrane potential = −69 mV.

A

2 mV

100 ms

B

10 ms

Fig. 4. A: Fluoroacetate does not act postsynaptically. Depicted are single traces, recorded intracellularly, following iontophoretic application (10 ms) of glutamate (0.5 M; retention current 4 nA, ejection current 200 nA) in control ACSF (arrow), and 30 min following application of 100 µM FAC. Fluoroacetate does not alter the peak of the response to glutamate. However, prolongation of the response is evident. Membrane potential = −79 mV. B: FAC prolongs the decay of evoked PSPs. Superimposed are averaged traces from control (arrow) and 30 min following FAC (100 µM) application. The amplitudes of the PSPs have been normalized to illustrate the increase in decay time with FAC. Actual amplitudes are control = 10.3 mV and FAC = 3.7 mV. Membrane potential = −73 mV.
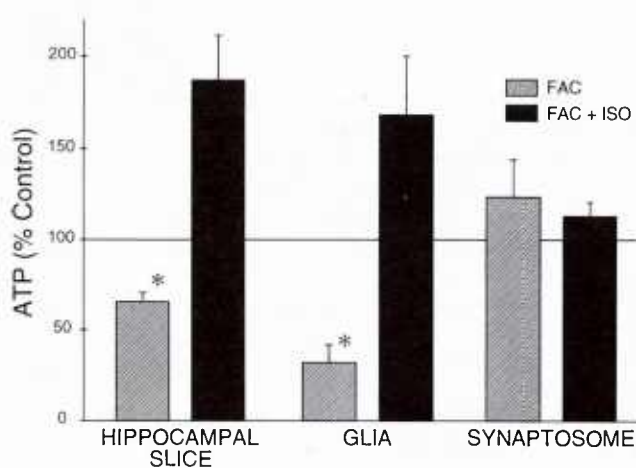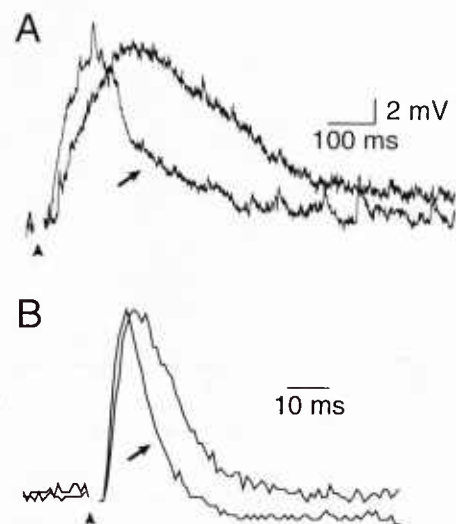

Fig. 3. Fluoroacetate decreases ATP levels in glia in an isocitrate sensitive manner. FAC was applied 30 min prior to the quick freezing of specimens in liquid nitrogen. Isocitrate (ISO) was added 30 min prior to the addition of FAC. Data are presented as percent of control measures. *Significantly different from control (P < 0.05; two-tailed Student's t-test). Control ATP levels were; hippocampal slice = 7.44 ± 2.18 nmol/mg protein, C6 glia = 32.08 ± 6.9 nmol/mg protein, and synaptosomes = 9.78 ± 1.6 nmol/mg protein and agree with previously reported measurements (Crumrine and Lamanna, 1991; Erecinska et al., 1991; Huang et al., 1991; Kass et al., 1992; Whittingham et al., 1989).

an 88% increase in ATP levels (Fig. 3). Similar yet more robust results (Fig. 3) were obtained using C6 cells, a pure glial preparation from a rat astroglial tumor cell line. A 67% decrease in ATP levels was observed in C6 glia treated with FAC (1 mM, P < 0.05) while addition of ISO (3 mM) to the same preparation resulted in a 69% increase. To assess neuronal sensitivity to FAC we measured ATP concentration in synaptosomes prepared from field CA1 of the hippocampus. ATP levels in the synaptosomal preparations were not sensitive to FAC (24% increase) or FAC + ISO (13% increase) suggesting that neuronal elements are not metabolically influenced by either FAC or ISO (Fig. 3).

As a further test of postsynaptic sensitivity to FAC we evaluated 100 µM FAC on postsynaptic responses to iontophoretically applied glutamate in stratum radiatum of CA1. While the evoked PSPs were blocked by FAC, the amplitude of the glutamate response was not altered in seven of seven cells tested (Fig. 4A). However, responses to iontophoretically applied glutamate were prolonged. Iontophoretic responses tended to be very long (i.e., >1 sec) and potentials were recorded for only 900 ms after the iontophoretic pulse. Consequently, while most cells showed at least a decay back to 50% of peak amplitude in that time frame some cells only showed a decay to 70%. Cells were therefore analyzed two ways:

the 90–50% decay time (n = 4) and the 90–70% decay time (n = 6). FAC caused an increase in decay times of 41% (CON = 260.13 ± 64.2 ms; FAC = 367.38 ± 57.6 ms; $P < 0.05$) and 47% (CON = 146.83 ± 27.2 ms; FAC = 220.17 ± 31.9 ms; $P < 0.05$), respectively, for the two groups. Both groups were significantly different using Student's paired t-test, two-tailed. Also of note is that certain iontophoretic responses had slower rise times following FAC treatment (Fig. 4A). Although this could suggest a postsynaptic effect of FAC, many other factors (e.g., changes in cellular morphology or iontophoretic electrode characteristics) could also account for the observed change. Since only a small number of cells exhibited measurable rise times, this was not explored further.

Similar analysis was performed on evoked PSP data. Because of the concomitant decrease in evoked PSP amplitude, the prolongation is evident only with normalization of the peaks (Fig. 4B). The time required for the potential to decay from 90 to 10% of peak amplitude was determined for responses in control and FAC-treated cells. Decay times were prolonged 33% by FAC (CON = 39.29 ± 8.2 ms; FAC = 52.29 ± 5.2 ms; $P < 0.05$; N = 5). The differences were statistically significant using Student's paired t-test, two-tailed. The number of cells in this experimental group is less than the total cells recorded because the PSP remaining after FAC treatment was frequently too small to make an accurate assessment of the 90% and 10% time points.

DISCUSSION

We have shown that FAC impairs synaptic transmission via specific block of glial metabolism without altering neuronal metabolism or postsynaptic sensitivity to neurotransmitter.

The metabolism of glial cells can be selectively inhibited by FAC. This specificity is supported by several lines of evidence. Acetate and citrate are specifically transported into a "small" metabolic compartment (Fonnum, 1985; Hassel et al., 1992; O'Neal and Koeppe, 1966) that has been identified as glial cells (see Fonnum 1985, 1993, for review). The fluorinated analogues, FAC and fluorocitrate, are also taken up into this small compartment where they inhibit the TCA cycle (Clarke et al., 1970; Hassel et al., 1992). After transport into glial cells, FAC is converted to fluorocitrate which is the active inhibitor of aconitase (Clarke, 1991), thereby blocking the TCA cycle at the conversion of citrate to isocitrate and inhibiting ATP production.

Anatomical evidence also supports the specificity of FAC and fluorocitrate for glial cells. With electron microscopy Paulsen et al. (1987) demonstrated morphological damage to glia but not to neurons. An autoradiographic study (Muir et al., 1986) demonstrated that FAC and acetate are localized to the neuropil but are not in the neuronal cell bodies, consistent with glial specific distribution.

Our present results are also consistent with the glial specificity of FAC and ISO. If specific metabolic block and subsequent ATP depletion of glial cells are responsible for the FAC-induced depression of evoked PSPs, then presynaptic and postsynaptic neuronal elements should be insensitive to FAC. Synaptosomes contain the same metabolic constituents found in neuronal somata and reflect neuronal metabolism but the preparation is devoid of intact glial cells. ATP levels were not affected by FAC in synaptosomal preparations while, in C6 glioma cells and hippocampal slices, significant reduction in ATP levels were seen, suggesting that neuronal elements are not metabolically influenced by FAC.

Metabolic substrates that feed into the TCA cycle beyond FAC's site of action should attenuate FAC-induced effects. ISO, with FAC present, does not affect synaptosomal ATP as it does that of C6 glioma cells and hippocampal slices. Both ISO and glutamine, a substrate that is converted to α-ketoglutarate for entry into the TCA cycle, effectively inhibited FAC-induced depression of PSPs. However, since glutamine is also taken up by neurons for glutamate production and can serve to replenish presynaptic glutamate stores, interpretation of the results with this substrate as a stabilization of glial metabolic integrity is tenuous. Further evidence of glial specificity of ISO comes from the observation that ISO, in the absence of glucose, can not support electrophysiological activity in the slice since it can not serve as a metabolic substrate in neurons.

With these pharmacological tools we evaluated glial cell influence on synaptic transmission by selectively eliminating glial activity. Our data demonstrate that functionally intact glial cells are required for normal synaptic transmission.

Metabolic disruption of glial cells and subsequent depletion of ATP stores initiate a cascade of events, any or all of which may contribute to FAC-induced depression of synaptic transmission. Among the potential consequences are 1) decreased production of glutamine, 2) disruption of ionic gradients, 3) accumulation of extracellular glutamate, and 4) morphological changes.

Perhaps the most plausible explanation for the depression of PSPs by FAC is the reduction of glutamate precursor supplied from glial cells to neurons. A decrease in glial ATP levels could reduce glutamate uptake and/or inhibit the energy-dependent metabolism of glutamate to glutamine (Paulsen et al., 1987, 1988; Paulsen and Fonnum, 1989; Szerb and Issekutz, 1987). Block of the glutamine-glutamate cycle would stop the supply of the glutamate precursor to the presynaptic terminal and eventually result in depletion of presynaptic glutamate stores and depression of neurotransmission. Additionally, the glutamine block of FAC-induced PSP depression supports such an hypothesis.

A decrease in glial ATPase activity would perturb ionic homeostasis. Both potassium and sodium gradients would potentially be disrupted by effects on the sodium/potassium ATPase. This would result in a decreased potassium buffering capability and a rise in extracellular potassium concentration. Since no general neuronal depolarization was observed in our system we conclude that potassium concentrations were

not significantly affected. Decreased sodium/potassium ATPase activity would also increase internal sodium concentration, accompanied by internal acidification and swelling of glial cells. However, it has been shown that glial swelling produces an increase in PSP amplitude (Ballyk et al., 1991), opposite to what is observed with FAC application, suggesting that accumulation of internal sodium is not sufficient to produce these changes within the time frame of our present experiments. A reduction in sodium/potassium ATPase activity could also decrease Na^+-dependent glutamate uptake, the predominant glutamate uptake system in glia. The reduction in ATPase activity would reduce the driving force for Na^+-dependent glutamate uptake and, ultimately, reduce the amount of glutamate taken up by glia. It has been shown that FAC and other metabolic inhibitors block glutamate uptake (Szerb and Issekutz, 1987; Szerb and O'Regan, 1984).

As glutamate uptake systems begin to fail glutamate concentrations at the synapse are sustained for longer periods of time. As would be expected with impairment of glial uptake of neurotransmitter (Clements et al., 1992; Korn and Dingledine, 1986; Thompson and Gahwiler, 1992) response decay times of iontophoretic responses to glutamate and the evoked synaptic responses significantly increased following application of FAC. Decreased GABA uptake could also contribute to the prolongation of the PSP observed in the present experiments since inverted inhibitory PSPs contribute to the PSP recorded with KCl electrodes. However, the actions of glutamate are likely to predominate since the contribution of inhibitory PSPs are small when potassium acetate electrodes are used and the prolongation of PSPs was the same regardless of the anion in the electrode.

It is difficult to attribute the FAC-induced depression of the evoked PSPs directly to a slowed removal of glutamate from the extracellular space but secondary consequences could be involved. Prolonged glutamate exposures at the synapse could activate presynaptic glutamate receptors leading to altered neurotransmitter release. Alternatively, desensitization could occur. However, ambient glutamate concentrations were not high enough to cause significant desensitization of postsynaptic glutamate receptors activated by iontophoresis.

An increase in extracellular glutamate concentration would also have direct effects on glial cells. Recent reports indicate that glial cells express a variety of glutamate receptors and respond to glutamate stimulation via classical ionotropic and second messenger pathways (Hansson, 1989; Murphy and Pearce, 1987; von Blankenfeld and Kettenmann, 1991) as well as with distinct changes in morphological structure (Cornell-Bell et al., 1990b; Noble et al., 1992; Wenzel et al., 1991). Glial response to increased glutamate activation may affect neurotransmission via some glial second messenger cascade or by physical disruption of the micro-architecture of the synaptic cleft. Others have reported that glial cells react dynamically to extracellular glutamate. Glial

pseudopodial extension or retraction, which have been reported to be glial responses to glutamate (Cornell-Bell et al., 1990b; Noble et al., 1992; Wenzel et al., 1991), may disrupt glial-neuronal coupling sufficiently to manifest a decrease in synaptic transmission. Further investigations on the coupling of glial cell morphology and synaptic modulation should prove helpful.

Hippocampal synaptic transmission has been the focus of much research in the past decade. Many factors, both presynaptic and postsynaptic, have been identified as important for modulation of synaptic transmission. However, many questions remain unanswered. It is of critical importance to keep in mind that 1) glial cells play an integral role in the maintenance of synaptic transmission and 2) glial cells may be a target for modulation of synaptic activity. It is evident from this work and others that synaptic communication relies heavily on the complex interplay of glial cells and neuronal elements.

ACKNOWLEDGMENTS

REFERENCES

Ballyk, B.A., Quackenbush, S.J., and Andrew, F.D. (1991) Osmotic effects on the CA1 neuronal population in hippocampal slices with special reference to glucose. *J. Neurophysiol.*, 65:1055–1066.

Barres, B.A. (1991) New roles for glia. *J. Neurosci.*, 11:3685–3694.

Clarke, D.D., Nicklas, W.J., and Berl, S. (1970) Tricarboxylic acid-cycle metabolism in brain. *Biochem. J.*, 120:345–351.

Clarke, D.D. (1991) Fluoroacetate and fluorocitrate: Mechanism of action. *Neurochem. Res.*, 16:1055–1058.

Clements, J.D., Lester, R.A.J., Tong, G., Jahr, C.E., and Westbrook, G.L. (1992) The time course of glutamate in the synaptic cleft. *Science*, 258:1498–1501.

Cornell-Bell, A.H., Finkbeiner, S.M., Cooper, M.S., and Smith, S.J. (1990a) Glutamate induces calcium waves in cultured astrocytes: Long-range glial signaling. *Science*, 247:470–473.

Cornell-Bell, A.H., Thomas, P.G., and Smith, S.J. (1990b) The excitatory neurotransmitter glutamate causes filopodia formation in cultured hippocampal astrocytes. *Glia*, 3:322–334.

Cornell-Bell, A.H. and Finkbeiner, S.M. (1991) Ca^{2+} waves in astrocytes. *Cell Calcium*, 12:185–204.

Crumrine, R.C. and Lamanna, J.C. (1991) Regional cerebral metabolites, blood flow, plasma volume, and mean transit time in total cerebral ischemia in the rat. *J. Cereb. Blood Flow Metab.*, 11:272–282.

Dodd, P.R., Hardy, J.A., Oakley, A.E., Edwardson, J.A., Perry, E.K., and Delaunoy, J.P. (1981) A rapid method for preparing synaptosomes: Comparison with alternative procedures. *Brain Res.*, 226:107–118.

Erecinska, M., Troeger, M.B., Wilson, D.F., and Silver, I.A. (1986) The role of glial cells in regulation of neurotransmitter amino acids in the external environment. Il. Mechanism of aspartate transport. *Brain Res.*, 369:203–214.

Erecinska, M. (1990) Metabolism and role of glutamate in mammalian brain. *Prog. Neurobiol.,* 35:245–296.

Erecinska, M., Dagani, F., Nelson, D., Deas, J., and Silver, I.A. (1991) Relations between intracellular ions and energy metabolism: A study with monensin in synaptosomes, neurons, and C6 glioma cells. *J. Neurosci.,* 11:2410–2421.

Finkbeiner, S. (1992) Calcium Waves in Astrocytes: Filling in the Gaps. *Neuron,* 8:1101–1108.

Fonnum, F. (1985) Determination of transmitter amino acid turnover. In: *Neuromethods: Amino Acids.* Boulton, A.A., Baker, G.B. and Wood, J.D., eds: Humana Press, Clifton, N.J., pp. 201–237.

Fonnum, F. (1993) Regulation of the synthesis of the transmitter glutamate pool. *Prog. Biophys. Molec. Biol.,* 60:47–57.

Gilman, S.C., Kumaroo, K.K., and Kallenbeck, J.M. (1986) Effects of pressure on uptake and release of calcium by brain synaptosomes. *J. Appl. Physiol.,* 60:1446–1450.

Hansson, E. (1989) Co-existence between receptors, carriers, and second messengers on astrocytes grown in primary cultures. *Neurochem. Res.,* 14:811–819.

Hassel, B., Paulsen, R.E., Johnsen, A., and Fonnum, F. (1992) Selective inhibition of glial cell metabolism in vivo by fluorocitrate. *Brain Res.,* 576:120–124.

Hatten, M.E. (1990) Riding the glial monorail: A common mechanism for glial-guided neuronal migration in different regions of the developing mammalian brain. *Trends Neurosci.,* 13:179–184.

Hatten, M.E. and Mason, C.A. (1990) Mechanisms of glial-guided neuronal migration in vitro and in vivo. *Experientia,* 46:907–916.

Huang, H.M., Toralbarza, L., and Gibson, G. (1991) Cytosolic free calcium and ATP in synaptosomes after ischemia. *Life Sci.,* 48:1439–1445.

Kass, I.S., Abramowicz, A.E., Cottrell, J.E., and Chambers, G. (1992) The barbiturate thiopental reduces ATP levels during anoxia but improves electrophysiological recovery and ionic homeostasis in the rat hippocampal slice. *Neuroscience,* 49:537–543.

Kollegger, H., Mcbean, G.J., and Tipton, K.F. (1991) The inhibition of glutamine synthetase in rat corpus striatum in vitro by methionine sulfoximine increases the neurotoxic effects of kainate and N-methyl-D-aspartate. *Neurosci. Lett.,* 130:95–98.

Korn, S.J. and Dingledine, R. (1986) Inhibition of GABA uptake in the rat hippocampal slice. *Brain Res.,* 368:247–255.

Krysotek, A. and Seeds, N.W. (1981) Plasminogen activator release at the neuronal growth cone. *Science,* 213:1532–1534.

Martin, D.L. (1992) Synthesis and release of neuroactive substances by glial cells. *Glia,* 5:81–94.

Moonen, G., Grau-Wagemans, M.P., and Selak, I. (1982) Plasminogen activator-plasmin system and neuronal migration. *Nature,* 298:753–755.

Muir, D., Berl, S., and Clarke, D.D. (1986) Acetate and fluoroacetate as possible markers for glial metabolism in vivo. *Brain Res.,* 380:336–340.

Murphy, S. and Pearce, B. (1987) Functional receptors for neurotransmitters on astroglial cells. *Neuroscience,* 22:381–394.

Noble, L.J., Hall, J.J., Chen, S., and Chan, P.H. (1992) Morphologic changes in cultured astrocytes after exposure to glutamate. *J. Neurotrauma,* 9:255–267.

O'Neal, R.M. and Koeppe, R.E. (1966) Precursors in vivo of glutamate, aspartate and their derivatives of rat brain. *J. Neurochem.,* 13:835–847,

Paulsen, R.E., Contestabile, A., Villani, L., and Fonnum, F. (1987) An in vivo model for studying function of brain tissue temporarily devoid of glial cell metabolism: The use of fluorocitrate. *J. Neurochem.,* 48:1377–1385.

Paulsen, R.E., Contestabile, A., Villani, L., and Fonnum, F. (1988) The effect of fluorocitrate on transmitter amino acid release from rat striatal slices. *Neurochem. Res.,* 13:637–641.

Paulsen, R.E. and Fonnum, F. (1989) Role of glial cells for the basal and Ca^{2+}-dependent K^+-evoked release of transmitter amino acids investigated by microdialysis. *J. Neurochem.,* 52:1823–1829.

Pellmar, T.C. (1987) Peroxide alters neuronal excitability in the CA1 region of guinea-pig hippocampus in vitro. *Neuroscience,* 23:447–456.

Schousboe, A., Svenneby, G., and Hertz, L. (1977) Uptake and metabolism of glutamate in astrocytes cultured from dissociated mouse brain hemispheres. *J. Neurochem.,* 29:999–1005.

Szerb, J.C. and Issekutz, B. (1987) Increase in the stimulation-induced overflow of glutamate by fluoroacetate, a selective inhibitor of the glial tricarboxylic cycle. *Brain Res.,* 410:116–120.

Szerb, J.C. and O'Regan, P.A. (1984) Glutamine enhances glutamate release in preference to gamma-aminobutyrate. *Can. J. Physiol. Pharmacol.,* 62:919–923.

Thompson, S.M. and Gahwiler, B.H. (1992) Effects of the GABA uptake inhibitor tiagabine on inhibitory synaptic potentials in rat hippocampal slice cultures. *J. Neurophysiol.,* 67:1698–1701.

von Blankenfeld, G. and Kettenmann, H. (1991) Glutamate and GABA receptors in vertebrate glial cells. *Mol. Neurobiol.,* 5:31–43.

Walz, W. (1989) Role of glial cells in the regulation of the brain ion microenvironment. *Prog. Neurobiol.,* 33:309–333.

Wenzel, J., Lammert, G., Meyer, U., and Krug, M. (1991) The influence of long-term potentiation on the spatial relationship between astrocyte processes and potentiated synapses in the dentate gyrus neuropil of rat brain. *Brain Res.,* 560:122–131.

Whittingham, T.S., Warman, E., Assaf, H., Sick, T.J., and Lamanna, J.C. (1989) Manipulating the intracellular environment of hippocampal slices: pH and high-energy phosphates. *J. Neurosci. Methods,* 28:83–91.

7

Single and Combination Cytokine Therapies for Treatment of Radiation-induced Hematopoietic Injury: Effects of *c-kit* Ligand and Interleukin-3

M.L. PATCHEN[1], R. FISCHER[1], T.J. MACVITTIE[1], F. SEILER[2] AND D.E. WILLIAMS[3]

[1]*Department of Experimental Hematology, Armed Forces Radiobiology Research Institute, 8901 Wisconsin Avenue, Bethesda, MD 20889-5603, USA,* [2]*Research Laboratories of Behringwerke AG, Marburg, Germany, and* [3]*Immunex Corporation, Seattle, WA, USA*

Abstract

Following radiation exposures, severe hematopoietic depression can result from injury to hematopoietic stem and progenitor cell populations. In recent years, a variety of recombinant cytokines have been demonstrated to possess hematopoietic activity. While some cytokines are lineage restricted in their activity, others such as *c-kit* ligand and interleukin-3 (IL-3) appear to be capable of affecting early multilineage hematopoietic cell populations. Using a $B_6D_2F_1$ murine model of severe ^{60}Co radiation-induced hematopoietic hypoplasia, we have evaluated the ability of *c-kit* ligand (recombinant murine mast cell growth factor; rmMGF) and rmIL-3 to accelerate hematopoietic regeneration when administered either alone or in combination following radiation exposure. Hematopoietic regeneration was based on spleen and bone marrow spleen colony forming unit (CFU-s$_{12}$) and granulocyte-macrophage progenitor cell (GM-CFC) recoveries. MGF alone, administered subcutaneously (s.c) on days 1–17 postirradiation at 100 μg/kg/day or 200 μg/kg/day, accelerated bone marrow and splenic GM-CFC as well as splenic CFU-s recoveries in a direct dose-dependent manner. IL-3 alone (100 μg/kg/day, s.c. on days 1–17)

also accelerated splenic GM-CFC and CFU-s recoveries. When these cytokines were co-administered (100 µg/kg/day each, s.c. on days 1–17), GM-CFC and CFU-s recoveries greater than those produced by either cytokine alone were observed. These studies illustrate a potential role for combined MGF and IL-3 in the treatment of radiation-induced hematopoietic injury.

Introduction

One of the most recent cytokines implicated in hematopoietic regulation is c-*kit* ligand, also known as mast cell growth factor (MGF), steel factor (SLF), and stem cell factor (SCF) (1–3). The c-*kit* ligand has been ascribed numerous hematopoietic and nonhematopoietic effects, although it was initially identified and purified based on its ability to stimulate mast cell growth (2–5). Multiple studies have focused on the *in vitro* effects of this factor, demonstrating that alone it has limited hematopoietic activity, but when combined with other hematopoietic cytokines, it synergizes to increase both the number and size of colonies generated from hematopoietic progenitors (3–11), and in some instances, to increase the replating potential of primitive progenitors (12). Furthermore, in combination with such factors, c-*kit* ligand also synergistically enhances the *in vitro* expansion of hematopoietic progenitors grown in liquid cultures (13–15). These effects are thought to result not only from the ability of c-*kit* ligand to potentiate progenitor cell proliferation but also from its ability to enhance progenitor cell survival (14,16).

IL-3, also known as multi-CSF, has previously been shown to enhance hematopoietic regeneration in irradiated animals based on recovery of peripheral blood white cells and platelets (17). Because *in vitro* studies have demonstrated synergistic hematopoietic stimulation produced by c-*kit* ligand combined with IL-3, we evaluated whether co-administration of these cytokines *in vivo* would synergize to further accelerate hematopoietic regeneration following radiation-induced hematopoietic hypoplasia.

Materials and methods

Cytokines

Recombinant murine c-*kit* ligand (MGF), was provided by Immunex (Seattle, WA). Recombinant murine IL-3 was provided by Behringwerke AG (Marburg, Germany). Cytokines were expressed in yeast and purified to homogeneity as previously described (10,18). Endotoxin contamination of cytokines was below the limit of detection using the Limulus amebocyte lysate assay. MGF was administered subcutaneously (s.c.) in a 0.1 ml volume at the dose of 100 or 200 µg/kg; IL-3 was administered s.c. at the dose of 100 µg/kg. In combination studies, mice received each cytokine at a separate injection site. All injections

were initiated 1 day following irradiation and continued daily for 17 days. Control mice were injected with an equal volume of sterile saline.

MICE

$B_6D_2F_1$ female mice (~20 g) were purchased from Jackson Laboratories (Bar Harbor, ME). Mice were maintained in an AAALAC (American Association for Accreditation of Laboratory Animal Care) accredited facility in Micro-Isolator cages on hardwood-chip contact bedding and were provided commercial rodent chow and acidified water (Ph 2.5) *ad libitum*. Animal rooms were equipped with full-spectrum light from 6 a.m. to 6 p.m. and were maintained at 70°F +/– 2°F with 50% +/– 10% relative humidity using at least 10 air changes per hour of 100% conditioned fresh air. Upon arrival, all mice were tested for *Pseudomonas* and quarantined until test results were obtained. Only healthy mice were released for experimentation. All animal experiments were approved by the Institute Animal Care and Use Committee prior to performance.

IRRADIATION

The ^{60}Co source at the Armed Forces Radiobiology Research Institute was used to administer bilateral total-body gamma radiation. Mice were placed in ventilated Plexiglas containers and irradiated with 7.75 Gy at a dose rate of 0.4 Gy/min. Dosimetry was performed using ionization chambers (19) with calibration factors traceable to the National Institute of Standards and Technology. The tissue-to-air ratio was determined to be 0.96. Dose variation within the exposure field was < 3%.

CELL SUSPENSIONS

Cell suspensions for each assay represented tissues from three normal, irradiated, or irradiated and cytokine-treated mice at each time point. Cells were flushed from femurs with 3 ml of McCoy's 5A medium (Flow Labs, McLean, VA) containing 10% heat-inactivated fetal bovine serum (Hyclone Labs, Logan, UT). Spleens were pressed through a stainless steel mesh screen, and the cells were washed from the screen with 6 ml medium. The number of nucleated cells in the suspensions was determined by Coulter counter. Femurs and spleens were removed from mice euthanized by cervical dislocation.

SPLEEN COLONY FORMING UNIT ASSAY

Exogenous spleen colony forming units (CFU-s) were evaluated by the method of Till and McCulloch (20). Recipient mice were exposed to 9 Gy of total-body radiation to reduce endogenous hematopoietic stem cells. Bone marrow or

spleen cells were intravenously (i.v.) injected into the irradiated recipients 3-5 h later. Twelve days after transplantation, the recipients were euthanized by cervical dislocation, and their spleens were removed. The spleens were fixed in Bouin's solution, and grossly visible spleen colonies were counted. Each treatment group consisted of five mice.

GRANULOCYTE-MACROPHAGE COLONY-FORMING CELL ASSAY

Hematopoietic progenitor cells committed to granulocyte and/or macrophage development were assayed using a double-layer agar granulocyte-macrophage colony forming cell (GM-CFC) assay in which mouse endotoxin serum (5% v/v) was added to feeder layers as a source of colony stimulating factors (21). Colonies (> 50 cells) were counted after 10 days of incubation in a 37°C humidified environment containing 5% CO_2. Triplicate plates were cultured for each cell suspension.

STATISTICS

Results of replicate experiments were pooled and are represented as the mean +/- standard error (SE) of pooled data. Statistical differences were determined by Behrens-Fisher t-test analysis. Significance level was set at $p < 0.05$.
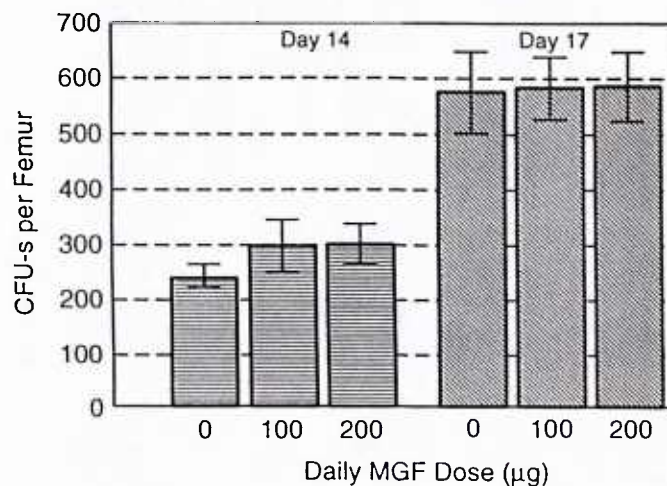
Results

The ability to accelerate hematopoietic regeneration in a murine model of severe radiation-induced hematopoietic hypoplasia was used to evaluate the potential of MGF and IL-3 to induce hematopoietic progenitor cell expansion *in vivo*. In preliminary studies, it was determined that a sublethal 7.75 Gy ^{60}Co radiation exposure induced severe hematopoietic hypoplasia from which recovery (especially in the spleen) became evident between days 14 and 17 post-irradiation (Figure 7.1). Based on these preliminary studies, subsequent studies evaluating the ability of cytokines to accelerate hematopoietic recovery focused on evaluation of bone marrow and splenic CFU-s and GM-CFC recoveries on days 14 and 17 post-irradiation.

The effects of MGF on CFU-s and GM-CFC recoveries in sublethally irradiated mice are illustrated in Figure 7.2 and Figure 7.3, respectively. At either the 100 µg/kg/day or 200 µg/kg/day dose, MGF alone accelerated bone marrow and splenic GM-CFC recovery. The 200 µg/kg/day MGF dose also accelerated splenic CFU-s recovery; however, no effect on bone marrow CFU-s recovery was observed at either MGF dose. Following administration of IL-3 alone, both splenic CFU-s (Figure 7.4B) and GM-CFC (Figure 7.5B) numbers were increased compared to saline-treated mice by day 17 postirradiation. No
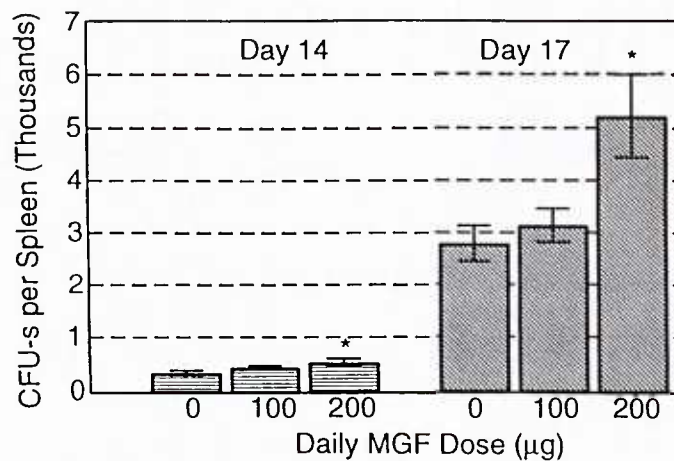
Figure 7.1   Hematopoietic suppression and recovery following a sublethal 7.75 Gy ^{60}Co radiation exposure in $B_6D_2F_1$ mice.
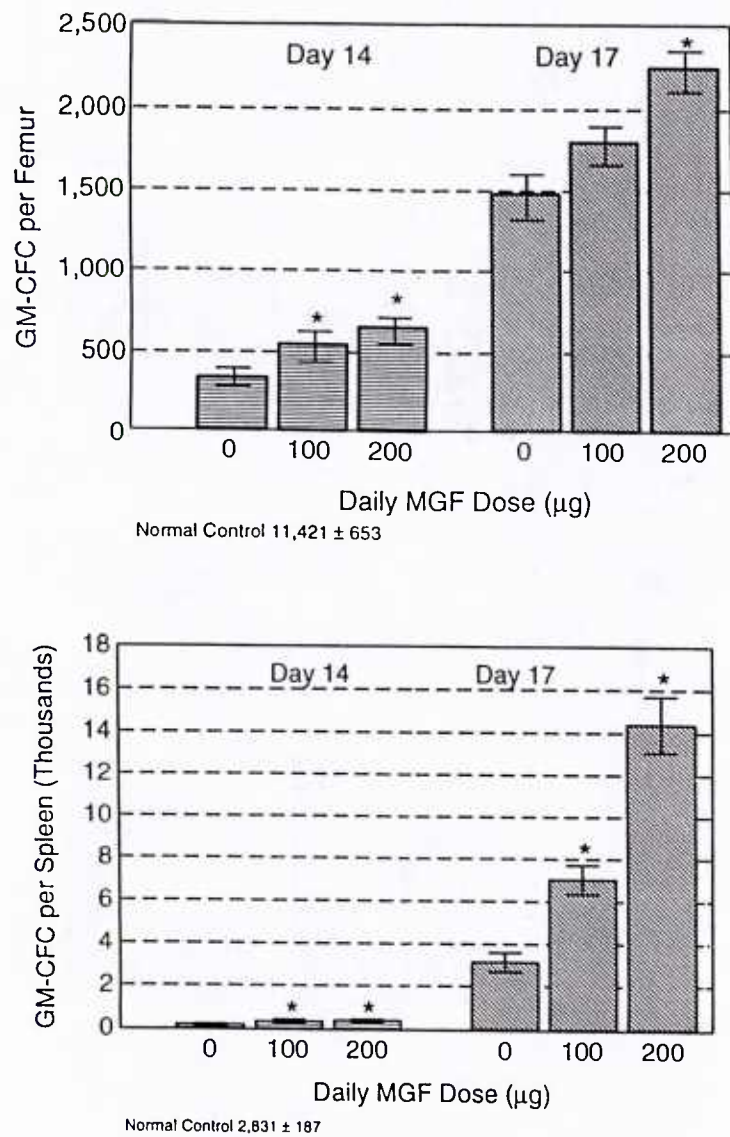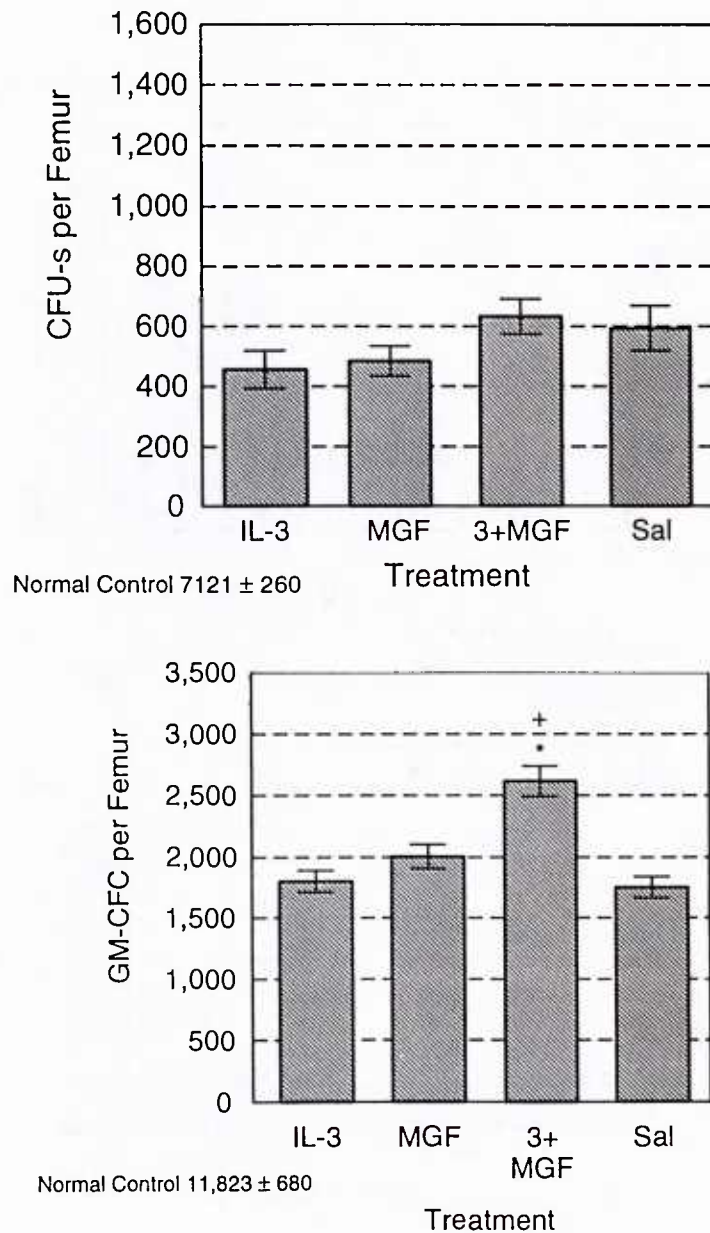
Normal Control 7,223 ± 150

Normal Control 2,722 ± 100

Figure 7.2   Effects of MGF administration (100 or 200 $\mu g/kg/day$, x17 day, s.c.) on bone marrow (A) and splenic (B) CFU-s recovery on days 14 and 17 after a 7.75 Gy radiation exposure in $B_6D_2F_1$ mice. Mean +/- SE; * $p < 0.05$, with respect to saline controls.

Normal Control 11,421 ± 653
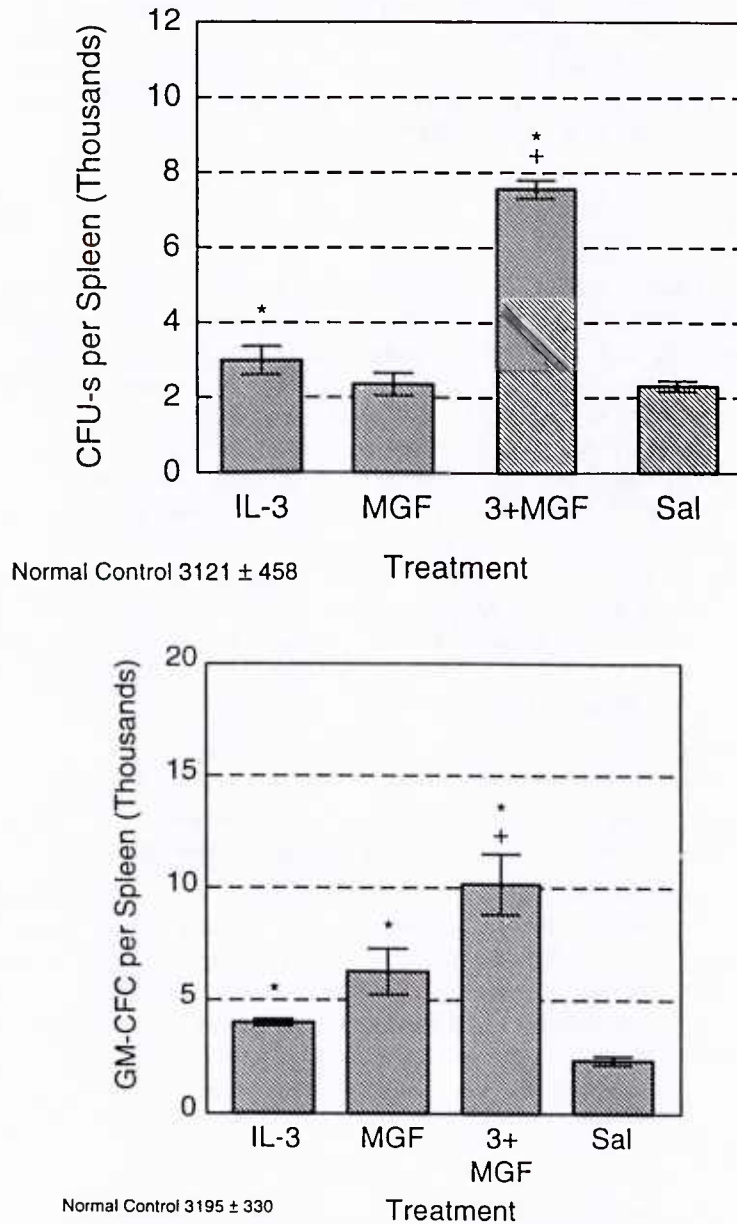

Normal Control 2,831 ± 187

Figure 7.3 Effects of MGF administration (100 or 200 µg/kg/day, x17 day, s.c.) on bone marrow (A) and splenic (B) GM-CFC recovery on days 14 and 17 after a 7.75 Gy radiation exposure in $B_6D_2F_1$ mice. Mean +/- SE; * $p < 0.05$, with respect to saline controls.

Figure 7.4 Effects of IL-3, MGF, and MGF plus IL-3 (each 100 µg/kg/day, x17 day, s.c.) on bone marrow (A) and splenic (B) CFU-s recovery on day 17 after a 7.75 Gy radiation exposure in $B_6D_2F_1$ mice. Mean +/- SE; * $p < 0.05$, with respect to saline controls; + $p < 0.05$, with respect to IL-3 values.

Normal Control 3121 ± 458

Normal Control 3195 ± 330

Figure 7.5 Effects of IL-3, MGF, and MGF plus IL-3 (each 100 µg/kg/day, x17 day, s.c.) on bone marrow (A) and splenic (B) GM-CFC recovery on day 17 after a 7.75 Gy radiation exposure in $B_6D_2F_1$ mice. Mean +/- SE; * $p < 0.05$, with respect to saline controls; + $p < 0.05$, with respect to MGF values.

IL-3 effects, however, were observed on bone marrow recovery. When MGF was administered to sublethally irradiated mice in combination with IL-3, CFU-s (Figure 7.4) and GM-CFC (Figure 7.5) recoveries greater than those induced by MGF alone or IL-3 alone were observed, with splenic effects being more dramatic than bone marrow effects.

Discussion

Sustained hematopoietic recovery following chemotherapy or radiation exposure requires surviving pluripotent stem cells to self-renew as well as to differentiate into multipotent and committed progenitors capable of giving rise to functional mature cells. In recent years, administration of single hematopoietic growth factors, including G-CSF, GM-CSF, MGF, and IL-6, has been shown to stimulate hematopoietic regeneration following radiation- or chemotherapy-induced myelosuppression. In addition, some cytokine combinations, such as GM-CSF plus IL-3, have proven to surpass the effectiveness of single agents. Because c-*kit* ligand, *in vitro*, has been shown to synergize with IL-3 in stimulating progenitor cell proliferation and expansion, we hypothesized that administration of MGF in combination with this cytokine *in vivo* may further improve hematopoietic regeneration beyond that obtained with only MGF or only IL-3.

Our studies demonstrate that in irradiated mice:

1. MGF alone can accelerate hematopoietic regeneration,
2. IL-3 alone can also accelerate hematopoietic regeneration, and
3. when MGF and IL-3 are co-administered, hematopoietic recovery greater than that produced by either single cytokine can be obtained.

It remains to be determined whether the apparent lack of effect of MGF, IL-3, or the combination of these cytokines on bone marrow CFU-s regeneration concomitant with significant splenic CFU-s regeneration may be due to cytokine mediated bone marrow CFU-s mobilization. In spite of this, these studies suggest a potential role for combined MGF plus IL-3 in the treatment of hematopoietic hypoplasia.

References

1. Witte ON. *Steel* locus defines new multipotent growth factor. *Cell* **63**:5, 1990
2. Williams DE, Eisenman J, Baird A, Rauch C, Van Ness K, March CJ, Park LS, Martin U, Mochizuki DY, Boswell HS, Burgess GS, Cosman D, Lyman SD. Identification of a ligand for the c-*kit* proto-oncogene. *Cell* **63**:167, 1990
3. Zsebo KM, Wypych J, McNeice IK, Lu HS, Smith KA, Karkare SB, Sachdev RK, Yuschenkoff VN, Brikett NC, Williams LR, Satyagal VN, Tung W, Bosselman RA,

Mendiaz EA, Langley KE. Identification, purification, and biological characterization of hematopoietic stem cell factor from buffalo rat liver-conditioned medium. *Cell* **63**:195, 1990

4. Nocka K, Buck J, Levi E, Besmer P. Candidate ligand for the c-*kit* transmembrane kinase receptor: KL, a fibroblast derived growth factor stimulates mast cells and erythroid progenitors. *EMBO J* **9**:3287, 1990

5. Williams DE, DeVries P, Namen AE, Widmer MB, Lyman SD. The *Steel* factor. *Develop Biol* **151**:368, 1992

6. Martin FH, Suggs SV, Langley KE, Lu HS, Ting J, Okino KH, Morris F, McNeice IK, Jacobsen FW, Mendiaz EA, Birkett NC, Smith KA, Johnson MJ, Parker VP, Flores JC, Patel AC, Fischer EF, Erjavec HO, Herrera CJ, Wypych J, Sachdev RK, Pope JA, Leslie I, Wen D, Lin CH, Cupples RL, Zsebo KM. Primary structure and functional expression of rat and human stem cell factor DNAs. *Cell* **63**:203, 1990

7. McNeice IK, Langley KE, Zsebo KM. Recombinant human stem cell factor synergizes with GM-CSF, G-CSF, IL-3, and Epo to stimulate human progenitor cells of the myeloid and erythroid lineages. *Exp Hematol* **19**:226, 1991

8. Broxmeyer HA, Hangoc G, Cooper S, Anderson D, Cosman D, Lyman SD, Williams DE. Influence of murine mast cell growth factor (c-*kit* ligand) on colony formation by mouse marrow hematopoietic progenitor cells. *Exp Hematol* **19**:143, 1991

9. Williams N, Bertoncello I, Kavnoudias H, Zsebo KM, McNeice I. Recombinant rat stem cell factor stimulates the amplification and differentiation of fractionated mouse stem cell populations. *Blood* **79**:58, 1992

10. Anderson DM, Lyman SD, Baird A, Wingnall JM, Eisenman J, Rauch C, March CJ, Boswell S, Gimpel SD, Cosman D, Williams DE. Molecular cloning of mast cell growth factor, a hematopoietin that is active in both membrane bound and soluble forms. *Cell* **63**:235, 1990

11. deVires P, Brasel KA, Eisenman JR, Alpert AR, Williams DE. The effect of recombinant mast cell growth factor on purified murine hematopoietic stem cells. *J Exp Med* **173**:1205, 1991

12. Carow CE, Hangoc G, Cooper SH, Williams DE, Broxmeyer HE. Mast cell growth factor (c-*kit* ligand) supports the growth of human multipotential progenitor cells with a high replating potential. *Blood* **78**:2216, 1991

13. Moore MAS. Clinical implications of positive and negative hematopoietic stem cell regulators. *Blood* **78**:1, 1991

14. Bernstein ID, Andrews RG, Zsebo KM. Recombinant human stem cell factor enhances the formation of colonies by CD34+ and CD34+Lin– cells, and the generation of colony-forming cell progeny from CD34+Lin– cells cultured with interleukin-3, granulocyte colony-stimulating factor, or granulocyte-macrophage colony-stimulating factor. *Blood* **77**:2316, 1991

15. Brandt J, Briddell RA, Srour EF, Leemhuis TB, Hoffman R. The role of c-*kit* ligand in the expansion of human hematopoietic progenitor cells. *Blood* **79**:634, 1992

16. Heyworth CM, Whetton AD, Nicholls S, Zsebo K, Dexter TM. Stem cell factor directly stimulates the development of enriched granulocyte-macrophage colony-forming cells and promotes the effects of other colony-stimulating factors. *Blood* **80**:2230, 1992

17. MacVittie TJ, Monroy RL, Farese AM, Patchen ML, Seiler FR, Williams DE. Cytokine therapy in canine and primate models of radiation-induced marrow aplasia. *Behring Inst Mitt* **90**:1, 1991

18. Urdal DL, Mochizuki D, Conlon PJ, March CJ, Remerowski ML, Eisenmann J, Ramthun C, Gillis S. Lymphokine purification by reversed phase high performance liquid chromatography. *J Chromatogr* **296**:171, 1984

19. Schulz J, Almond PR, Cunningham JR, Holt JG, Loevinger R, Suntharalingam N, Wright KA, Nath R, Lempert D. A protocol for the determination of absorbed dose for high energy photon and electron beams. *Med Phys* **10**:741, 1983
20. Till JE, McCulloch EA. A direct measurement of the radiation sensitivity of normal mouse bone marrow cells. *Radiat Res* **14**:213, 1961
21. Patchen ML, MacVittie TJ. Hematopoietic effects of intravenous soluble glucan administration. *J Immunopharmacol* **8**:407, 1986

**Experimental
Hematology**

Mast cell growth factor enhances multilineage hematopoietic recovery in vivo following radiation-induced aplasia

M.L. Patchen,[1] R. Fischer,[1] E.A. Schmauder-Chock,[1] D.E. Williams[2]

[1]Department of Experimental Hematology, Armed Forces Radiobiology Research Institute, Bethesda, MD;
[2]Immunex Corporation, Seattle, WA

Offprint requests to: Dr. Myra L. Patchen, Department of Experimental Hematology, Armed Forces Radiobiology Research Institute, 8901 Wisconsin Avenue, Bethesda, MD 20889-S603

Abstract

Based on in vitro studies, mast cell growth factor (MGF; also known as steel factor, stem cell factor, and c-*kit* ligand) has been implicated as an important hematopoietic regulator, especially in the presence of additional hematopoietic cytokines. Since hematopoietic regeneration follows sublethal radiation–induced hematopoietic injury and is thought to be mediated by endogenously produced cytokines, the ability to accelerate recovery from radiation-induced hematopoietic hypoplasia was used to evaluate in vivo effects of MGF administration. Female $B_6D_2F_1$ mice were exposed to a sublethal 7.7S-Gy dose of ^{60}Co radiation followed by subcutaneous administration of either saline or 100, 200, or 400 µg/kg/d recombinant murine MGF on days 1 to 17 postirradiation. Recoveries of bone marrow and splenic spleen colony-forming units (CFU-S), granulocyte-macrophage colony-forming cells (GM-CFC), and peripheral white blood cells (WBC), red blood cells (RBC), and platelets (PLT) were determined on days 14 and 17 during the postirradiation recovery period. MGF accelerated hematopoietic recovery at the 100 and 200 µg/kg/d doses. The 100 µg/kg/d dose accelerated recovery of only GM-CFC, while the 200 µg/kg/d dose accelerated CFU-S, GM-CFC, WBC, and PLT recoveries. In contrast, hematopoietic recovery was delayed in mice receiving the 400 µg/kg/d dose. These studies demonstrate the in vivo dose-dependent ability of MGF to accelerate multilineage hematopoietic regeneration following radiation-induced hematopoietic hypoplasia. They also document detrimental effects of providing "supraoptimal" doses of this growth factor and suggest caution in dose-escalation trials in humans.

Key words: MGF—Irradiation—Aplasia—c-*kit* ligand—Therapy—Stem cells—Stem cell factor

Introduction

Neutropenia and thrombocytopenia are major factors contributing to morbidity and mortality associated with hematopoietic injury. Agents capable of enhancing regeneration of cellular elements necessary for efficient host defense mechanisms and facilitating hematopoietic hemostasis would be useful in treating hematopoietic hypoplasia caused by accidental radiation exposures, radiotherapy, and chemotherapy.

Hematopoietic proliferation and differentiation are known to be regulated by a variety of colony-stimulating factors and interleukins [1,2]. Mast cell growth factor (MGF), also known as steel factor (SLF), stem cell factor (SCF), and c-*kit* ligand, is the most recent cytokine implicated in hematopoietic regulation [3–S]. This factor was initially identified and purified based on its ability to stimulate mast cell growth; however, it has subsequently been ascribed numerous hematopoietic and nonhematopoietic effects [4–7].

In vitro, c-*kit* ligand has been shown to synergize with numerous hematopoietic cytokines, including granulocyte colony-stimulating factor (G-CSF), granulocyte-macrophage colony-stimulating factor (GM-CSF), interleukin-1 (IL-1), IL-3, IL-6, IL-7, and erythropoietin (Epo) [S–19]. The observations that c-*kit* ligand in combination with other cytokines appears to generate large numbers of both committed colony-forming cells (CFC) and pre-CFC suggest that this factor may act earlier than other hematopoietic factors described to date.

c-*kit* ligand has also been implicated in hematopoietic regulation in vivo. Most notably, mice with mutations at the *Steel* (*Sl*) locus, which encodes c-*kit* ligand, are defective in hematopoietic cell development, exhibiting severe macrocytic anemia that is resistant to erythropoietin treatment [20], profound deficiencies in tissue mast cells [21], abnormalities in megakaryocytopoiesis [22], and reduced granulocytopoiesis [23]. The hematopoietic defects in *Steel* mice can be partially corrected by the administration of c-*kit* ligand [24]. In addition to the data accumulated on *Steel* mice, a limited number of studies have recently reported the ability of c-*kit* ligand to alter hematopoiesis in normal mice, rats, and nonhuman primates [2S–27]. In rats, a single intravenous (IV) injection of recombinant rat (rr) c-*kit* ligand induced a rapid and transient neutrophilia and lymphocytosis; prolonged (14-day) administration resulted in bone marrow mast cell hyperplasia but erythroid and lymphoid hypoplasia [25]. When rr c-*kit* ligand was administered daily for 21 days in mice, it was found to be only a modest stimulator of peripheral blood neutrophil production but a potent stimulator of splenic CFU-S production [26]. In baboons, continuous infusion of recombinant human (rh) c-*kit* ligand caused an increase in peripheral blood erythrocyte, neutrophil, lymphocyte, monocyte, eosinophil, and basophil numbers, as well as an increase in bone marrow cellularity, GM-CFC, and erythroid burst-forming units (BFU-E) [27].

In contrast to previous studies performed with c-*kit* ligand in normal animals, we have evaluated the ability of this factor to stimulate hematopoiesis in the more clinically relevant condition of hematopoietic hypoplasia. Because hematopoietic recovery in the sublethal murine radiation model used in our studies is presumed to be mediated by endogenously produced hematopoietic cytokines [28,29], and because c-*kit* ligand has been shown to synergize with other cytokines, we hypothesized that c-*kit* ligand may synergize

with endogenous cytokines in irradiated mice and accelerate hematopoietic recovery.

Materials and methods

MGF
Recombinant murine c-*kit* ligand, henceforth referred to as MGF, was provided by Immunex (Seattle, WA). It was expressed in yeast and purified to homogeneity as previously described [12]. Endotoxin contamination was below the limit of detection using the limulus amebocyte lysate assay. MGF was administered subcutaneously (s.c.) in a 0.1-mL volume at doses of 100, 200, or 400 μg/kg. Injections were initiated 1 day following irradiation and continued daily for 17 days. Control mice were injected with an equal volume of sterile saline.

Mice
$B_6D_2F_1$ female mice (~20 g) were purchased from Jackson Laboratories (Bar Harbor, ME). Mice were maintained in a facility accredited by the American Association for Accreditation of Laboratory Animal Care (AAALAC) in Micro-Isolator cages on hardwood-chip contact bedding and were provided with commercial rodent chow and acidified water (pH 2.5) ad libitum. Animal rooms were equipped with full-spectrum light from 6 a.m. to 6 p.m. and were maintained at $21 \pm 1°C$ with $50 \pm 10\%$ relative humidity using at least 10 air changes per hour of 100% conditioned fresh air. On arrival, all mice were tested for *Pseudomonas* and quarantined until test results were obtained. Only healthy mice were released for experimentation. All animal experiments were approved by the Institute Animal Care and Use Committee.

Irradiation
The ^{60}Co source at the Armed Forces Radiobiology Research Institute was used to administer bilateral total-body gamma radiation. Mice were placed in ventilated Plexiglas containers and irradiated with 7.75 Gy at a dose rate of 0.4 Gy/min. Dosimetry was performed using ionization chambers [30] with calibration factors traceable to the National Institute of Standards and Technology. The tissue-to-air ratio was 0.96. Dose variation within the exposure field was <3%.

Peripheral blood cell counts
Blood was obtained from halothane-anesthetized mice by cardiac puncture using a heparinized syringe attached to a 20-gauge needle. WBC, RBC, and PLT counts were performed using a Coulter counter.

Cell suspensions
Cell suspensions for each assay represented tissues from three normal, irradiated, or irradiated-plus-MGF-treated mice at each time point. Cells were flushed from femurs with 3 mL McCoy's 5A medium (Flow Labs, McLean, VA) containing 10% heat-inactivated fetal bovine serum (Hyclone Labs, Logan, UT). Spleens were pressed through a stainless steel mesh screen, and cells were washed from the screen with 6 mL medium. The number of nucleated cells in the suspensions was determined by Coulter counter. Femurs and spleens were removed from mice killed by cervical dislocation.

GM-CFC assay
Hematopoietic progenitor cells committed to granulocyte and/or macrophage development were assayed using a double-layer agar GM-CFC assay in which mouse endotoxin serum (5% vol/vol) was added to feeder layers as a source of colony-stimulating factors [31]. Colonies (>50 cells) were counted after 10 days of incubation in a 37°C humidified environment containing 5% CO_2. Triplicate plates were cultured for each cell suspension.

CFU-S assay
Exogenous CFU-S were evaluated by the method of Till and McCulloch [32]. Recipient mice were exposed to 9 Gy total-body radiation to reduce endogenous hematopoietic stem cells. Three to 5 hours later, bone marrow, spleen, or peripheral blood cells were injected IV into the irradiated recipients. Twelve days after transplantation, the recipients were killed by cervical dislocation, their spleens were removed and fixed in Bouin's solution, and grossly visible spleen colonies were counted. Each treatment group consisted of five mice.

Survival assay
Recipient mice were exposed to 9.5 Gy total-body radiation, and various numbers of bone marrow or spleen cells were injected IV. Animal survival was recorded daily for 60 days.

Histopathology
Mice were killed by cervical dislocation, and the spleen, bone marrow, and proximal small intestine were removed and immersion-fixed for 2 hours in a modified Karnovsky's fixative consisting of 2% paraformaldehyde, 2.5% glutaraldehyde, and 4 mM $MgCl_2$ in 100 mM cacodylate buffer (pH 7.3). Specimens were postfixed in 1% osmium tetroxide, dehydrated in acetone, and embedded in Epon 812. To enhance the visualization of mast cells, sections were stained with methylene blue-azure II, a metachromatic stain. With this stain, the granules of nonsecreted connective tissue mast cells stain dark purple while secreted granules appear pink. Sections were examined and photographed with a Zeiss Ultraphot microscope.
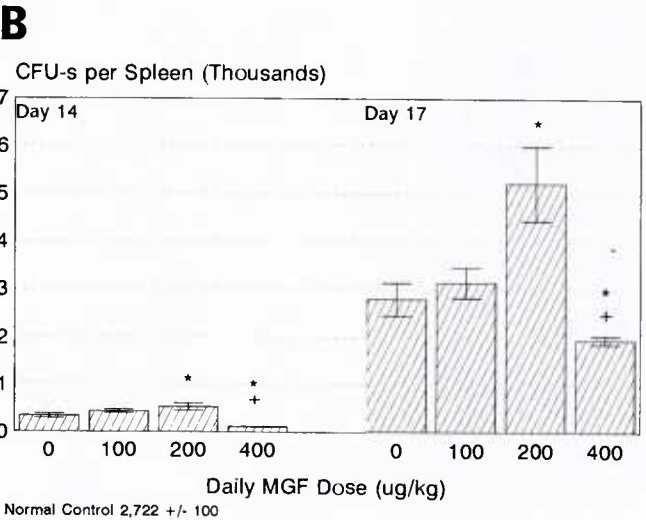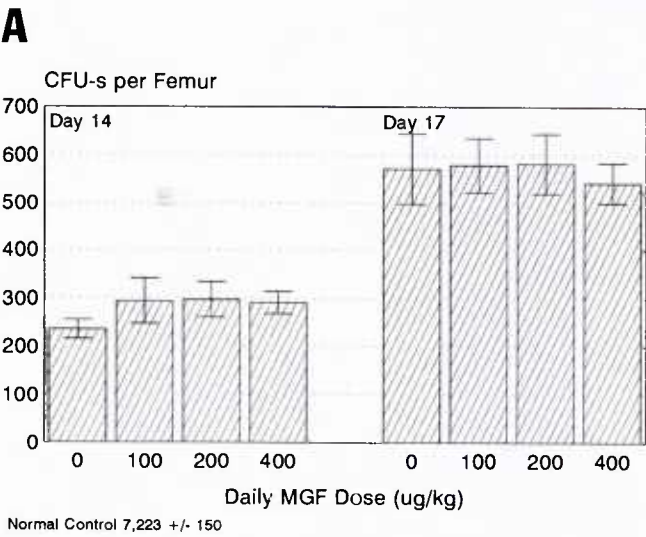
Statistical analysis
Results of replicate experiments were pooled and are represented as the mean ± standard error (SE) of pooled data. Bone marrow and splenic hematopoietic colony and blood cell data were analyzed by Student's *t*-test, survival data were analyzed by Fisher's exact test, and peripheral blood CFU-S data were analyzed by a two-way analysis of variance (ANOVA). Significance level was set at $p<0.05$.
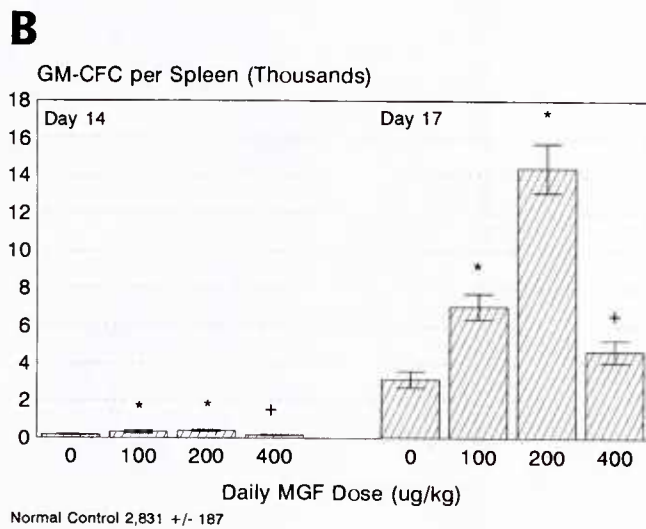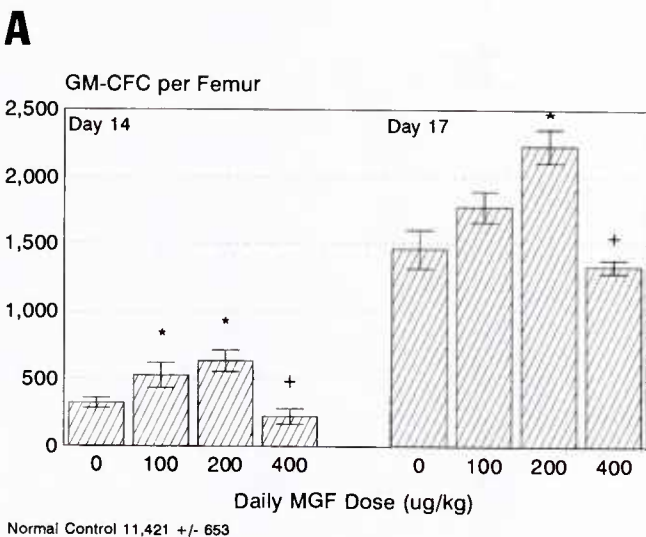
Experimental design
The ability to accelerate hematopoietic regeneration in a murine model of radiation-induced hematopoietic hypoplasia was used to evaluate the in vivo effects of MGF. Mice were exposed to a sublethal (7.75 Gy) dose of ^{60}Co radiation to induce severe hematopoietic hypoplasia. MGF was administered s.c. daily on days 1 to 17 postexposure. On days 14 and 17 during the postirradiation recovery period, three mice from each treatment group were randomly selected and bone marrow and splenic cellularity; CFU-S and GM-CFC recoveries; peripheral blood CFU-S, WBC, RBC, and PLT recoveries; and tissue histopathological changes were evaluated. The day-14 and day-17 assay points were chosen to bracket the most dynamic period of hematopoietic recovery expected following the 7.75-Gy radiation exposure, and were based on our previous knowledge regarding the kinetics of hematopoietic recovery in this murine radiation model [33].

Results
Compared to saline-treated irradiated mice, some irradiated mice given daily injections of MGF exhibited enhanced

A

CFU-s per Femur

Normal Control 7,223 +/- 150

B

CFU-s per Spleen (Thousands)

Normal Control 2,722 +/- 100

A

GM-CFC per Femur

Normal Control 11,421 +/- 653

B

GM-CFC per Spleen (Thousands)

Normal Control 2,831 +/- 187

Fig. 1. Effect of MGF (100, 200, or 400 µg/kg/d, s.c.) on postirradiation recovery of bone marrow (A) and splenic (B) CFU-S in sublethally irradiated (7.75 Gy) $B_6D_2F_1$ mice. Data represent the mean ± SE of values obtained from three replicate experiments. *$p<0.05$ with respect to saline controls; $^+p<0.05$ with respect to 200 µg/kg/d MGF. Average background CFU-S number in recipient mice not injected with cells was 0.2 ± 0.2.
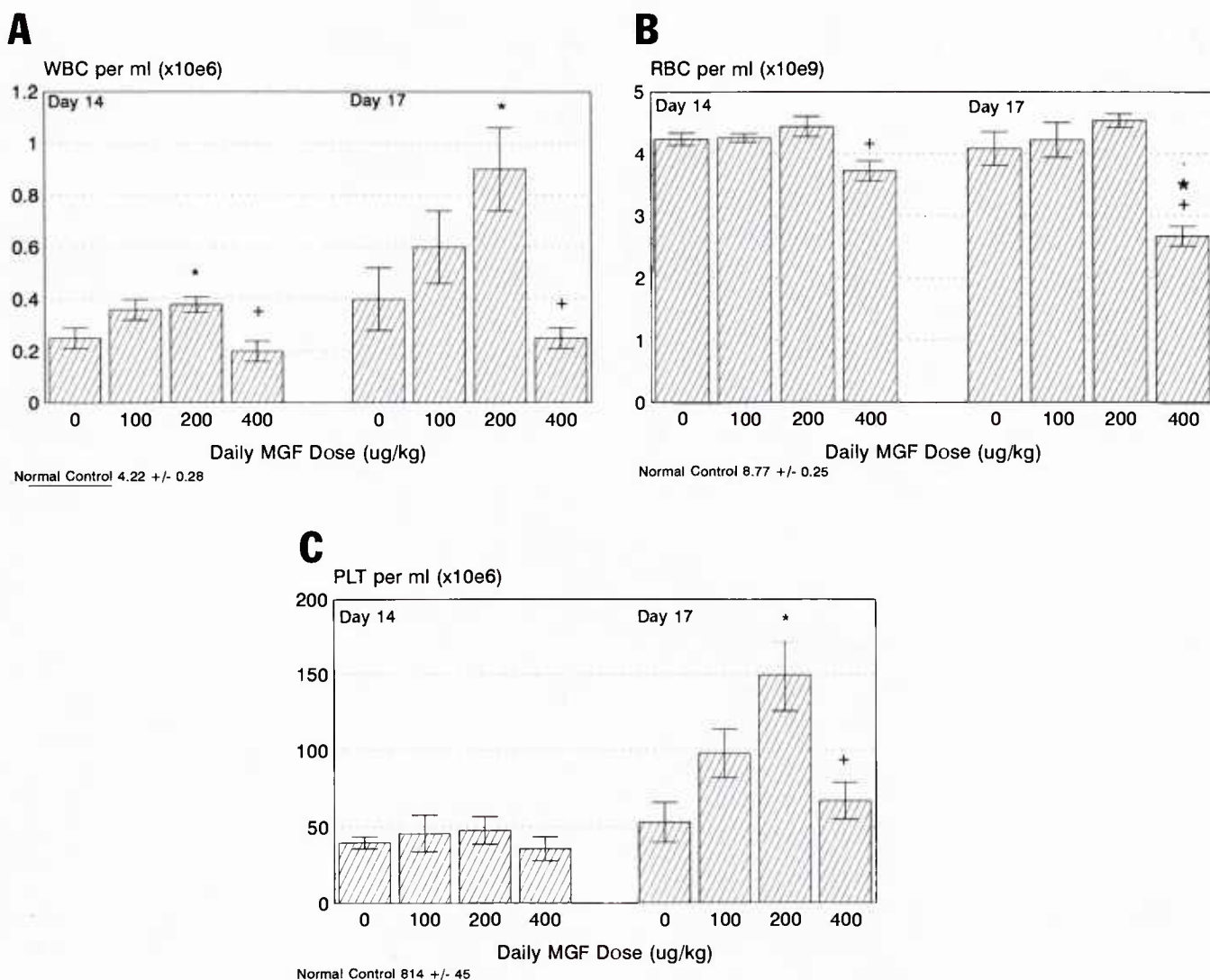
Fig. 2. Effect of MGF (100, 200, or 400 µg/kg/d, s.c.) on postirradiation recovery of bone marrow (A) and splenic (B) GM-CFC in sublethally irradiated (7.75 Gy) $B_6D_2F_1$ mice. Data represent the mean ± SE of values obtained from three replicate experiments. *$p<0.05$ with respect to saline controls; $^+p<0.05$ with respect to 200 µg/kg/d MGF.

regeneration of all hematopoietic parameters evaluated, with the exception of bone marrow CFU-S and peripheral RBC (Figs. 1, 2, and 3). Effects were clearly dose-dependent, with the most significant stimulatory effects observed in mice receiving 200 µg/kg/d MGF. In these mice, hematopoietic parameters increased more, and in some instances were observed earlier, than in mice treated with only 100 µg/kg/d MGF. Surprisingly, the 400 µg/kg/d-MGF dose induced less hematopoietic recovery than the 200 µg/kg/d dose; furthermore, splenic CFU-S and peripheral RBC recoveries in these mice were even less than in saline-treated irradiated mice.

Because c-kit ligand has been shown capable of mobilizing primitive marrow cells into the circulation, peripheral blood

CFU-S levels were evaluated to determine whether CFU-S effects in the bone marrow of MGF-treated mice may be masked by mobilization. Table 1 illustrates that CFU-S mobilization occurred in all MGF-treated mice. This phenomenon was directly dose-dependent, the most significant mobilization being observed following administration of the highest (400 µg/kg/d) MGF dose. Furthermore, in all treatment groups, CFU-S mobilization was more pronounced at day 17 postirradiation than at day 14 postirradiation.

Additional studies were performed to determine the effects of MGF on the subsequent reconstitutional potential of regenerated bone marrow and spleen cells from the sublethally irradiated mice. Recipient mice were irradiated with 9.5 Gy ^{60}Co and transplanted with various doses of bone marrow or spleen cells obtained from regenerating, sublethally irradiated

A

WBC per ml (x10e6)

B

RBC per ml (x10e9)

C

PLT per ml (x10e6)

Fig. 3. Effect of MGF (100, 200, or 400 μg/kg/d, s.c.) on postirradiation recovery of peripheral white blood cells (**A**), red blood cells (**B**), and platelets (**C**) in sublethally irradiated (7.75 Gy) $B_6D_2F_1$ mice. Data represent the mean ± SE of values obtained from three replicate experiments. *$p<0.05$ with respect to saline controls; $^+p<0.05$ with respect to 200 μg/kg/d MGF.

mice that had been treated for 17 days with either saline or MGF. Transplanted mice were then monitored for survival over a 60-day posttransplant period (Table 2). The survival-enhancing ability of bone marrow cells obtained from irradiated mice treated with either 100 or 200 μg/kg/d MGF was superior to that obtained from saline-treated mice; effects were more dramatic in mice transplanted with cells obtained from mice receiving 200 μg/kg/d MGF. For example, compared to 0% and 5% survival provided by 5×10^4 or 10×10^4 bone marrow cells obtained from saline-treated mice, 60% survival and 100% survival, respectively, were obtained with these cell numbers obtained from the 200 μg/kg/d MGF–treated mice. Survival-enhancing effects were less obvious in mice transplanted with spleen cells, yet spleen cells from mice treated with 200 μg/kg/d MGF did increase survival. In contrast, bone marrow and spleen cells obtained from mice treated with 400 μg/kg/d MGF exhibited a reduced ability to reconstitute irradiated mice.

No adverse effects were observed in mice treated with the 100 μg/kg/d-MGF dose; however, the higher doses induced some lethality in otherwise sublethally irradiated mice. Twelve percent of mice receiving 200 μg/kg/d and 22% of mice receiving 400 μg/kg/d died before day 17, the final assay point. Most of these animals died between days 14 and 17 postirradiation. Mice receiving 400 μg/kg/d MGF also appeared to become progressively emaciated and lost significantly more weight than mice in the other treatment groups; at day 14 postirradiation, body weight had decreased ~15% in these mice compared to only a 5% decrease in saline-treated mice and a 7 to 8% decrease in the 100 or 200 μg/kg/d MGF–treated mice (Table 3).

Because of the possibility that the detrimental effects observed in mice treated with the higher MGF doses may be related to MGF-induced mast cell proliferation and/or degranulation, the bone marrow, spleen, and small intestine (murine tissues that typically exhibit easily detectable mast cells in

Table 1. MGF-induced mobilization of CFU-S into the peripheral blood of irradiated mice

Daily MGF dose (µg/kg)	Day 14 postirradiation		Day 17 postirradiation	
	CFU-S/mL	CFU-S/10^5 mononuclear cells	CFU-S/mL	CFU-S/10^5 mononuclear cells
0 (saline)	3.50±0.83	0.82±0.31	4.65±0.84	1.34±0.25
100	3.65±0.35	0.99±0.09	5.77±1.37	1.38±0.23
200	5.48±0.98	1.09±0.19	6.10±1.25	2.23±0.55
400	6.67±1.85	1.46±0.40	10.09±2.08	2.73±0.57

Five irradiated (9.0 Gy) $B_6D_2F_1$ recipient mice were injected with peripheral blood obtained from mice on days 14 and 17 after irradiation (7.75 Gy) and daily treatment with saline or the indicated doses of MGF. A two-way ANOVA was performed using the endpoints CFU-S/mL and CFU-S/10^5 mononuclear cells with MGF dose and postirradiation days as factors. For the endpoint CFU-S/mL, a dose effect significant at $p=0.0127$ and a day effect significant at $p=0.0517$ were found. For the endpoint CFU-S/10^5 mononuclear cells, a dose effect significant at $p=0.0311$ and a day effect significant at $p=0.0027$ were found. The average number of background CFU-S in recipient mice not injected with cells was 0.15 ± 0.15.

Table 2. Survival of lethally irradiated mice transplanted with bone marrow or spleen cells

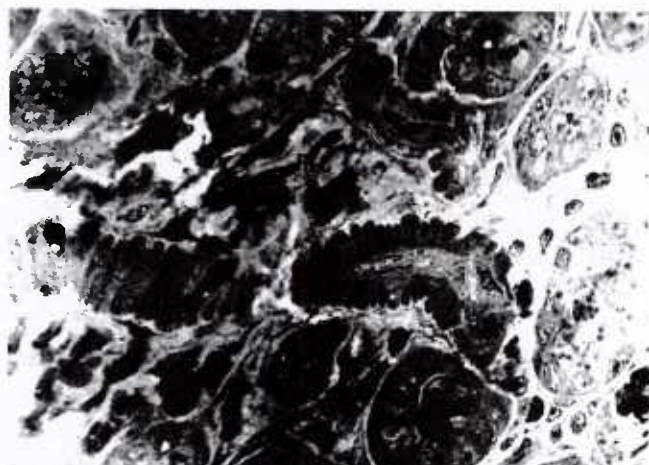|	Number of cells injected				
	5×10^4	10×10^4	5×10^5	10×10^5	20×10^5
Bone marrow					
Normal	100%	100%	—	—	—
Saline	0%	5%	—	—	—
MGF 100 µg/kg/d	30%[a]	70%[a]	—	—	—
MGF 200 µg/kg/d	60%[a]	100%[a]	—	—	—
MGF 400 µg/kg/d	0%[b]	0%[b]	—	—	—
Spleen					
Normal	—	—	50%	100%	100%
Saline	—	—	20%	60%	95%
MGF 100 µg/kg/d	—	—	20%	70%	90%
MGF 200 µg/kg/d	—	—	40%	100%[a]	100%
MGF 400 µg/kg/d	—	—	0%[b]	40%[b]	60%[a,b]

Ten to 20 irradiated (9.5 Gy) recipient $B_6D_2F_1$ mice were transplanted with the indicated number of bone marrow or spleen cells from nonirradiated normal control mice, saline-treated mice 17 days after sublethal 7.75-Gy irradiation, or MGF-treated mice 17 days after sublethal 7.75-Gy irradiation. Survival was monitored for 60 days posttransplant. [a]$p<0.05$ with respect to saline values; [b]$p<0.05$ with respect to 200 µg/kg/d-MGF values.

Table 3. Weight loss in irradiated mice treated with MGF

	Daily MGF dose (µg/kg)			
	0	100	200	400
Preirradiation (g)	21.8±0.4	21.0±0.6	21.5±0.5	21.6±0.6
Day 14 postirradiation (g)	20.7±0.4	19.5±1.1	19.7±0.9	18.4±1.1[a]
Loss (g)	1.1	1.5	1.8	3.2
Percent loss	5.0%	7.1%	8.4%	14.8%

Twelve mice in each group were irradiated with 7.75 Gy ^{60}Co and daily injected s.c. with either saline or the indicated dose of MGF. [a]$p<0.05$ with respect to preirradiation values.

Fig. 4. Light micrograph of connective tissue mast cells (mc) in the gut of $B_6D_2F_1$ mice, demonstrating these easily detectable cells using metachromatic stain.
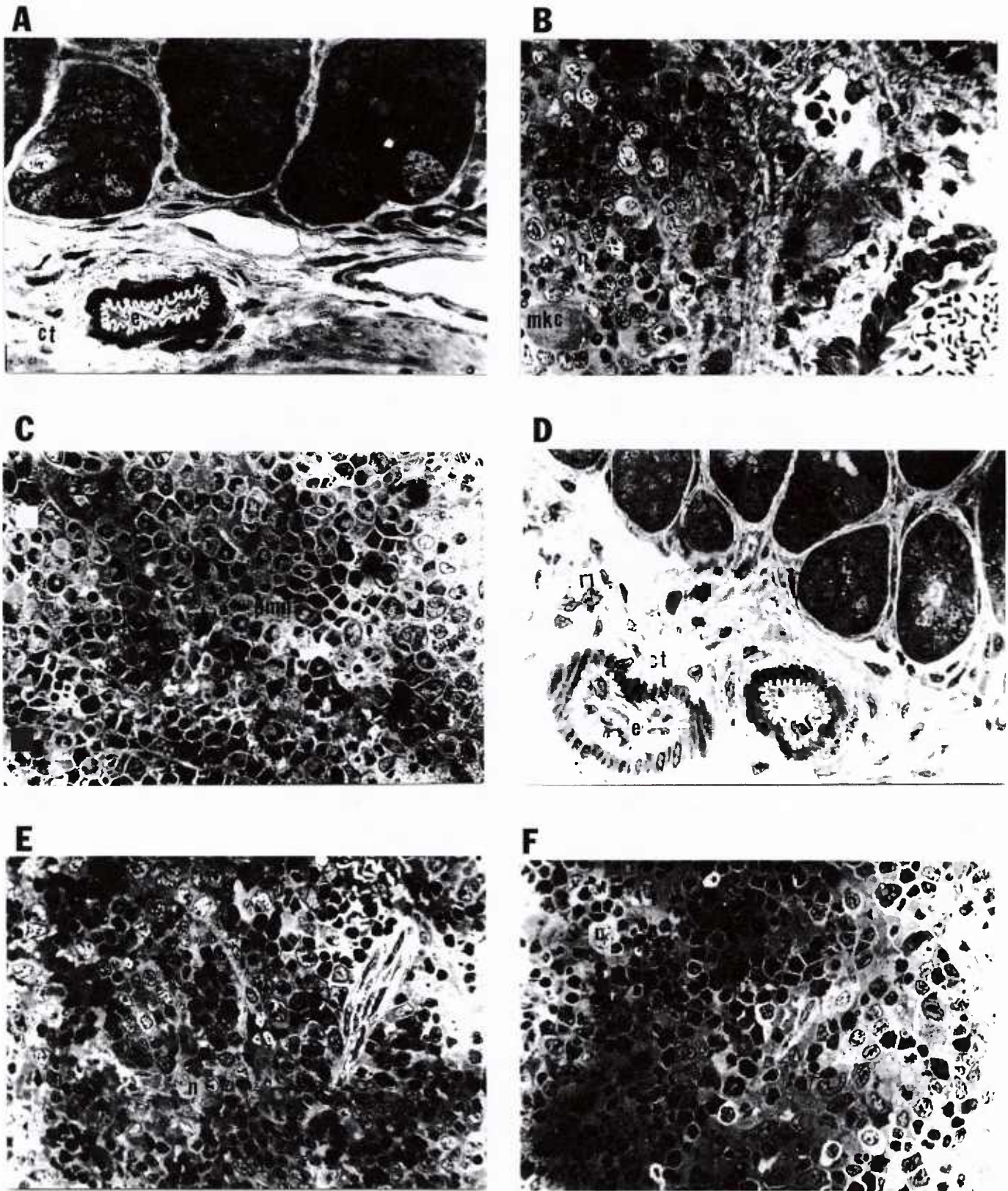
connective tissue areas as illustrated in Fig 4) were histologically evaluated for the presence of mast cells and mast-cell degranulation. Almost no mast cells were detected in any tissue of irradiated saline- or MGF-treated mice at either day 14 or day 17 postirradiation. Furthermore, no other obvious histological differences were observed in MGF-treated mice compared to saline-treated mice. The gut spleen, and bone marrow in both treatment groups appeared similar in terms of cell numbers and composition (Fig. 5).

Discussion

Morbidity and mortality associated with high-level radiation exposures can be directly attributed to infectious and hemorrhagic complications resulting from radiation-induced neutropenia and thrombocytopenia. In recent years, several hematopoietic growth factors have been shown to stimulate hematopoietic regeneration following radiation- or chemotherapy-induced myelosuppression, most notably G-CSF, GM-CSF, IL-6, and the GM-CSF/IL-3 fusion protein, PIXY321 [33–37]. Following sublethal radiation exposure, hematopoietic recovery gradually occurs and appears to be mediated by endogenously produced hematopoietic cytokines [28,29]. Because c-kit ligand has been shown to have little hematopoietic effect alone, but rather to synergize with a variety of hematopoietic cytokines to enhance their effects, we hypothesized that sublethally irradiated mice should provide a good model in which to evaluate the potential in vivo effects of MGF.

Our results demonstrate that a 17-day treatment course of MGF can alter multiple-lineage hematopoietic regeneration following radiation injury. Effects were dose-dependent, 100 or 200 µg/kg/d stimulating recovery and 400 µg/kg/d appearing to inhibit recovery. The hematopoietic stimulatory effects observed in our studies at the 200 µg/kg/d MGF dose confirmed results published by Scheuning et al. in which 200 µg/kg/d recombinant canine SCF administered for 21 days postirradiation in dogs was shown to enhance recovery from otherwise lethal hematopoietic injury [38] Furthermore, our studies at the 100 µg/kg MGF dose expand observations of Zsebo et al. in which even a single 100-µg/kg injection of rrSCF administered to lethally irradiated mice 4 hours postex-

Fig. 5. Light micrograph of gut **(A, D)**, spleen **(B, E)** and bone marrow **(C, F)** from irradiated (7.75 Gy) $B_6D_2F_1$ mice treated for 17 days with 400 µg/kg/d of MGF **(A–C)** or saline **(D–F)**. Gut endothelial cells (e) are hypertrophied. Both spleen and bone marrow are cellular, and normoblasts (n), megakaryocytes (mkc), and neutrophils (pmn) are prominent. The cell in **D** adjacent to the arteriole is a macrophage (m). If present, mast cells would be visible in connective tissue (ct) areas as in Figure 4.

posure extended mean survival time, presumably through enhancement of hematopoietic recovery [39].

An initial enigma in our studies was the observation that, while increased numbers of both CFU-S and GM-CFC were observed in the spleens of MGF-treated mice, only GM-CFC numbers were increased in the bone marrow. Since recent studies in normal mice have demonstrated the ability of c-*kit* ligand to mobilize into the peripheral circulation large numbers of cells capable of engrafting irradiated animals [40,41], we suspected that the apparent lack of CFU-S proliferation in the bone marrow of our MGF-treated mice may be due to the mobilization of these cells out of the marrow as rapidly as they were being produced. Studies presented in Table 1 verify that CFU-S mobilization did occur in the MGF-treated mice, suggesting that CFU-S proliferation in the marrow most likely was occurring but was not apparent due to this mobilization phenomenon.

As described, the 400 µg/kg/d MGF dose appeared to inhibit hematopoiesis. This effect did not appear to be due merely to "toxicity" since, although 22% of mice treated with the 400 µg/kg/d MGF dose died before evaluation, 12% of mice receiving 200 µg/kg/d MGF and exhibiting the greatest hematopoietic stimulation also died before evaluation. The cause of the lethality and weight loss observed in otherwise sublethally irradiated mice given high-dose MGF remains unknown, but mast cells do not appear to be involved. Although high doses of MGF have previously been shown to induce extensive mast-cell degranulation associated with respiratory distress [42], histopathological evaluation of tissues typically exhibiting mast cells in the mouse revealed almost no mast cells in any of the irradiated mice. Since mast cells are ultimately generated from the radiosensitive hematopoietic stem cells [43,44], apparently recovery of these cells to detectable levels had not yet occurred in our irradiated mice.

c-*kit* ligand in combination with additional cytokines has been demonstrated to stimulate the proliferation and differentiation of primitive hematopoietic precursors [11,15]. Because of this, the possibility that stem cell exhaustion may occur following prolonged MGF administration cannot be excluded as a possible explanation for the observed MGF-induced inhibition of hematopoiesis. Indeed, our results in Table 2 indicate that as the MGF dose was increased from 100 to 200 µg/kg/d, the reconstitutional potential of bone marrow and spleen cells increased; however, at 400 µg/kg/d such reconstitutional potential decreased. Thus, following the 400 µg/kg/d MGF dose, primitive cells may have been stimulated to proliferate to the point of exhaustion. Had this occurred, however, an increase in downstream progenitor populations would have been expected; this was not observed in the 400 µg/kg/d MGF–treated mice.

An alternate explanation for the apparent hematopoietic inhibitory effects observed following administration of the highest MGF dose may relate to the nature of the MGF used in our studies and receptor-ligand interactions. c-*kit* ligand is known to exist in two biologically active forms: (1) an integral membrane protein with an extracellular domain, transmembrane domain, and intracytoplasmic domain, and (2) a soluble protein produced by proteolytic cleavage of the membrane-associated form [12]. Membrane-associated c-*kit* ligand has been shown to be prevalent in bone marrow stromal cells [45,46]. Since primitive hematopoietic cells possess c-*kit* (that is, the receptor for c-*kit* ligand [47]), under in situ conditions it can be envisioned that, via c-*kit*, hematopoietic cells bind cell-associated c-*kit* ligand on stromal cells, positioning themselves in proximity to respond to additional stromal-derived hematopoietic cytokines. Since the MGF used in our studies

was a soluble c-*kit* ligand, high doses of MGF may have saturated c-*kit* on hematopoietic cells, preventing the binding of these receptors with stromal-associated c-*kit* ligand and therefore preventing subsequent stromal–hematopoietic cell interactions that lead to proliferation and differentiation, resulting in reduced hematopoietic recovery in irradiated mice. The fact that mice treated with the 400 µg/kg/d MGF dose exhibited decreased splenic CFU-S numbers concurrent with the greatest CFU-S mobilization may suggest an inability of these cells to attach to the splenic microenvironment.

In conclusion, these studies demonstrate a dose-dependent ability of MGF to stimulate multilineage hematopoietic regeneration following radiation-induced hematopoietic injury. Detrimental effects observed following high-dose MGF treatment do not appear to be mast cell related, and their cause remains to be determined. However, the effects observed with "supraoptimal" doses of MGF suggest that caution should be taken in dose-escalation trials in humans.

References

1. Robinson BE, Quesenberry P (1990) Review: Hemopoietic growth factors: overview and clinical applications, part I. Am J Med Sci 300:163
2. Moore MAS (1991) Clinical implications of positive and negative hematopoietic stem cell regulators. Blood 78:1
3. Witte ON (1990) *Steel* locus defines new multipotent growth factor. Cell 63:5
4. Williams DE, Eisenman J, Baird A, Rauch C, Van Ness K, March CJ, Park LS, Martin U, Mochizuki DY, Boswell HS, Burgess GS, Cosman D, Lyman SD (1990) Identification of a ligand for the c-*kit* proto-oncogene. Cell 63:167
5. Zsebo KM, Wypych J, McNiece IK, Lu HS, Smith KA, Karkare SB, Sachdev RK, Yuschenkoff VN, Brikett NC, Williams LR, Satyagal VN, Tung W, Bosselman RA, Mendiaz EA, Langley KE (1990) Identification, purification, and biological characterization of hematopoietic stem cell factor from buffalo rat liver-conditioned medium. Cell 63:195
6. Nocka K, Buck J, Levi E, Besmer P (1990) Candidate ligand for the c-*kit* transmembrane kinase receptor: KL, a fibroblast derived growth factor stimulates mast cells and erythroid progenitors. EMBO J 9:3287
7. Williams DE, DeVries P, Namen AE, Widmer MB, Lyman SD (1992) The *Steel* factor. Develop Biol 151:368
8. Martin FH, Suggs SV, Langley KE, Lu HS, Ting J, Okino KH, Morris F, McNiece IK, Jacobsen FW, Mendiaz EA, Birkett NC, Smith KA, Johnson MJ, Parker VP, Flores JC, Patel AC, Fischer EF, Erjavec HO, Herrera CJ, Wypych J, Sachdev RK, Pope JA, Leslie I, Wen D, Lin CH, Cupples RL, Zsebo KM (1990) Primary structure and functional expression of rat and human stem cell factor DNAs. Cell 63:203
9. McNiece IK, Langley KE, Zsebo KM (1991) Recombinant human stem cell factor synergizes with GM-CSF, G-CSF, IL-3, and Epo to stimulate human progenitor cells of the

myeloid and erythroid lineages. Exp Hematol 19:226

10. Broxmeyer HA, Hangoc G, Cooper S, Anderson D, Cosman D, Lyman SD, Williams DE (1991) Influence of murine mast cell growth factor (c-*kit* ligand) on colony formation by mouse marrow hematopoietic progenitor cells. Exp Hematol 19:143

11. Williams N, Bertoncello I, Kavnoudias H, Zsebo KM, McNiece I (1992) Recombinant rat stem cell factor stimulates the amplification and differentiation of fractionated mouse stem cell populations. Blood 79:58

12. Anderson DM, Lyman SD, Baird A, Wingnall JM, Eisenman J, Rauch C, March CJ, Boswell S, Gimpel SD, Cosman D, Williams DE (1990) Molecular cloning of mast cell growth factor, a hematopoietin that is active in both membrane bound and soluble forms. Cell 63:235

13. deVries P, Brasel KA, Eisenman JR, Alpert AR, Williams DE (1991) The effect of recombinant mast cell growth factor on purified murine hematopoietic stem cells. J Exp Med 173:1205

14. McNiece IK, Langley KE, Zsebo KM (1991) The role of recombinant stem cell factor in early B cell development: synergistic interaction with IL-7. J Immunol 146:3785

15. Carow CE, Hangoc G, Cooper SH, Williams DE, Broxmeyer HE (1991) Mast cell growth factor (c-*kit* ligand) supports the growth of human multipotential progenitor cells with a high replating potential. Blood 78:2216

16. Bernstein ID, Andrews RG, Zsebo KM (1991) Recombinant human stem cell factor enhances the formation of colonies by CD34$^+$ and CD34$^+$Lin$^-$ cells, and the generation of colony-forming cell progeny from CD34$^+$Lin$^-$ cells cultured with interleukin-3, granulocyte colony-stimulating factor, or granulocyte-macrophage colony-stimulating factor. Blood 77:2316

17. Brandt J, Briddell RA, Srour EF, Leemhuis TB, Hoffman R (1992) The role of c-*kit* ligand in the expansion of human hematopoietic progenitor cells. Blood 79:634

18. Heyworth CM, Whetton AD, Nicholls S, Zsebo K, Dexter TM (1992) Stem cell factor directly stimulates the development of enriched granulocyte-macrophage colony-forming cells and promotes the effects of other colony-stimulating factors. Blood 80:2230

19. Migliaccio G, Migliaccio AR, Valinsky J, Langley K, Zsebo KM, Visser JWM, Adamson JW (1991) Stem cell factor induces proliferation and differentiation of highly enriched murine hematopoietic cells. Proc Natl Acad Sci USA 88:7420

20. Bernstein SE, Russell ES, Keighley G (1968) Two hereditary mouse anemias (*Sl/Sl^d* and *W/W^v*) deficient in response to erythropoietin. Ann NY Acad Sci 149:475

21. Kitamura Y, Go S (1979) Decreased production of mast cells in *Sl/Sl^d* anemic mice. Blood 53:492

22. Ebbe S, Phalen E, Stohlman FJ (1973) Abnormal megakaryocytopoiesis in *Sl/Sl^d* mice. Blood 42:865

23. Ruscetti FN, Boggs DR, Torok BJ, Boggs SS (1976) Reduced blood and marrow neutrophils and granulocytic colony-forming cells in *Sl/Sl^d* mice. Proc Soc Exp Biol Med 152:398

24. Zsebo KM, Williams DA, Geissler EN, Broudy VC, Martin FH, Atkins HL, Hsu RY, Birkett NC, Okino KH, Murdock DC, Jacobsen FW, Langley KE, Smith KA, Takeishi T, Cattanach BM, Galli SJ, Suggs SV (1990) Stem cell factor is encoded at the *Sl* locus of the mouse and is the ligand for the c-*kit* tyrosine kinase receptor. Cell 63:213

25. Ulich TR, Castillo J, Yi ES, Yin S, McNiece I, Yung YP, Zsebo KM (1991) Hematologic effects of stem cell factor in vivo and in vitro in rodents. Blood 78:645

26. Molineux G, Migdalska A, Szmitkowski M, Zsebo KM, Dexter TM (1991) The effects of hematopoiesis of recombinant stem cell factor (ligand for c-*kit*) administered in vivo to mice either alone or in combination with granulocyte colony-stimulating factor. Blood 78:961

27. Andrews RG, Knitter GH, Bartelmez SH, Langley KE, Farrar D, Hendren W, Appelbaum FR, Bernstein ID, Zsebo KM (1991) Recombinant human stem cell factor, c-*kit* ligand, stimulates hemopoiesis in primates. Blood 78:1975

28. Baker WH, Limanni A, Chang CM, Williams JL, Patchen ML (1992) Comparison of interleukin-1 mRNA expression in murine spleens after lethal and sublethal cobalt-60 irradiation. Exp Hematol 20:771

29. Chang CM, Baker WH, Limanni A, Williams JL, Fragoso L, Patchen ML (1992) In vivo gene expression in interleukin-3, granulocyte-macrophage colony-stimulating factor, and c-*kit* ligand in murine bone marrow and spleen after sublethal irradiation. Exp Hematol 20:775

30. Schulz J, Almond PR, Cunningham JR, Holt JG, Loevinger R, Suntharalingam N, Wright KA, Nath R, Lempert D (1983) A protocol for the determination of absorbed dose for high energy photon and electron beams. Med Phys 10:741

31. Patchen ML, MacVittie TJ (1986) Hemopoietic effects of intravenous soluble glucan administration. J Immunopharmacol 8:407

32. Till JE, McCulloch EA (1961) A direct measurement of the radiation sensitivity of normal mouse bone marrow cells. Radiat Res 14:213

33. Patchen ML, Fischer R, MacVittie TJ (1993) Effects of combined administration of interleukin-6 and granulocyte colony-stimulating factor on recovery from radiation-induced hemopoietic aplasia. Exp Hematol 21:338

34. Moore MAS (1991) The clinical use of colony stimulating factors. Ann Rev Immunol 9:159

35. Brugger W, Bross KJ, Lindemann A, Kantz L, Mertelsmann R (1992) Role of hematopoietic growth factor combinations in experimental and clinical oncology. Sem Oncol 19:8

36. Patchen ML, MacVittie TJ, Williams JL, Schwartz GN, Souza LM (1991) Administration of interleukin-6 stimulates multilineage hematopoiesis and accelerates recovery from radiation-induced hematopoietic depression. Blood 77:472

37. Williams DE, Dunn JT, Park LS, Frieden EA, Seiler FR, Farese AM, MacVittie TJ (1993) A GM-CSF/IL-3 fusion protein promotes neutrophil and platelet recovery in sublethally irradiated rhesus monkeys. Biotechnol Ther 4:17

38. Scheuning FG, Appelbaum FR, Deeg HJ, Sullivan-Pepe M, Graham TC, Hackman R, Zsebo KM, Storb R (1993) Effects of recombinant canine stem cell factor, a c-*kit* ligand, and recombinant granulocyte colony-stimulating factor on hematopoietic recovery after otherwise lethal total body irradiation. Blood 81:20

39. Zsebo KM, Smith KA, Hartley CA, Greenblatt M, Cooke K, Rich W, McNiece IK (1992) Radioprotection of mice by recombinant rat stem cell factor. Proc Natl Acad Sci USA 89:9464

40. Andrews RG, Bensinger WI, Knitter GH, Bartelmez SH, Longin K, Bernstein ID, Appelbaum FR, Zsebo KM (1992) The ligand for c-*kit*, stem cell factor, stimulates the circulation of cells that engraft lethally irradiated baboons. Blood 80:2715

41. Fleming WH, Alpern E, Uchida N, Ikuta K, Weissman IL (1993) *Steel* factor influences the distribution and activity

of murine hematopoietic stem cells in vivo. Proc Natl Acad Sci USA 90:3760

42. Lynch DH, Jacobs C, DuPont D, Eisenman J, Foxworthe D, Martin U, Miller RE, Roux E, Liggitt D, Williams DE (1992) Pharmacokinetic parameters of recombinant mast cell growth factor (rMGF). Lymphokine Cytokine Res 11:233

43. Kitamura Y, Shimada M, Go S, Matsuda H, Hatanaka K, Seki M (1979) Distribution of mast-cell precursors in hematopoietic and lymphopoietic tissue of mice. J Exp Med 150:482

44. Kitamura Y, Yokoyama H, Matsuda H, Ohno T (1981) Spleen colony-forming cell as common precursor for mouse mast cells and granulocytes. Nature 291:159

45. Flanagan JG, Leder P (1990) The c-*kit* ligand: A cell surface molecule altered in *Steel* mutant fibroblasts. Cell 63:185

46. Aye MT, Hashemi S, Leclair B, Zeibdawi A, Trudel E, Halpenny M, Fuller V, Cheng G (1992) Expression of stem cell factor and c-*kit* mRNA in cultured endothelial cells, monocytes, and cultured human bone marrow stromal cells (CFU-RF). Exp Hematol 20:523

47. Papayannopoulou T, Brice M, Broudy VC, Zsebo KM (1991) Isolation of c-*kit* receptor–expressing cells from bone marrow, peripheral blood, and fetal liver: functional properties and composite antigenic profile. Blood 78:1403

INCREASED FIBRINOGEN SYNTHESIS IN MICE DURING THE ACUTE PHASE RESPONSE: CO-OPERATIVE INTERACTION OF INTERLEUKIN 1, INTERLEUKIN 6, AND INTERLEUKIN 1 RECEPTOR ANTAGONIST

Hanna Rokita,*   Ruta Neta,†   Jean D. Sipe‡

Interleukin 6 (IL-6) stimulates fibrinogen (Fg) gene expression both in vivo and in vitro; while interleukin 1 (IL-1) paradoxically stimulates in vivo, yet inhibits in vitro, Fg synthesis. The naturally occurring interleukin 1 receptor antagonist (IL-1ra) and passive immunization with anti-IL-6 antiserum were used to study the in vivo mechanism of action of IL-1 on Fg gene expression. Changes in plasma Fg and hepatic Fg mRNA concentrations were measured following administration of exogenous IL-1ra together with IL-6 or IL-1 to CD2F1 mice. Our results suggest that in vivo, IL-1 per se inhibits Fg production since when IL-1ra was co-administered with IL-6, greater concentrations of Fg were observed than when IL-6 was administered alone. The data suggest that IL-1 stimulates Fg production through intermediate production of IL-6, since stimulation was abrogated when either IL-1ra or anti-IL-6 antiserum was co-administered with IL-1. An in vivo role for IL-1ra in the stimulation of Fg by IL-1 was supported by the observation that within 1 h of IL-1 administration to mice, IL-1ra mRNA was detectable in liver. It appears that IL-1, an early mediator of inflammation, inhibits constitutive expression of Fg genes and stimulates the IL-1ra and IL-6 genes. The inhibitory effect of IL-1 is reversed by endogenous IL-1ra and by the direct stimulation of Fg gene expression by IL-6.

Changes in hepatic protein synthesis are a major manifestation of the acute phase response and are mainly regulated by the mononuclear phagocyte system through secretion of cytokines such as interleukin 6 (IL-6) and interleukin 1 (IL-1).[1-6] IL-6 and, to a lesser extent, IL-1 have been implicated as modulators of hepatic serum amyloid A (SAA) and fibrinogen (Fg) mRNA and/or protein synthesis in humans and mice.[4-7] Treatment of mice with endotoxin and the two lipopolysaccharide-induced cytokines, IL-1 and TNF, caused an increase in plasma Fg concentration.[8] IL-1 is an early and pluripotent mediator of the acute phase response, with capacity to induce itself. IL-6 and a structurally related receptor ligand with antagonist activity, termed IL-1 receptor antagonist (IL-1ra). Recently, recombinant generated preparations of IL-1ra, a 17 kDa protein with 26–30% homology to IL-1 beta and 19% to IL-1 alpha have been used to distinguish physiological roles of IL-1 from closely related cytokines such as IL-6.[9-17] Since several in vitro studies[5,18-21] indicate that constitutive and IL-6 stimulated Fg gene expression in hepatoma cell lines is inhibited by IL-1, the present study was undertaken to investigate the basis of the in vivo stimulatory effect of IL-1 on Fg gene expression.

RESULTS

IL-1ra Inhibits IL-1, but Enhances IL-6, Stimulation of Plasma Fibrinogen

In vivo administration of exogenous cytokines demonstrates biological activity and permits com-

parison of dose response and sensitivity to individual cytokines. Although IL-1 alpha and IL-6 both stimulated a concentration-related elevation in Fg, IL-1 was more effective on a weight basis than IL-6 (Table 1).

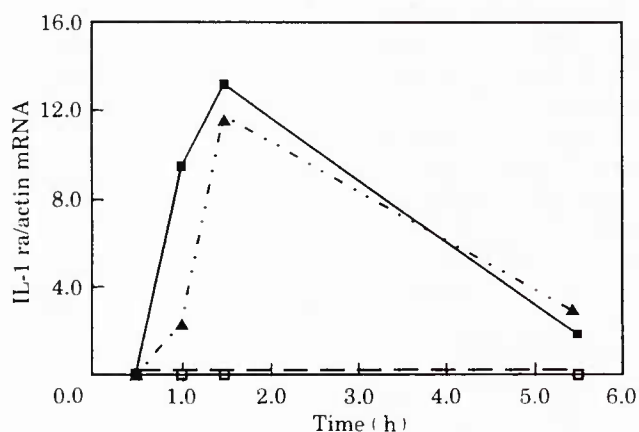**TABLE 1. Stimulation of in vivo fibrinogen production by cytokines.**

	Treatment			Fibrinogen (% control)
	IL-1 (ng)	IL-6 (µg)	IL-1ra (µg)	
1.	–	–	–	100
2.	10		–	147 ± 15
3.	300	–	–	264 ± 5
4.	–	0.25	–	146
5.	–	1.25	–	157 ± 20
6.	300	–	100	115 ± 15
7.	–	–	75	110
8.	–	1.25	10	167 ± 7
9.	–	1.25	75	194 ± 7
10.	–	1.25	100	213 ± 23

Mice were bled 24 h after injections. Values are means and standard errors of two to three experiments, each three or four mice per group. Exceptions are numbers 4 and 7 where data from one experiment were available.

The stimulatory effect of IL-1 on Fg production was blocked by the co-administration of IL-1ra with IL-1. In contrast, the stimulation of Fg by IL-6 was enhanced by co-administration of IL-1ra and IL-6.

Endogenous IL-1ra Production in Response to IL-1 but Not IL-6

Endogenous expression of IL-1ra mRNA in liver was detectable 1 and 1.5 h after administration of IL-1 alone and in combination with IL-6, but not after IL-6 alone (Fig. 1). The polyadenylated RNA enriched

Figure 1. Kinetics of IL-1ra mRNA, relative to beta-actin mRNA in livers of mice.

Results are given 0, 1, 1.5 and 5 h after administration of IL-1 (---▲---; 300 ng). IL-6 (---☐---; 1.25 µg) alone or in combination (---■---) to mice. Northern blots were prepared from mouse liver RNA enriched in polyadenylated mRNA, 3–5 µg/lane. Results are representative of four experiments.

fractions contained varying amounts of ribosomal RNA, leading to fluctuation in the relative abundance of beta-actin mRNA. Therefore the results shown in Fig. 1 are normalized for the content of beta actin in each preparation; the quantities of beta-actin and GAPDH mRNA were comparable. IL-1ra mRNA was not detectable at 30 min, appeared to reach maximal levels at 2–3 h and was expressed at a diminished level by 5.5 h after IL-1 administration.

IL-1 Stimulates Fg and SAA Production by Induction of IL-6
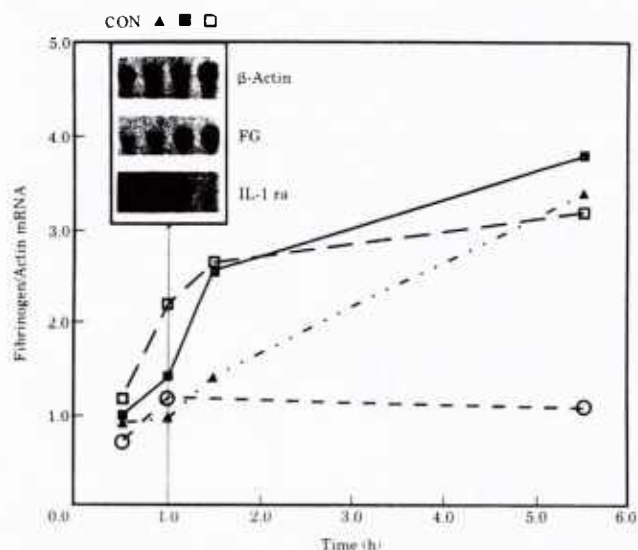
IL-6 has been shown to mediate other in vivo responses to IL-1;[22,23] the role of IL-6 in IL-1 stimulated Fg gene expression was indicated by the reduction in stimulation of Fg after administration of 20 ng IL-1 to mice passively immunized with anti-IL-6 antiserum 16 h earlier (Table 2) as compared with Fg

TABLE 2. Passive immunization with anti-IL-6 antibodies blocks stimulation of fibrinogen by IL-1.

Pretreatment	Fibrinogen		SAA (µg/ml)
	Protein (% control)	mRNA (Fg/Actin mRNA)	
None	176 ± 15	1.0	248 ± 25
Anti-IL-6	118 ± 17	0.6	93 ± 4
Rat Ig Control	310 ± 15	nd	196 ± 2
G113, Ab Control	182 ± 9	1.2	220 ± 16

Each of three mice per group were injected with 600 µg of each Ig 16–20 h prior to stimulation with 20 ng of IL-1. Values are mean and standard errors of individual plasma samples obtained 24 h after administration of IL-1. nd = not done. Results are representative of two to four experiments.

concentration in mice that received no pretreatment or received control immunoglobulins. The ratio of hepatic Fg mRNA to hepatic actin mRNA 1 h after administration of IL-1 to mice pretreated with anti-IL-6 antibodies was 50% of that in mice treated with control immunoglobulins or in mice with no pretreatment (Fig. 2). The in vivo production of IL-6 following IL-1 was further demonstrated by reduction in plasma SAA (Table 2) which is known to be produced in response to the synergistic action of IL-1 and IL-6.[24] We used a hybridization probe for gamma-Fg in these studies; expression of alpha, beta and gamma chains has been shown to proceed essentially co-ordinately[25] and in our study hybridization with either gamma-Fg or alpha-Fg specific cDNA probes revealed similar kinetics (Figs 1, 2).

Figure 2. Kinetics of Fg and IL-1ra (mRNA, relative to beta-actin mRNA in livers of mice.

Results are given 0, 1, 1.5 and 5 h after administration of IL-1 (20 ng). IL-6 (1.25 μg) alone and in combination to mice that received anti-IL-6 antibodies (600 μg), control immunoglobulins (600 μg) or no treatment 16 h earlier. ---▲---, IL-1; —-□—-, IL-6; —■—, IL-1 + IL-6; —-○—-, IL-1 + anti IL-6. Northern blots were prepared from mouse liver RNA enriched in polyadenylated mRNA. 3–5 μg/lane. Insert shows the Northern hybridization signal for the 1 h time point. Results are representative of four experiments.

DISCUSSION

This study has addressed the conflicting observations that IL-1 suppresses Fg gene expression in hepatoma cell lines, yet enhances Fg gene expression in mice.[1,2,5] The basis for increased concentrations of plasma Fg during the acute phase response, has, for the first time, been investigated by combining an analysis of plasma protein changes with changes in mRNA expression in liver. Using IL-1ra together with IL-6 we can confirm in the in vivo situation the previously reported in vitro inhibition of Fg gene expression by IL-1. Our results also provide strong evidence that, in vivo, IL-1 counteracts its direct inhibitory effect on Fg gene expression by stimulation of IL-1ra and IL-6 gene expression. In turn, IL-6 directly stimulates Fg gene expression and IL-1ra blocks inhibition of Fg gene expression by IL-1 leading to increased Fg production in the presence of IL-6.

The observation of IL-1ra mRNA expression in mice following IL-1 but not IL-6 administration (Fig. 2) suggests that IL-1ra exerts both temporal and bidirectional quantitative regulation of acute phase changes in liver protein synthesis by counteracting

both the synergistic interaction of IL-1 with IL-6 required for SAA induction and its antagonistic effect on Fg induction by IL-6.[5,18–22,24] IL-1 has been shown to influence the effects of IL-6 on plasma proteins other than Fg. For example, IL-1 acts synergistically with IL-6 to enhance SAA gene expression by Hep 3B and Hep G2 cells.[24] IL-1 has been shown to decrease the stimulatory effect on IL-6 on alpha-2-macroglobulin as well as Fg in Hep G2 cells.[5] These reports together with our findings in this paper indicate that IL-1 and IL-6 interactions may be one of the factors that contribute to the unique kinetic changes that individual acute phase reactants undergo during the acute phase response.

The mechanism by which IL-1 reduces constitutive Fg production and IL-6 induced Fg gene up-regulation is not understood. The Fg genes are expressed constitutively in liver and are further stimulated by dexamethasone and IL-6 and indirectly by IL-1 and TNF.[1,3,22,26] The studies of Huber and co-workers demonstrated the interplay between IL-6 and glucocorticoid responsive elements in the promoter region of Fg genes.[26] Fluctuation in receptor ratios and/or occupancy may play a role in the inhibitory effect of IL-1 on Fg gene expression. The recent studies of Nesbitt and Fuller[27] indicate that IL-1 and, to a lesser extent, IL-6, may elicit a transient reduction in the number of IL-6 receptors in rat hepatocytes, whereas IL-6 and IL-1 increased IL-6 receptor mRNA in human primary hepatocytes.[28] Other explanations may lie in the selective interaction of transcription factors. Thus, while our study has resolved the paradox of the conflicting in vivo and in vitro effects of IL-1 on Fg gene expression, the question as to how IL-1 down-regulates Fg remains.

MATERIALS AND METHODS

Experimental Animals

Female CD2F1-mice, 6–8 weeks of age, free from overt disease, were employed. All animal handling procedures were performed as described[29] in compliance with guidelines from the National Research Council and the Armed Forces Radiobiology Research Institute. At various time points, citrated plasma was collected and livers were removed and snap-frozen in liquid nitrogen and stored at −85°C for subsequent mRNA analysis.

Reagents

Recombinant human IL-1 alpha was the gift of Dr Peter Lomedico of Hoffman-LaRoche, Nutley, NJ. The preparation, lot IL-1 2/88 was stored in aliquots at −20°C until use. Recombinant human interleukin 6, lot PPG9001 was provided by Dr E. Liehl, Sandoz Pharme AG, Basel,

Switzerland. The IL-1ra was provided by Dr Robert Thompson, Synergen, Boulder, CO. Rat monoclonal antibody to recombinant mouse IL-6 (MP5 20F3) was prepared using partially purified Cos-7 mouse IL-6 as immunogen (22). Rat monoclonal antibody to beta-galactosidase was used as an isotype control.[23]

Protein Assays

Fibrinogen in citrated plasma was measured as the rate of conversion of fibrinogen to fibrin in the presence of excess thrombin using the Sigma Diagnostic Kit (Sigma Chemical Co., St Louis, MO) as calibrator to express the data as milligrams of fibrinogen per 100 ml plasma. Measurements of fibrin clot formation were performed on a fibrometer (Becton-Dickinson Co., Fairleigh, N.J.). Mouse SAA was measured by ELISA (Hemagen Diagnostics, Waltham, MA).

RNA Extraction and Northern Blot Hybridization Analysis

Polyadenylated RNA was extracted from individual and pooled livers using Mini RiboSep mRNA isolation kits (Collaborative Research, Bedford, MA) according to the manufacturer's instructions. RNA was denatured by glyoxylation and size-fractionated by electrophoresis through 1.5% agarose, and transferred to Genescreen Plus nylon membranes (Dupont NEN, Boston, MA). The quantity of IL-1ra,[16] fibrinogen,[30] actin[31] and GAPDH[32] mRNA in each lane was determined by hybridization with the corresponding cDNA probes labelled with alpha-32P-dCTP (Dupont NEN, Boston, MA) using a random priming oligonucleotide labelling kit (Bethesda Research Laboratories, Gaithersburg, MD). Unincorporated cCTP was removed from the reaction mixture through the use of Nensorb columns (Dupont NEN). Following overnight hybridization at 42°C, filters were washed as previously described[33] and exposed to X-ray film at −70°C for 2–24 h. The relative abundance of SAA mRNA was measured relative to beta actin by scanning densitometry of autoradiographs following Northern blot hybridization.

Acknowledgements

REFERENCES

1. Gordon AH, Koj A (1985) The Acute Phase Response to Injury and Infection. Elsevier, Amsterdam. pp 1–339.

2. Sipe JD (1989) The molecular biology of interleukin-1 and the acute phase response. Adv Internal Med 34:1–20.

3. Baumann H, Gauldie J (1990) Regulation of hepatic acute phase plasma protein genes by hepatocyte stimulating factors and other mediators of inflammation. Mol Biol Med 7:147–159.

4. Magielska-Zero D, Bereta J, Czuba-Pelech B, Pajdak W, Gauldie J, Koj A (1988) Inhibitory effect of recombinant human interferon gamma on synthesis of some acute phase proteins in human hepatoma HepG2 stimulated by leukocyte cytokines, TNF alpha and INF-beta2/BSF2/IL-6. Biochem Int 17:17–23.

5. Darlington GJ (1989) Response of liver genes to acute phase mediators. Ann NY Acad Sci 557:310–315.

6. Neta R, Vogel SN, Sipe JD, Wong GG, Nordan RP (1988) Comparison of in vivo effects of human recombinant IL-1 and human recombinant IL-6 in mice. Lymphokine Res 7:403–412.

7. Rokita H, Szuba K (1991) Regulation of acute phase reaction by transforming growth factor beta in cultured murine hepatocytes. Acta Biochim Polon 38:241–249.

8. Bertini R, Bianchi M, Erroi A, Villa P, Ghezzi P (1989) Dexamethasone modulation of in vivo effects of endotoxin, tumor necrosis factor, and interleukin-1 on liver cytochrome P-450, plasma fibrinogen, and serum iron. J Leuk Biol 46:254–262.

9. Arend WP (1991) Interleukin-1 receptor antagonist. A new member of the interleukin 1 family. J Clin Invest 88: 1445–1451.

10. Eisenberg SP, Evans RJ, Arend WP, Verderber E, Brewer MT, Hannum CH, Thompson RC (1990) Primary structure and functional expression from complementary DNA to a human interleukin-1 receptor antagonist. Nature 343:341–346.

11. Carter DB, Deibel MR, Dunn CJ, Tomich C-SC, Laborde AL, Slightom AL, Berger AE, Bienkowski MJ, Sun FF, McEwan RN, Harris PKW, Yem AW, Waszak GA, Chosay JG, Sieu LC, Hardee MM, Zurcher-Neely HA, Reardon IM, Heinrikson RL, Truesdell SE, Shelly JA, Eessalu TE, Taylor BM, Tracey DE (1990) Purification, cloning, expression and biological characterization of an interleukin-1 receptor antagonist protein. Nature 344:633–638.

12. Vogel SN, Henricson BE, Neta R (1991) Roles of interleukin-1 and tumor necrosis factor in lipopolysaccharide-induced hypoglycemia. Infect Immun 59:2494–2498.

13. Henricson BE, Neta R, Vogel SN (1991) Interleukin-1 receptor antagonist blocks lipopolysaccharide-induced colony-stimulating factor production and early endotoxin tolerance. Infect Immun 59:1188–1191.

14. Neta R, Abrams J, Perlstein R, Rokita H, Sipe JD, Vogel SN, Whitnall M (1992) Interaction of cytokines, IL-1, TNF and IL-6 in in vivo host responses. In Revel M (ed.), IL-6, Physiopathology and Clinical Potential, Raven Press, New York, pp 195–202.

15. Numerof R, Sipe JD, Zhang Z, Dinarello CA, Mier JW (1990) Use of the IL-1 receptor antagonist (IL-1ra) in IL-2 treated mice. Lymphokine Res 9:612.

16. Zahedi K, Seldin MF, Rits MF, Ezekowitz AB, Whitehead AS (1991) Mouse IL-1 receptor antagonist protein. Molecular characterization, gene mapping, and expression of mRNA in vitro and in vivo. J Immunol 146:4228–4233.

17. McIntyre KW, Stepan GJ, Kolinsky KD, Benjamin WR, Plocinski JM, Kaffka KL, Campen CA, Chizzonite RA, Kilian PL (1991) Inhibition of interleukin-1 (IL-1) binding and bioactivity in vitro and modulation of acute inflammation in vivo by IL-1 receptor antagonist and anti-IL-1 receptor monoclonal antibody. J Exp Med 173:931–939.

18. Mackiewicz A, Speroff T, Ganapathi MK, Kushner I (1991) Effects of cytokine combinations on acute phase protein production in two human hepatoma cell lines. J Immunol 146:3032–3037.

19. Malawista SE, Van Damme J, Sipe JD, Duff GW, Weiss MC (1989) Independent effects of interleukin 6 (IL-6) and interleukin 1 (IL-1) on accumulation of specific mRNA for fibrinogen and for serum amyloid A in human hepatoma (HepG2) cells. Ann NY Acad Sci 557:518–520.

20. Darlington GJ, Wilson DR, Lachman LB (1986) Monocyte-conditioned medium, interleukin-1 and tumor necrosis factor stimulate the acute phase response in human hepatoma cell lines. J Cell Biol 103:787–793.

21. Heinrich P, Castell JV, Andus T (1990) Interleukin-6 and the acute phase response. Biochem J 265:621–636.

22. Starnes HF, Pearce MK, Tewari A, Yim JH, Zou JC, Abrams JS (1990) Anti-IL-6 monoclonal antibodies protect against lethal Escherichia coli infection and lethal tumor necrosis factor a challenge in mice. J Immunol 145:4185–4191.

23. Neta R, Perlstein R, Vogel SN, Ledney GD, Abrams J (1992) Role of interleukin 6 (IL-6) in protection from lethal irradiation and in endocrine responses to IL-1 and tumor necrosis factor. J Exp Med 175:689–694.

24. Sipe JD, Rokita H, Bartle LM, Loose LD, Neta R (1991) The IL-1 receptor antagonist simultaneously inhibits SAA and stimulates fibrinogen synthesis in vivo and in vitro: a proposed mechanism of action. Cytokine 3:497.

25. Fuller GM, Otto JM, Woloski BM, McCary CT, Adams MA (1985) The effects of hepatocyte stimulating factor on fibrinogen biosynthesis in hepatocyte monolayers. J Cell Biol 101:1481–1486.

26. Huber P, Laurent M, Dalmon J (1990) Human beta-fibrinogen gene expression. Upstream sequences involved in its tissue specific expression and its dexamethasone and interleukin 6 stimulation. J Biol Chem 265:5695–5701.

27. Nesbitt JE, Fuller GM (1992) Differential regulation of interleukin-6 receptor and gp130 gene expression in rat hepatocytes. Mol Biol Cell 3:103–112.

28. Bauer J, Bauer TM, Kalb T, Taga T, Lengyel G, Hirano T, Kishimoto T, Acs G, Mayer L, Gerok W (1989) Regulation of interleukin-6 receptor expression in human monocytes and monocyte-derived macrophages. J Exp Med 170:1537–1549.

29. Perlstein RS, Mougey EH, Jackson WE, Neta R (1991) Interleukin-1 and interleukin-6 act synergistically to stimulate the release of adrenocorticotropic hormone in vivo. Lymphokine Cytokine Res 10:141–146.

30. Bolyard MG, Lord ST (1988) High-level expression of a functional human fibrinogen gamma chain in Escherichia coli. Gene 66: 183–192.

31. Bond JF, Farmer SF (1983) Regulation of tublin and actin mRNA production in rat brain: Expression of a new beta tubulin mRNA with development. Mol Cell Biol 3:1333–1342.

32. Tso JY, Sun X-H, Kao T-h, Reece KS, Wu R (1985) Isolation and characterization of rat and human glyceraldehyde-3-phosphate dehydrogenase cDNAs: genomic complexity and molecular evolution of the gene. Nucleic Acids Res 13:2485–2502.

33. Rokita H, Shirahama T, Cohen AS, Meek RL, Benditt EP, Sipe JD (1987) Differential expression of the amyloid SAA3 gene in liver and peritoneal macrophages of mice undergoing dissimilar inflammatory episodes. J Immunol 139:3849–3853.

Ulstrastructural localization of tumour necrosis factor-alpha

ELSA A. SCHMAUDER-CHOCK[1], STEPHEN P. CHOCK[2] and MYRA L. PATCHEN[1]

[1]*Department of Experimental Hematology, Armed Forces Radiobiology Research Institute, Bethesda, Maryland 20889-5603, and*

[2]*The Department of Biochemistry and Molecular Biology, Howard University College of Medicine, Washington, DC 20059, USA*

Summary

The application of an antibody against tumour necrosis factor-alpha (TNF) to thin sections of plastic-embedded mouse tissue has identified sites of TNF activity in normal and endotoxin-treated C_3N/HeN mice. Prior to endotoxin treatment, TNF was observed in the secretory granules of the antibacterial Paneth cell and one type of crypt endocrine cell. Four hours after endotoxin treatment, these two types of intestinal cell were found to have degranulated. In addition, endotoxin treatment resulted in the appearance of TNF in the secretory granules of all eosinophils, neutrophils and monocytes in the bone marrow, spleen, lung and the proximal intestine. TNF was also observed in the internal elastic lamina (IEL) of arterioles. These results suggest that the process of TNF induction specifically targets the immune system and the vasculature. An invasive stimulus, such as circulating endotoxin, can provoke the immune cells to be armed with TNF. That same stimulus may cause arteriole smooth muscle cells to secrete TNF. TNF secretion in the presence of arteriole smooth muscle cells may play a role in the adjustment of arteriole tone. In the venules, TNF may be responsible for platelet and neutrophil accumulation which leads to embolism formation.

Introduction

The relationship between endotoxin and septic shock with tissue injury has been well documented (Tracey *et al.*, 1986; Rothstein & Schreiber, 1988; Havell, 1989; Natanson *et al.*, 1989; Hinshaw *et al.*, 1990; Wakabayashi *et al.*, 1991). It has been suggested by Natanson and others, that endotoxin is not a requirement for septic shock since microorganisms, with or without endotoxin, can provoke a similar vascular response. It was thought that the invading microorganisms might be able to induce the expression of endogenous host mediators to target the vasculature and the immune system. The over-expression of these factors would ultimately cause the dysfunction of the target tissues. The cytokine tumour necrosis factor-alpha (TNF) (cachectin), has been considered to be one of the host factors involved. An invasive stimulus, such as sepsis, initiates TNF synthesis. Excessive secretion of TNF leads to the condition of cachexia which is manifested by shock, multiple organ failure, wasting and death (Beutler & Cerami, 1986).

To better understand the mechanism by which an invasive stimulus targets the vasculature and the immune system, we have applied immunocytochemical techniques to localize TNF in tissues from normal and endotoxin-treated mice. In normal mice, we found the presence of TNF in the secretory granules of Paneth cells and endocrine cells in the crypts of Lieberkuhn of the proximal small intestine. Endotoxin treatment resulted in the appearance of TNF in the secretory granules of all neutrophils, eosinophils and monocytes examined. TNF was also localized in the internal elastic lamina of arterioles. The relationship between the site of TNF localization and the manifestation of tissue injury will be discussed.

Materials and methods

Animals

C3H/HeN female mice of about 20 g in body-weight were purchased from Charles River Laboratories (Raleigh, NC). Mice were maintained in Micro-Isolator cages (Lab Products, Marywood, IL) and maintained on commercial rodent chow and acidified water (pH 2.5) *ad libitum* in a facility accredited by the American Association for Accreditation of Laboratory Animal Care. All animals were quarantined on arrival and tested for

Pseudomonas. Only healthy mice were released for experimentation. All animal protocols were pre-approved by an in-house Animal Care and Use Committee.

Endotoxin

Lipopolysaccharide derived from *Escherichia coli* (number 437635, Calbiochem Corp., San Diego, CA) was diluted to a concentration of 50 μg ml^{-1} with sterile saline, and 0.1 ml (5 μg) was injected into the lateral tail vein of each mouse. Four hours later, mice were killed by cervical dislocation and specimens removed and fixed. Specimens obtained from uninjected mice were used as controls.

Specimen preparation

Specimens were obtained from the proximal small intestine, spleen, bone marrow and lung and were immediately immersion-fixed in 1% paraformaldehyde (J. T. Baker Chemical, Phillipsburg, NJ) in a 100 mM cacodylate buffer (pH 7.3) containing 4 mM MgCl$_2$. Tissue specimens were dehydrated in a graded series of methanol and embedded in L.R. White acrylic resin (The London Resin Co. Ltd, England) at 38°C in gelatin capsules. Thick sections were stained with a mixture of Methylene Blue (1%) and Azure II (1%) and photographed with a Zeiss Ultrophot microscope. Thin sections after cytochemistry were stained with 1% uranyl acetate in water and photographed with an Hitachi 7000 electron microscope. Because paraformaldehyde fixative has the disadvantage of not preserving cellular fine structure as well as glutaraldehyde does, attempts were made to perform studies using half-strength Karnovsky's fixative (a glutaraldehyde-containing fixative). Although it improved the general tissue appearance, this fixative also eliminated all binding of TNF antibody in the immunocytochemical assay. Washing tissue overnight to remove excess glutaraldehyde did not improve antibody binding.

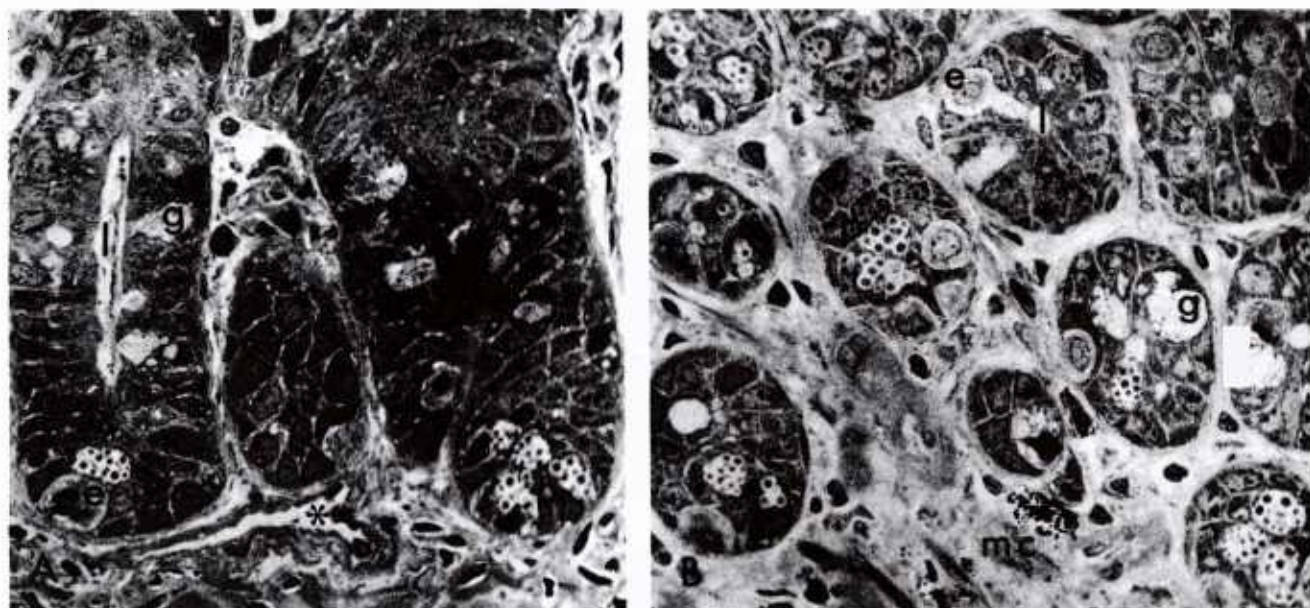Because of this limitation, paraformaldehyde was used as the fixative agent.

Antibody labelling

All thin sections were first floated on 20% normal whole goat serum (number 5006-1380 Cappel, Organon Teknika Corp., West Chester, PA). Without rinsing, sections were then floated overnight at room temperature on a 1:5 dilution of anti-TNF (number 654300 Calbiochem Corp., Mouse, Rabbit, IgG fraction), in antibody diluent. The antibody diluent was composed of 20 mM HEPES (N-2-hydroxyethylpiperazine-N'-2-ethansulphonic acid), 10 mM EGTA (ethyleneglycol-*bis*-(β-aminoethyl ether) N,N,N',N'-tetraacetic acid), 1% Tween 20, 1% bovine serum albumin, sodium chloride 0.43 M in deionized water. Control specimens were incubated overnight on a 1:100 dilution of normal rabbit serum (number 5012-1380 Cappel, Organon Teknika Corp., West Chester, PA) in antibody diluent. The following morning the specimens were rinsed with five changes of antibody diluent and then floated on a 1:10 dilution of 10 nm gold-conjugated goat anti-rabbit immunoglobulin G (number G-3766 Sigma, St Louis, MO) in antibody diluent for 1 h.
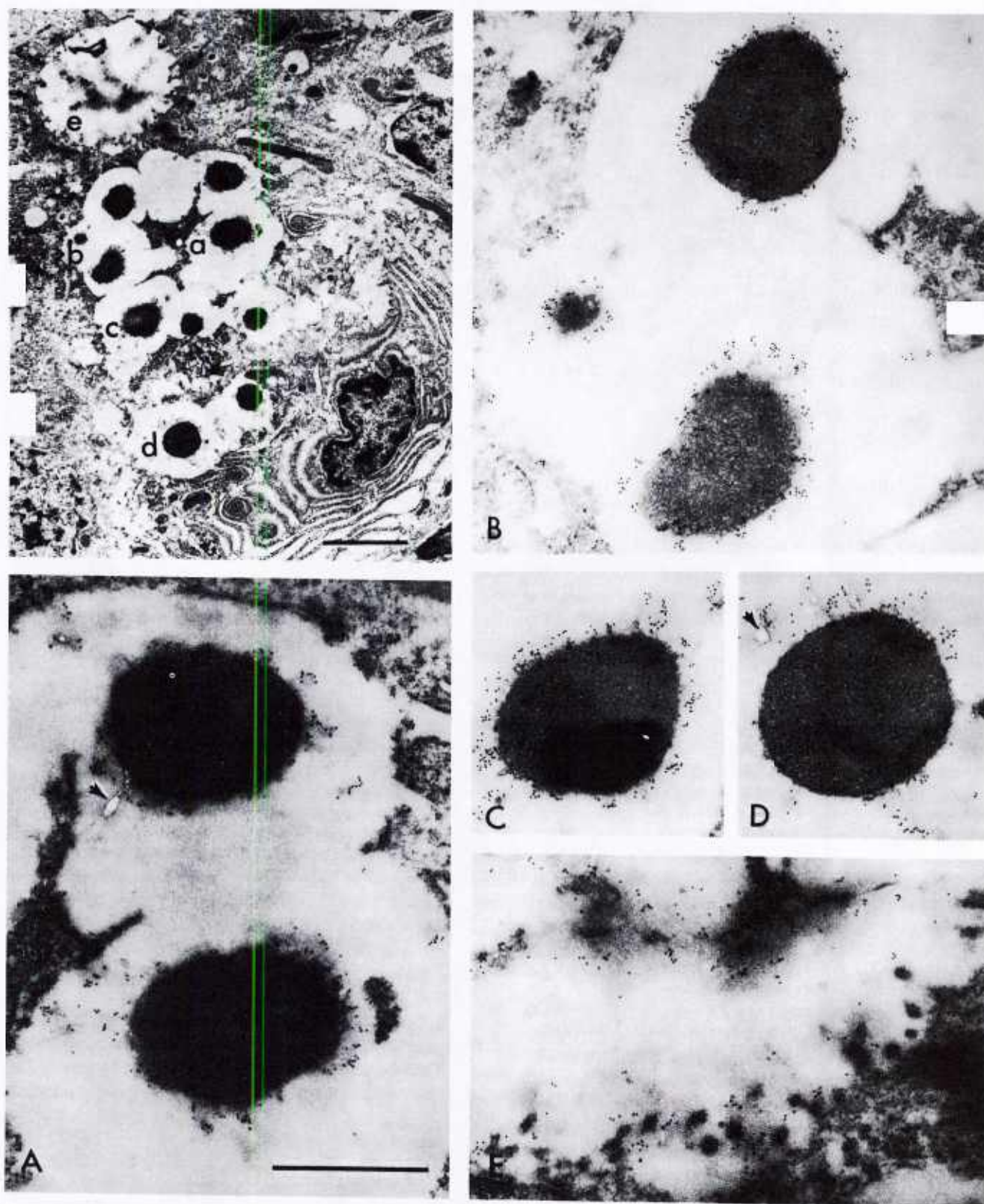
Results

Localization of TNF in specimens from normal mice

In normal (non-endotoxin-treated) mice, TNF label was found only in the granules of the Paneth cell and the endocrine cell in the intestinal crypt. Many granule-bearing cells, as a result of paraformaldehyde fixation, appeared to have been activated. This can be seen in the light microscopic image (Fig. 1). In Fig. 1A, the crypt region was sectioned longitudinally and its base was seen

Fig. 1. Light-microscopic images of the crypts of Lieberkuhn in the proximal small intestine of the mouse. Goblet cells (g) have secreted while the Paneth cells (p) are partially secreted. Endocrine cells (e) can be identified by their low optical density. Mast cells (mc) can be seen in the connective tissue. The lumen (l) is centrally located in each crypt. (A) Longitudinal section of the intestine containing a lymphatic duct (*). (B) Cross-section of the crypt region. ×1000.

144

Fig. 2. TNF localization in a Paneth cell. TNF label was observed in the granules (a–d) and in the crypt lumen (e). Low-magnification image = ×5075. Bar = 3 μm. (A–E) High-magnification images of areas marked (a) through (e) in the Paneth cell. The apparent bubbles (arrowheads) at the periphery of the activated granules are vesicles, and reflect the phospholipid content of the granules. High magnification = ×27 750. Bar = 1 μm.

Fig. 3. Localization of TNF in the secretory granules of an intestinal endocrine cell. A secreting Paneth cell (p) in the upper right corner, a second endocrine cell (e) in the upper left corner, and a circulating red blood cell (rbc) in a capillary in the lower right corner are also shown. Low-magnification image = ×7350. Bar = 2 µm. (A, B) High-magnification images of areas marked (a) and (b) in the endocrine cell. High magnification = ×38 500. Bar = 0.5 µm.

Fig. 4. Localization of TNF in the secretory granules of an eosinophil in the bone marrow after endotoxin administration. TNF label was observed in the secretory granules (a–c). Low-magnification image of cell = 11 900. Bar = 1 μm (A–C) High-magnification images of areas marked a–c in the eosinophil. High magnification = ×51 000. Bar = 0.2 μm.

to be occupied by Paneth cells and an unidentified endocrine cell. An endocrine cell with its cell body facing the submucosa and with a finger-like cytoplasmic extension touching the lumen was also seen (Fig. 1B). The connective tissue beneath the crypts is rich in lymphatic ducts and vasculature. The cross section of the crypts (Fig. 1B) also showed a large number of granule-bearing secretory cells.

The immunocytochemical localization of TNF in a typical Paneth cell is shown in Fig. 2. The activated granules were heavily labeled with anti-TNF, especially in the peripheral regions of the granules where their

matrices had become unravelled and dispersed. The inner domains of the granules which remained condensed appeared to have less TNF labelling (Fig. 2, A–D). This may occur because these compact hydrophobic areas are less accessible to antibody penetration. The surface of the luminal mucosa contained TNF as a result of Paneth cell secretion (Fig. 2E)

TNF was also observed in association with the granules of the endocrine cells in the crypt (Fig 3). These cells are normally located in areas adjacent to Paneth cells. The part of the cell body which contains the granules is usually located near the serosa and centrifugally from the

intestinal lumen aperture. These cells sample the luminal environment (Fig. 1B) and they release their granules near the basement membrane in response to stimuli arising in the lumen. They were easily identified by light- or electron-microscopy due to the low optical and electron density of their nucleus and cytoplasm.

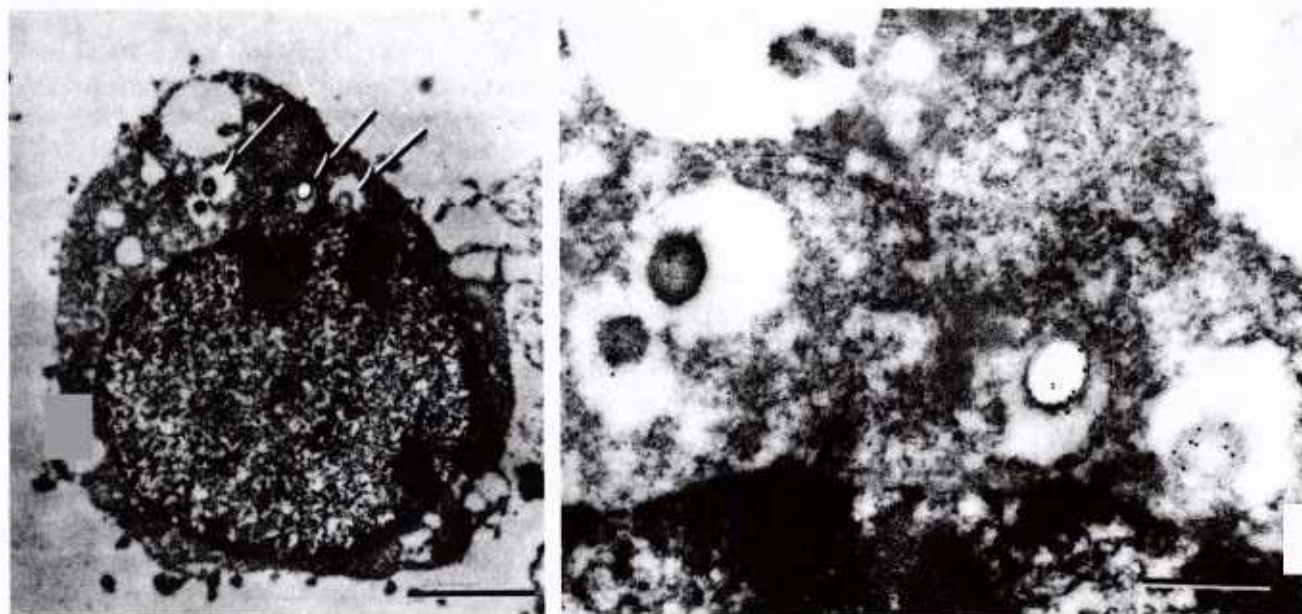*Localization of TNF in specimens from endotoxin-treated mice*
Endotoxin treatment resulted in the extensive degranulation of both the Paneth cells and the endocrine cells. Furthermore, endotoxin treatment also resulted in the appearance of TNF in the secretory granules of all eosinophils, monocytes and neutrophils in all tissues examined. Figures 4–6 show examples of labelled cells. In Fig. 4, an eosinophil in the bone marrow, after host endotoxin treatment, showed intense TNF activity in the secretory granules. TNF was also localized in bone marrow monocyte granules, as shown in Fig. 5. Several neutrophils in an intestinal venule were seen with light microscopy (Fig. 6A). One of these neutrophils (arrow), when examined with the electron microscope (Fig. 6B), exhibited cytoplasmic granules that contained TNF (Fig. 6, C–D). Circulating neutrophils of endotoxin-treated animals contained fewer granules than untreated controls, indicating that these cells had secreted as a result of endotoxin treatment. A large accumulation of platelets was seen adjacent to the neutrophils in the venule (Fig. 6A); within this accumulation there were amorphous materials that revealed a TNF content with high magnification (Fig. 6E). The platelets themselves did not exhibit TNF activity while the neighbouring neutrophils did. The neutrophils were assumed to be the source of this secreted TNF.

TNF was also localized in the internal elastic lamina (IEL) of arterioles in the bone marrow (Fig. 7). The images in Fig. 7 represent longitudinal sections through the lumen of an arteriole. The specific binding of TNF antibodies to the IEL was obvious. However, the origin of this TNF was not apparent because no significant localization of TNF was observed within either the adjacent endothelial cells or the underlying smooth muscle cells. Since the TNF label was seen in the elastin surrounding each smooth muscle cell in addition to the large ribbon which comprised the IEL, it can be assumed that the endotoxin-induced TNF might have been secreted by the smooth muscle cells with the elastin.
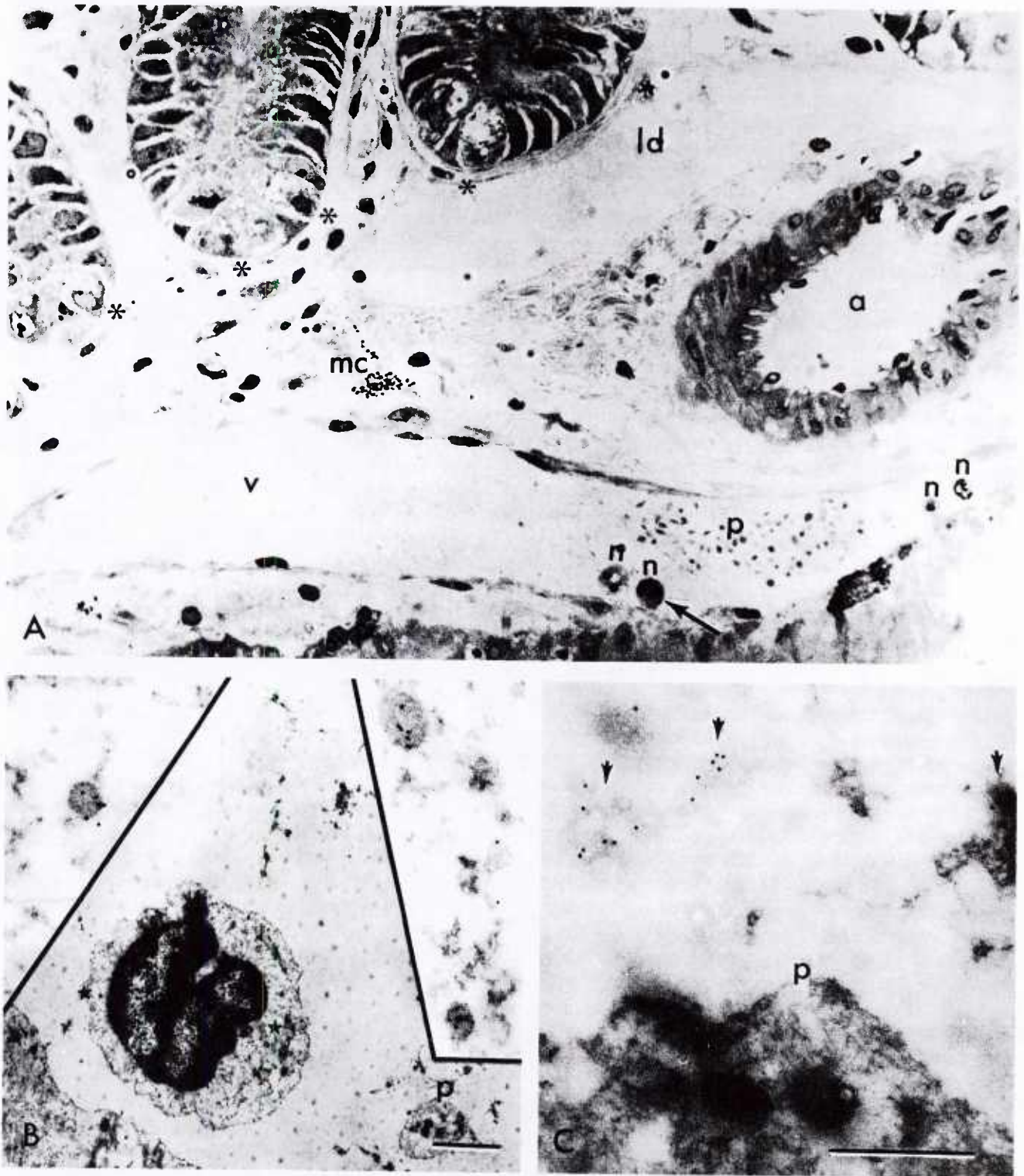
Specimens treated with normal pre-immune serum as control did not exhibit gold labelling.

Discussion

The role of TNF in terms of the immune function has been difficult to assign due to the many apparently opposing aspects of its actions. It has been implicated in derangement of host physiology as manifested by shock, wasting, multiple organ failure and death (Beutler & Cerami, 1986; Tracey *et al.*, 1986; Rothstein & Schreiber, 1988; Varani *et al.*, 1988; Luedke & Humes, 1989; Natanson *et al.*, 1989; Hinshaw *et al.*, 1990). Our observation of the sites of TNF localization has led us to believe that TNF may serve as a 'signal' to the host of an invasive trauma or threat. In this study, that threat was the presence of circulating endotoxin which was perceived by the host as a systemic bacterial infection. The host responded to this threat by inducing the synthesis and the release of TNF by cells of the immune system and vasculature.
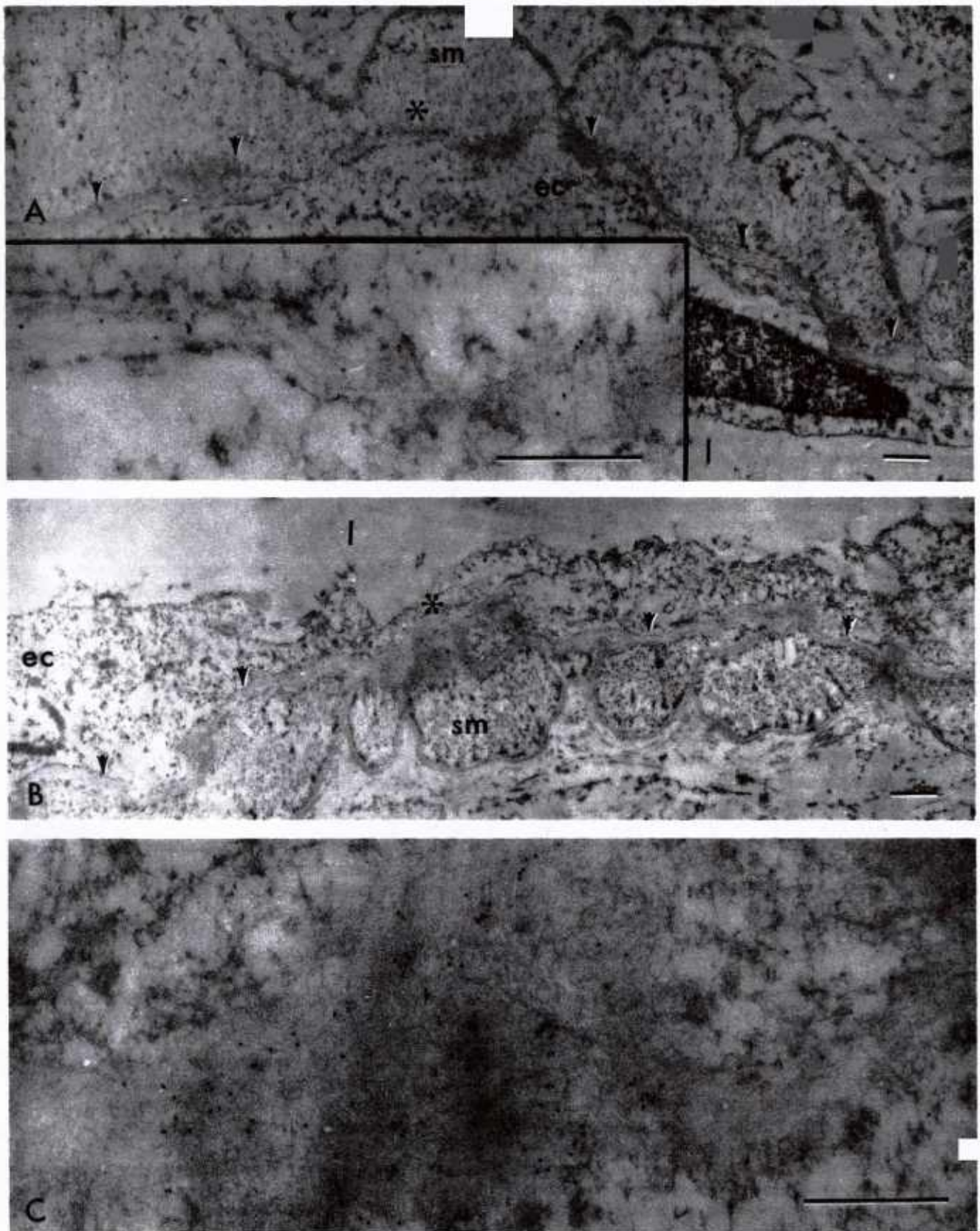

Fig. 5. Localization of TNF in the secretory granules of a monocyte in the bone marrow. On the left is the low-magnification image of the monocyte at ×8575. Bar = 2 μm. On the right is the high-magnification image of the area marked with arrows in the monocyte. ×34 500. Bar = 0.5 μm.

Fig. 6. The intestinal crypt area 4 hours after endotoxin treatment. (A) Light micrograph. Paneth and endocrine cells have totally secreted their granules (*). The close proximity of the crypts to a lymphatic duct (ld), an arteriole (a) and a venule (v), can be seen. Neutrophils (n) in the venule are in association with an accumulation of platelets (p) in what may represent early embolism formation. A mast cell (mc) is seen in the connective tissue Light-micrograph magnification = ×1000. (B) Electron-micrograph of the neutrophil indicated with an arrow in the light-micrograph. (p) is a platelet. Areas indicated by stars (*) in (B) are seen in high magnification in insets where the granules show label for TNF. Magnification for (B) = 5600. Bar = 2 μm. (C) Electron-micrograph of area adjacent to platelet (p) shows an amorphous material labelled for TNF (arrowheads). Magnification for (C) and the insets in (B) = ×50 250. Bar = 0.5 μm.

Fig. 7. Localization of TNF in the internal elastic lamina of a bone marrow arteriole. (A) and (B) represent low-magnification images of longitudinal sections showing the lumen (l), endothelial cells (ec), smooth muscle cells (sm) and the internal elastic lamina (arrowheads) of an arteriole. ×8550. Bars = 1 µm. The inset represents a high-magnification image of the elastin (*) shown in (A), while (C) represents the elastin (*) shown in (B). High magnification = ×52 500. Bars = 0.5 µm.

The Paneth cell and the intestinal endocrine cell reside within the crypts of Lieberkuhn. These crypts are pockets in the gut wall where bacteria, including endotoxin-producing Gram-negative bacteria, are normally present (Fig. 1). Our observations indicate that the chronic presence of bacteria in the gut induced TNF synthesis in the Paneth cell and the endocrine cell of normal, non-endotoxin-treated, animals (Figs 2 and 3). The administration of exogenous endotoxin caused these two types of cell to degranulate and release TNF further. The Paneth cell secretes TNF into the lumen and this may serve to signal the intestinal mucosa of a bacterial threat. The Paneth cell, which also secretes lysozyme and immunoglobulin A (Rodning et al., 1976; Hauptman & Tomasi, 1976), may be an important component of the host intestinal immune defence system. Due to the strategic location of the endocrine cell granules, TNF secretion from these cells would be directed toward the vicinity of the vasculature and the lymphatic ducts in the connective tissues. This may serve to signal the circulating immune cells of a local presence of bacteria. This endocrine cell and the Paneth cell may play an important role in immune functions.

The injection of endotoxin into the general circulation induced the synthesis and the packaging of TNF in the secretory granules of all eosinophils, monocytes and neutrophils examined (Figs 4–6). The neutrophils and probably the monocyte, besides containing TNF in their granules, also exhibited fewer than a normal complement of granules. This might suggest that endotoxin had stimulated these cells to secrete their TNF into the circulation (Djeu et al., 1990; Dubravec et al., 1990). Neutrophils were often observed in the presence of large numbers of platelets within the venules (Fig. 6) in what appeared to be early embolism formation. The increased number of platelets in association with neutrophils was only observed in venules, and not in arterioles.

Following endotoxin treatment, TNF also appeared in the elastin surrounding each smooth muscle cell. This TNF was more apparent in the thick elastic ribbon, the IEL, which comprises the physical substrate for the attachment of endothelial cells in the arterioles (Fig. 7). The presence of TNF in the IEL and the release of TNF by neutrophils and other circulating immune cells in the arteriole, represents a potential exposure of the endothelial cells to TNF sources from both the lumen as well as the attachment matrix.

In our experiments we did not detect TNF labelling in the macrophage. This may be due to the fact that the maximal level of TNF induction in the macrophage usually occurs within one hour and declines rapidly thereafter (Chensue et al., 1991). This narrow window of TNF production must have been missed in our four-hour time period between endotoxin injection and tissue fixation.

Rothstein & Schreiber (1988) have studied the endotoxin response in pathogen-free mice. They concluded that, for tissue injury to occur, four criteria needed to be met. These included endotoxin priming, TNF secretion,

neutrophil activation, and an unidentified 'cellular responsiveness'. In our experiment, we have also observed TNF secretion and neutrophil activation following endotoxin priming. Furthermore, we have also consistently observed a response by the vasculature. This vascular responsiveness to endotoxin includes neutrophil and platelet aggregation (embolism formation) in the venules and an accumulation of TNF in the arteriole wall, that may imply a change in the arteriole tone.

We propose that, once the 'signal' of an invasive threat is perceived by the host, circulating granulocytes and monocytes become armed with TNF. They circulate normally and will secrete their TNF only when and where they are challenged by a specific stimulus. This makes the release of TNF very site-specific and localized.

In our experiments, endotoxin was injected systemically into the circulation, causing cells of the immune system and vasculature to become armed with TNF. Since neutrophils specifically respond to bacteria, the systemic presence of endotoxin could potentially trigger all neutrophils to secrete their TNF throughout the circulation.

The stimulation of neutrophils is accompanied by the release of lipid mediators such as platelet activating factor (Sisson et al., 1987; Warren et al., 1990; Mozes et al., 1991). In the venules, the endotoxin-triggered release of TNF and lipid mediators may be instrumental in causing the aggregation of platelets and neutrophils resulting in clot formation and venule occlusion.

The drastic drop in the mean arterial blood pressure associated with endotoxic shock has been linked to the release of lipid mediators such as prostaglandin E_2 (PGE_2), a well known vasodialator substance (Messina et al., 1976; Kettelhut et al., 1987; Mozes et al., 1991). The localization of cyclo-oxygenase and PGE_2 in the secretory granule, and the localization of PGE_2 in the IEL of intestinal arterioles, have also been reported (Schmauder-Chock & Chock, 1989, 1992). It can be implied that TNF and lipid mediators may be responsible for the drop in arterial tone associated with septic shock. Our localization of TNF, and additionally, the previous localization of PGE_2 to the IEL, lead us to consider that the arterial smooth muscle may react to circulating stimuli with the production of vaso-active mediators such that they may self-regulate their own tonicity. This may be a means of regulating the local blood flow.

Venule occlusion may be an intrinsic mechanism of the vasculature to confine invasive bacteria to the capillary bed and prevent their distribution into the general circulation. Venule occlusion, when coupled with a drop in the arteriole tone, may serve to increase the capillary blood volume and to facilitate the influx of immune cells to combat the invasive bacteria. Therefore, in the micro-environments, these mechanisms serve to limit the scope of an invasive threat and facilitate the elimination of bacteria from the circulation. However, when they function systemically, they may induce shock, multiple organ failure, wasting and death.

Acknowledgements

References

BEUTLER, B. & CERAMI, A. (1986) Cachectin and tumor necrosis factor as two sides of the same biological coin. *Nature* **320**, 584–8.

CHENSUE, S. W., TEREBUH, P. D., REMICK, D. G., SCALES, W. E. & KUNKEL, S. L. (1991) *In vivo* biologic and immunohistochemical analysis of interleukin-1 alpha, beta and tumor necrosis factor during experimental endotoxemia. Kinetics, Kupffer cell expression, and glucocorticoid effects. *Am. J. Pathol.* **138**, 395–402.

DJEU, J. Y., SERBOUSEK, D. & BLANCHARD, D. K. (1990) Release of tumor necrosis factor by human polymorphonuclear leukocytes. *Blood* **76**, 1405–9.

DUBRAVEC, D. B., SPRIGGS, D. R., MANNICK, J. A. & RODRICK, M. L. (1990) Circulating human peripheral blood granulocytes synthesize and secrete tumor necrosis factor α. *Proc. Natl Acad. Sci. USA* **87**, 6758–61.

HAUPTMAN, S. P. & TOMASI, T. B. (1976) The secretory immune system. In *Basic and Clinical Immunology* (edited by FUDENBERG, H. H., STITES, D. P., CALDWELL, D. P. & WELLS, J. V.) pp. 170–81. Los Altos, CA: Lange Medical Publications.

HAVELL, E. A. (1989) Evidence that tumor necrosis factor has an important role in antibacterial resistance. *J. Immunol.* **143**, 2894–9.

HINSHAW, L. B., TEKAMP-OLSON, P., CHANG, A. C. K., LEE, P. A., TAYLOR, F. B. JR, MURRAY, C. K., PEER, G. T., EMERSON, T. E., PASSEY, R. B. & KUO, G. C. (1990) Survival of primates in LD$_{100}$ septic shock following therapy with antibody to tumor necrosis factor (TNFα). *Circulatory Shock* **30**, 279–92.

KETTELHUT, I. C., FIERS, W. & GOLDBERG, A. L. (1987) The toxic effects of tumor necrosis factor *in vivo* and their prevention by cyclooxygenase inhibitors. *Proc. Natl Acad. Sci. USA* **84**, 4273–7.

LUEDKE, E. S. & HUMES, J. L. (1989) Effect of tumor necrosis factor on granule release and LTB$_4$ production in adherent human polymorphonuclear leukocytes. *Agents Actions* **27**, 451–4.

MESSINA, E. J., WEINER, R. & KALEY, G. (1976) Prostaglandins and local circulatory control. *Fed. Proc.* **35**, 2367–75.

MOZES, T., ZIJLSTRA, F. J., HEILIGERS, J. P. C., TAK, C. J. A. M., BEN-EFRAIM, S., BONTA, I. L. & SAXENA, P. R. (1991) Sequential release of tumor necrosis factor, platelet activating factor and eicosanoids during endotoxin shock in anaesthetized pigs; protective effects of indomethacin. *Br. J. Pharmacol.* **104**, 691–9.

NATANSON, C., DANNER, R. L., ELIN, R. J., HOSSEINI, J. M., PEART, K. W., BANKS, S. M., MACVITTIE, T. J., WALKER, R. I. & PARRILLO, J. E. (1989) Role of endotoxemia in cardiovascular dysfunction and mortality. *Escherichia coli and Staphylococcus aureus* challenges in a canine model of human septic shock. *J. Clin. Invest.* **83**, 243–51.

RODNING, C. B., WILSON, I. D. & ERLANDSEN, S. L. (1976) Immunoglobulins within human small-intestinal Paneth cells. *Lancet* **1**, 984–7.

ROTHSTEIN, J. L. & SCHREIBER, H. (1988) Synergy between tumor necrosis factor and bacterial products causes hemorrhagic necrosis and lethal shock in normal mice. *Proc. Natl Acad. Sci. USA* **85**, 607–11.

SCHMAUDER-CHOCK, E. A. & CHOCK, S. P. (1989) Localization of cyclo-oxygenase and prostaglandin E$_2$ in the secretory granule of the mast cell. *J. Histochem. Cytochem.* **37**, 1319–28.

SCHMAUDER-CHOCK, E. A. & CHOCK, S. P. (1992) Protaglandin E$_2$ localization in the rat ileum. *Histochem. J.* **24**, 663–72.

SISSON, J. H., PRESCOTT, S. M., MCINTYRE, T. M. & ZIMMERMAN, G. A. (1987) Production of platelet-activating factor by stimulated human polymorphonuclear leukocytes. *J. Immunol.* **138**, 3918–26.

TRACEY, K. J., BEUTLER, B., LOWRY, S. F., MERRYWEATHER, J., WOLPE, S., MILSARK, I. W., HARIRI, R. J., FAHEY, T. J. III, ZENTELLA, A., ALBERT, J. D., SHIRES, G. T. & CERAMI, A. (1986) Shock and tissue injury induced by recombinant human cachectin. *Science* **234**, 470–4.

VARANI, J., BENDELOW, M. J., SEALEY, D. E., KUNKEL, S. L., GANNON, D. E., RYAN, U. S. & WARD, P. A. (1988) Tumor necrosis factor enhances susceptibility of vascular endothelial cells to neutrophil-mediated killing. *Lab. Invest.* **59**, 292–5.

WAKABAYASHI, G., GELFAND, J. A., JUNG, W. K., CONNOLLY, R. J., BURKE, J. F. & DINARELLO, C. A. (1991) *Staphylococcus epidermidis* induces complement activation, tumor necrosis factor and interleukin-1, a shock-like state and tissue injury in rabbits without endotoxemia. Comparison to *Escherichia coli. J. Clin. Invest.* **87**, 1925–35.

WARREN, J. S., BARTON, P. A., MANDEL, D. M. & MATROSIC, K. (1990) Intrapulmonary tumor necrosis factor triggers local platelet-activating factor production in rat immune complex alveolitis. *Lab. Invest.* **63**, 746–54.

THE ROLE OF INTERLEUKIN-6 IN LIPOPOLYSACCHARIDE-INDUCED WEIGHT LOSS, HYPOGLYCEMIA AND FIBRINOGEN PRODUCTION, IN VIVO

Gideon Strassmann, Miranda Fong, Sandra Windsor, Ruth Neta*

It was recently shown that interleukin (IL)-6 is an important mediator involved in the Colon (C)-26 model of experimental cancer cachexia. In this study, we wished to determine whether IL-6 is also involved in several metabolic changes associated with lipopolysaccharide (LPS) challenge. Administration of a relatively high amount of LPS to mice induced a transient weight loss, hypoglycemia, hypertriglyceridemia and an increase in the hepatic acute phase reactant, fibrinogen. Pretreatment of mice with the rat anti-murine IL-6 antibody (20F3), but not with a control antibody, resulted in a significant improvement of LPS-induced hypoglycemia and weight loss as well as a significant decrease of plasma fibrinogen. Anti- IL-6 antibody had no effect on LPS-induced hypertriglyceridemia. On the other hand, the pretreatment of mice with anti-murine TNF (TN3.19) antibody was able to completely inhibit elevation of triglycerides and modestly improve LPS-induced weight loss although it had no effect on hypoglycemia and fibrinogen production. Taken together, these results suggest that IL-6 plays a role in some of the metabolic changes associated with both an acute (i.e. LPS challenge) and chronic (C-26 cachexia) inflammatory conditions.

Prolonged exposure to an inflammatory stimulus may result in chronic wasting or cachexia. In neoplastic diseases, the presence of wasting of muscle and fat tissues is quite frequent[1] and complicates therapeutic intervention.[2] Tumor necrosis factor (TNF) has been suggested as a mediator of cancer cachexia because it suppresses metabolic enzymes such as lipoprotein lipase (LPL) activity and induces anorexia and weight loss when administered into experimental animals.[3-5] Recently, however, an experimental cachexia model has been identified that appears to involve another factor. This model involves a cell line derived from colon (C)-26 adenocarcinoma, which retains the transplantability of the original tumor and causes severe weight loss in syngeneic hosts.[6] In this model, we showed that interleukin (IL)-6 appears to have a more significant role than TNF in mediating the various parameters of wasting. This was based on the finding that the monoclonal antibody (MAb) against murine IL-6 (20F3) but not a MAb against murine TNF (TN3.19) could prevent the development of key parameters of cachexia, including weight loss, hypoglycemia and hepatic acute phase response.[6] More recently, IL-6 was also found to reduce LPL activity in vitro and in vivo.[7]

Profound metabolic disturbances are not restricted to chronic diseases but can also occur during infection.[8] Many of these metabolic changes can be reproduced by the administration of bacterial products such as lipopolysaccharides (LPS).[9,10] LPS induces TNF, IL-1 and IL-6, each of which is thought of as primary mediator of acute inflammation, since direct administration of each of them mimics some inflammatory events. The overlapping effects of cytokines, together with their induction of each other, as in the case of IL-1 and TNF, as well as the induction of IL-6 by both IL-1 and TNF, has complicated the precise determination of their individual contributions to events associated with acute inflammation.

In this report, using neutralizing anti-cytokine MAb, we attempted to determine the relative contribution of TNF and IL-6 in several metabolic changes associated with endotoxin shock in vivo.

RESULTS

LPS Induces Transient Weight Loss

To determine whether LPS induces weight loss in CD_2F_1 mice, increasing amounts of LPS were injected and the change in body weight was recorded at 24 h intervals (see Materials and Methods). The results in Table 1 show that LPS administration induces a transient but significant weight loss. Maximal change could be seen at 48 h after injection of 100 µg/mouse of LPS. Of note, maximal serum TNF and IL-6 levels in this system were found at 1–2 h and 3–4 h post-endotoxin (30 µg/mouse), respectively (data not shown). These results confirm those obtained previously.[11]

Inhibition of Weight Loss by Anti-IL-6 MAb

Next, we attempted to reverse the endotoxin-induced weight loss by the neutralizing anti-IL-6 antibody 20F3. Table 2 shows that pretreatment of mice with anti-IL-6 significantly reduced LPS-induced weight loss (10.9% in RIgG vs 3.2% in 20F3 treated

mice at 24 h and 14.1% in RIgG vs 4.7% in 20F3 treated mice, 48 h post-endotoxin). Anti-TNF MAb reduced by c. 50% the LPS-induced weight loss, but only within 48 h.

Differential Involvement of IL-6 and TNF in LPS-Induced Metabolic Changes

Table 3 clearly demonstrates that pretreatment of mice with MAb anti-IL-6 significantly inhibits LPS-induced hypoglycemia. In the same set of experiments, the pretreatment of mice with anti-TNF MAb did not improve hypoglycemia. The same pattern of differential involvement of these cytokines, could be observed with regard to LPS induction of the hepatic acute phase reactant fibrinogen. Table 4 shows that whereas the anti-IL-6 MAb 20F3 significantly reduced plasma fibrinogen concentrations, anti-TNF antibody did not affect the level of this LPS-induced inflammatory marker. On the other hand, pretreatment with anti-TNF almost completely blocked the LPS-induced increase in serum triglycerides (Table 5), whereas the anti-IL-6 MAb failed to block LPS-induced hypertriglyceridemia.

Modulation of Serum IL-6 Levels by Anti-TNF and Anti-IL-6 MAb

To determine whether the anti-cytokine MAb used in this study affected LPS-induced IL-6 levels,

TABLE 1. Time and dose dependent responses of LPS-induced weight loss.

Treatment	24 h	% weight loss 48 h	72 h	96 h
PBS	0	-1.0 ± 0.5	-1.0 ± 0.5	2.0 ± 0.5
LPS (10 µg/mouse)	5.1 ± 1.3	2.1 ± 1.0	3.2 ± 1.0	-1.2 ± 0.5
LPS (30 µg/mouse)	8.2 ± 1.7	9.5 ± 2.5	5.3 ± 2.0	-1.8 ± 0.5
LPS (100 µg/mouse)	10.4 ± 0.9	16.2 ± 1.2	8.1 ± 0.8	2.1 ± 0.2
LPS (300 µg/mouse)	10.0 ± 1.1	16.1 ± 1.5	8.3 ± 0.8	NT

CD_2F_1 male mice received an i.p. injection of 0.25 ml of PBS or the indicated amount of LPS. Weight loss was determined as described in Materials and Methods on six mice per group. Results are expressed as mean ± SD of cumulative % weight loss. NT =

TABLE 2. Inhibition of LPS induces weight loss by anti-IL-6 MAb.

Group	Pretreatment	Treatment	% weight loss at 24 h	% weight loss at 48 h
1	PBS	PBS	0	0
2	PBS	LPS	12.2 ± 1.5	15.0 ± 1.7
3	RIgG	LPS	10.9 ± 1.6	14.1 ± 1.5
4	HIgG	LPS	11.6 ± 2.6	16.5 ± 1.6
5	20F3	LPS	$3.2 \pm 2.9^*$	$4.7 \pm 1.5^*$
6	TN3.19	LPS	10.6 ± 1.2	$8.1 \pm 1.0^*$

CD_2F_1 mice (six per group) were pretreated 16 h before LPS injection (100 µg) with 0.6 mg per mouse of RIgG and 20F3 or with 0.3 mg per mouse of HIgG and TN3.19. Percent weight loss between the time of LPS injection and 24 and 48 h was recorded. Results are expressed as mean ± SD. Asterisk represents a P value less than 0.01 of group 5 from 3 and 6 from 4.

mice were pretreated with antibody and at various time points after LPS injection, mice were bled and serum IL-6 levels were quantified by both the B-9 bioassay and an ELISA. Table 6 shows that pretreatment of mice with TN3.19 anti-TNF MAb reduced the amount of serum IL-6 by c. 50% as compared with the controls (PBS or HIgG). In contrast, pretreatment with anti-IL-6 MAb resulted in a tremendous increase in both bioactive and immunoreactive IL-6 levels as compared to the controls. At 4 and 6 h post-endotoxin, 20F3 increased the circulating IL-6 levels by 28- and 274-fold, respectively. Of note, these results were reproduced twice with similar results. Also, the addition of fresh 20F3 MAb to diluted serum sample from all the groups in the experiment abrogated the cellular proliferation of B-9 cells in the bioassay.

DISCUSSION

Pro-inflammatory cytokines, IL-1, TNF and IL-6 have been implicated in the pathophysiological events associated with septic shock, bacterial toxemia and a variety of chronic inflammatory conditions. This was based in part on experiments where the administration of recombinant cytokines could mimic most of the changes associated with inflammation. For example, injections of IL-1 and TNF induce fever, neutrophilia, hypotension, hepatic acute phase response, activate the hypothalamic–pituitary–adrenal axis, weight loss, hypertriglyceridemia, hypoglycemia as well as stimulate the induction of secondary mediators including IL-6. However, the relative contribution of each of these cytokines to the overall metabolic changes asso-

TABLE 3. IL-6 is involved in LPS-induced hypoglycemia.

Pretreatment	Treatment	Expt. 1	Expt. 2	Expt. 3	Expt. 4
PBS	PBS	148 ± 9	131 ± 8	130 ± 10	NT
PBS	LPS	86 ± 9	90 ± 3	NT	100 ± 5
RIgG	LPS	83 ± 5	89 ± 4	74 ± 3	96 ± 11
HIgG	LPS	81 ± 16	83 ± 5	NT	NT
20F3	LPS	115 ± 4*	106 ± 5*	112 ± 5*	123 ± 4
TN3.19	LPS	78 ± 3	82 ± 5	NT	NT
20F3	PBS	NT	NT	148 ± 10	NT
RIgG	PBS	NT	NT	126 ± 15	NT

CD_2F_1 male mice were pretreated as described in Table 2. In experiments 1, 3 and 4 the amount of LPS used was 30 µg/mouse. In experiment 2 the amount of LPS used was 100 µg/mouse. There were 4–5 mice per group. Mice were bled at 4 h post-LPS injection, except in experiment 4 where mice were bled at 6 h post-endotoxin. Results are expressed in mg/dl ± SD. NT = not tested.
* $P < 0.01$ from RIgG injected group.

TABLE 4. IL-6 is involved in LPS-induced elevation of fibrinogen.

Pretreatment	Treatment	Expt. 1	Expt. 2	Expt. 3
PBS	PBS	257 ± 15	239 ± 31	300 ± 61
PBS	LPS	568 ± 47	711 ± 160	523 ± 123
RIgG	LPS	619 ± 127	824 ± 49	454 ± 136
HIgG	LPS	693 ± 77	734 ± 48	554 ± 92
20F3	LPS	396 ± 5*	480 ± 78*	293 ± 22*
TN3.19	LPS	640 ± 61	860 ± 16	445 ± 76

See footnote to Table 3. Plasma was collected 24 h post-endotoxin. Results are expressed in mg/dl ± SD.
* $P < 0.01$ from RIgG-injected mice.

TABLE 5. TNF but not IL-6 is involved in LPS-induced hypertriglyceridemia.

Pretreatment	Treatment	Expt. 1	Expt. 2	Expt. 3
PBS	PBS	98 ± 10	112 ± 18	96 ± 10
PBS	LPS	171 ± 12	161 ± 28	170 ± 18
RIgG	LPS	NT	176 ± 33	180 ± 32
HIgG	LPS	178 ± 20	198 ± 25	169 ± 25
20F3	LPS	156 ± 17	163 ± 23	165 ± 8
TN3.19	LPS	116 ± 4*	106 ± 15*	100 ± 16*

See footnote to Table 3. Results are expressed in mg/dl ± SD. NT = not tested.
* $P < 0.01$ from HIgG-injected mice.

TABLE 6. Anti-TNF reduces and anti-IL-6 elevates circulating IL-6 levels.

Post-endotoxin assay		2 h B-9	4 h		6 h B-9
Pretreatment	Treatment		ELISA	B-9	
PBS	LPS	NT	31 ± 10	33 ± 3	6 ± 3
RIgG	LPS	72 ± 10	32 ± 13	31 ± 10	7 ± 3
20F3	LPS	401 ± 50	975 ± 150	880 ± 100	1922 ± 300
HIgG	LPS	NT	NT	35 ± 7	NT
TN3.19	LPS	NT	17 ± 7	12 ± 3	NT

CD_2F_1 male mice (3–6 per group) were pretreated with PBS or antibodies as indicated in Table 2. At the indicated time points relative to LPS (30 μg/mouse) injection, mice were bled and serum samples were subjected to IL-6 bioassay (B-9) and ELISA. Results are expressed in units × 10^{-3}/ml or ng/ml for B-9 assay and ELISA, respectively. Normal levels of IL-6 in CD_2F_1 mice are 0.02 ± 0.01 ng/ml in ELISA. The addition of fresh 20F3 (10 μg/ml) abrogated cellular proliferation of B-9 cells in all samples tested. NT = not tested.

ciated with endogenously produced cytokines during inflammation is not fully appreciated.

Recently, we showed that IL-6 is involved in key parameters of wasting associated with the development of C-26 tumors in vivo. Thus, hypoglycemia, acute phase response and the loss of muscle and fat tissues were prevented by the rat anti-murine IL-6 MAb-20F3.[6] TNF did not appear to play a role in this experimental model, since anti-TNF MAb-TN3.19, did not improve cachexia. Therefore, it was of interest to determine how general is the role of IL-6 in inducing metabolic changes, especially in an experimental system where TNF is known to be produced. In this paper, we show that anti-IL-6 MAb inhibited LPS-induced weight loss, hypoglycemia and acute phase response. Interestingly, anti-TNF antibody only modestly reversed weight loss, did not improve the extent of hypoglycemia and acute phase response, but was very effective in blocking LPS-induced hypertriglyceridemia. Thus, these results appear to support our previous data obtained in the C-26 chronic inflammation model and to extend the role of IL-6 in mediating several metabolic alterations to an acute type inflammatory condition.

Chronic and acute infections have been associated with changes in glucose metabolism which could be reproduced by administration of IL-1, TNF but not IL-6. Typically, these changes involve an enhanced rate of glucose utilization in a variety of tissues, including liver, spleen, ileum and lung.[12] However, in septic animals or following TNF infusion, a corresponding increase in hepatic glucose production, probably related to elevation in glucagon levels,[13] partially compensates for the increase in glucose uptake resulting only in a modest hypoglycemia. Indeed, high doses of LPS used in our study reduced glucose levels by only 30 to 40%.

The finding that anti-IL-6, and not anti-TNF antibody, reverses significantly LPS-induced hypoglycemia confirms and extends previous findings

which demonstrated that IL-1 receptor antagonist, but not anti-TNF antibody partially reverses LPS-induced hypoglycemia.[14,15] Whereas TNF itself, given in a sufficient dose (5–7.5 μg/mouse), induced a modest hypoglycemia, which was partially reversed by anti-IL-6 treatment,[16] the administration of IL-6 to mice did not lead to a reduction of blood glucose levels (our unpublished results). Surprisingly, anti-IL-6 antibody did not affect IL-1-induced hypoglycemia.[16] Taken together, these blocking experiments suggest that IL-6, like IL-1, contributes to LPS-induced hypoglycemia. However, unlike IL-1, which when given by itself induces hypoglycemia, IL-6 may require an interaction with other LPS-induced factors, the identity of which remains to be determined.

In contrast, our experiments with anti-TNF clearly show that the elevation in triglyceride levels—known to occur during infection[8]—involves TNF. These findings support previous results. Daily administration of TNF to animals induces hypertriglyceridemia,[17] which was linked to TNF-induced decrease in LPL activity.[3,4] More recent studies, however, suggested that TNF increases serum triglycerides by stimulating hepatic lipogenesis and not by inhibiting adipose tissue LPL activity or triglyceride clearance (for review see ref. 18).

Results presented here also show that the improvement in several LPS-induced inflammatory markers such as hypoglycemia, weight loss and acute phase response which involves IL-6 cannot be directly linked to a reduced serum level of this cytokine. Paradoxically, the anti-IL-6 20F3 induced a significant increase in serum IL-6 levels. This observation was recently made in 20F3-treated mice when the generalized Schwartzman reaction was induced. The 20F3 MAb provided partial but a significant protection against the reaction and yet resulted in an increase of circulating IL-6 levels.[19] Also, this phenomenon is not restricted to the 20F3 MAb, as anti-human IL-6 MAb prolonged serum IL-6 levels in mice injected

with recombinant human IL-6.[20] One explanation of this observation may involve an antibody-dependent slower clearance of the cytokine. However, the difficulty with this is that the increased level of IL-6 does not represent inactive antigen–antibody complexes. This is based on the following findings. First, the IL-6 in the circulation of anti-IL-6-treated and LPS-challenged animals is still active in the B-9 assay. Second, this activity in the bioassay was fully neutralized when fresh 20F3 was added. Third, a significant signal was obtained in an IL-6 specific enzyme-linked immunosorbent assay (ELISA) where the capturing antibody was 20F3. Together, this would argue that the increase in serum IL-6 may represent free cytokine in a form which is not bound to the antibody. A second explanation of this phenomenon is a potential feedback mechanism where the presence of the antibody in vivo induces excess synthesis of IL-6. However, it is difficult to assume that antibody-dependent increase in IL-6 level in vivo results in a protection against LPS-induced deleterious changes. IL-6 is currently designated as a pro-inflammatory cytokine, which is based in part on its ability to stimulate hepatic acute phase protein production[21] and pituitary hormones such as ACTH,[22] and to inhibit LPL activity in vivo.[7] Together with the demonstration that in our system, anti-IL-6 treatment greatly reduced fibrinogen levels, these data support the notion that the effect of IL-6 on the liver and possibly other tissues as well in LPS-treated mice, was neutralized. Furthermore, with a different assay system, no IL-6 could be found in the sera of IL-1 treated mice.[16] Thus, the significance of the increase in the B-9 assay and in the ELISA, in sera of mice receiving blocking antibody to IL-6, will require further investigation.

MATERIALS AND METHODS

Mice

Male Balb/C × DBA/2 (CD_2F_1) mice were purchased from Charles River Breeding Laboratories (Wilmington, MA), and were used at 10–12 weeks of age.

Reagents and Antibodies

LPS from *E. coli* 055:B5 was obtained from Sigma (St. Louis, MO). The rat IgG_1 anti-murine IL-6 MAb, 20F3 was originated by Dr J. Abrams (DNAX, Palo Alto, CA). For in-vivo studies, pharmaceutical-grade antibody was used (a gift from Dr C.O. Jacob, Syntex, Palo Alto, CA). The antibody was purified to > 98% by Prosep Protein A (Proton Products, Maidenhead, UK). The MAb TN3.19 was the kind gift of Dr R. Schreiber (Washington University, St. Louis, MO) and was purified on protein A agarose. Purified rat IgG (RIgG) and hamster IgG (HIgG) as control antibody for 20F3 and TN3.19 respectively, were purchased from Sigma.

Measurements of Glucose, Fibrinogen and Triglycerides

Mice were injected with antibodies intraperitoneally 16 h before LPS challenge as indicated in Tables 1–6. The quantity of 20F3 and RIgG was 0.6 mg/mouse and the quantity of TN3.19 and HIgG was 0.3 mg/mouse. Serum was collected for glucose and triglyceride determinations which were performed using an Ektachem DT-60 analyser (Eastman Kodak Co, Rochester, NY). Plasma fibrinogen was determined using a kit from Sigma (St. Louis, MO). Human fibrinogen was used as a standard.

Measurements of IL-6

IL-6 assays were performed as previously described.[23] One unit of IL-6 was defined as the amount required for half maximal stimulation of cell proliferation in the assay. The addition of 10 μg/ml of 20F3 abrogated proliferation of B-9 cells in response to diluted test samples. IL-6 was also quantified using a murine IL-6 ELISA from Endogen (Boston, MA). This ELISA uses 20F3 as a capturing antibody.

Statistical Analysis

Differences in weights and glucose, fibrinogen and triglyceride levels were compared by using computerized analysis of variance (ANOVA).

REFERENCES

1. Langstein HN, Norton JA (1991) Mechanisms of cancer cachexia. Hematol Oncol Clin North Am 5:747–753.

2. Tisdale MJ (1991) Cancer Cachexia. Br J Cancer 63:337–342.

3. Butler B, Mahoney J, Letrang N, Pekala P, Cerami A (1985) Purification of cachectin, a lipoprotein lipase suppressing hormone from endotoxin induced RAW-2667 cells. J Exp Med 161:986–994.

4. Butler B, Greenwald D, Holmes JD, Chang M, Pan V, Mathison J, Ulevich R, Cerami A (1985) Identity of tumor necrosis factor and of the macrophage secreted factor cachectin. Nature 316:552–554.

5. Semb H, Peterson J, Tarvernir J, Olivecrona T (1987) Multiple effects of tumor necrosis factor on lipoprotein lipase in vivo. J Biol Chem 261:8390–8394.

6. Strassmann G, Fong M, Kenney JS, Jacob CO (1992) Evidence for the involvement of interleukin 6 in experimental cancer cachexia. J Clin Invest 89:1681–1684.

7. Greenberg AS, Norton JP, McIntosh J, Calvo JC, Scow RO, Jablons D (1992) Interleukin 6 reduces lipoprotein lipase activity in adipose tissue of mice in vivo and in 3T3-L1 adipocytes. A possible role of IL-6 in cancer cachexia. Cancer Res 52:4113–4116.

8. Beisel WR (1975) Metabolic response to infection. Ann Rev Med. 26:9–20.

9. Kaufmann RL, Matson CF, Beisel WR (1976) Hypertriglyceridemia produced by endotoxin: role of impaired triglyceride disposal mechanisms. J Infec Dis 133:548–555.

10. Lang CH, Bagby GJ, Spitzer JJ (1985) Glucose kinetics and body temperature after lethal and non-lethal doses of endotoxin. Am J Physiol 248:471–478.

11. Vogel SN, Moore RN, Sipe GD, Rosenstrich DL (1980) BEG induced enhancement of endotoxin sensitivity in C3H/HeJ mice. 1. In vivo Studies. J Immunol 124:2000–2009.

12. Lang CH, Dobrescu C, Bagby GJ (1992) Tumor necrosis factor impairs insulin action on peripheral glucose disposal and hepatic glucose output. Endocrinol 130:43–52.

13. Lang CH, Dobrescu C (1991) Gram negative infection increases noninsulin mediated glucose disposal. Endocrinol 128:645–652.

14. Vogel SN, Hennricson BE, Neta R (1991) Roles of interleukin 1 and tumor necrosis factor in lipopolysaccharide induced hypoglycemia. Infect Immun 59:2494–2498.

15. Vogel SN, Havell EA (1990) Differential inhibition of lipopolysaccharide induced phenomena by anti tumor necrosis factor alpha antibody. Infect Immun 58:2397–2400.

16. Neta R, Perlstein R, Vogel SN, Ledney GD, Ahrams J (1992) Role of IL-6 in protection from lethal irradiation and in endocrine responses to IL-1 and TNF. J Exp Med 175:689–694.

17. Tracey KJ, Wei H, Monague KR, Fong Y, Hesse DG, Nguyen HT, Kuo GC, Butler B, Cotran RS, Cerami A, Lowry SF (1988) Cachectin/tumor necrosis factor induces cachexia, anemia and inflammation. J Exp Med 167:1211–1231.

18. Grunfeld C, Feingold KR (1991) The metabolic effects of tumor necrosis factor and other cytokines. Biotherapy 3:143–158.

19. Hermans H, Dillen D, Put W, Damme JV, Billiau A (1992) Protective effect of anti interleukin-6 antibody against endotoxin associated with paradoxically increased IL-6 levels. Eur J Immunol 22:2395–2601.

20. Mihara M, Koishihara Y, Fukui H, Yasukawa Y, Ohsugi Y (1991) Murine anti human IL-6 monoclonal antibody prolongs the half life in circulating blood and thus prolongs the bioactivity of human IL-6 in mice. Immunology 74:55–59.

21. Marinkovic S, Jahreis GP, Wong GG, Baumann H (1989) IL-6 modulates the synthesis of a specific set of acute phase plasma proteins in vivo. J Immunol 142:808–812.

22. Perlstein RS, Mougey EH, Jackson WE, Neta R (1991) Interleukin-1 and interleukin-6 act synergistically to stimulate the release of adrenocorticotropic hormone in vivo. Cytokine Res 10:141–146.

23. Strassmann G, Bertolini DR, Kerhy SB, Fong M (1991) Regulation of murine mononuclear phagocytes inflammatory products by macrophage colony stimulating factor. J Immunol 147:1279–1285.

DISTRIBUTION LIST

DEPARTMENT OF DEFENSE

ARMED FORCES INSTITUTE OF PATHOLOGY
ATTN: RADIOLOGIC PATHOLOGY DEPARTMENT

ARMED FORCES RADIOBIOLOGY RESEARCH INSTITUTE
ATTN: PUBLICATIONS DIVISION
ATTN: LIBRARY

ARMY/AIR FORCE JOINT MEDICAL LIBRARY
ATTN: DASG-AAFJML

ASSISTANT TO SECRETARY OF DEFENSE
ATTN: AE
ATTN: HA(IA)

DEFENSE NUCLEAR AGENCY
ATTN: TITL
ATTN: DDIR
ATTN: RARP
ATTN: MID

DEFENSE TECHNICAL INFORMATION CENTER
ATTN: DTIC-DDAC
ATTN: DTIC-FDAC

FIELD COMMAND DEFENSE NUCLEAR AGENCY
ATTN: FCFS

INTERSERVICE NUCLEAR WEAPONS SCHOOL
ATTN: TCHTS/RH

LAWRENCE LIVERMORE NATIONAL LABORATORY
ATTN: LIBRARY

UNDER SECRETARY OF DEFENSE (ACQUISITION)
ATTN: OUSD(A)/R&AT

UNIFORMED SERVICES UNIVERSITY OF THE HEALTH SCIENCES
ATTN: LIBRARY

DEPARTMENT OF THE ARMY

AMEDD CENTER AND SCHOOL
ATTN: HSMC-FCM

HARRY DIAMOND LABORATORIES
ATTN: SLCHD-NW
ATTN: SLCSM-SE

SURGEON GENERAL OF THE ARMY
ATTN: MEDDH-N

U.S. ARMY AEROMEDICAL RESEARCH LABORATORY
ATTN: SCIENTIFIC INFORMATION CENTER

U.S. ARMY CHEMICAL RESEARCH, DEVELOPMENT, AND ENGINEERING CENTER
ATTN: SMCCR-RST

U.S. ARMY INSTITUTE OF SURGICAL RESEARCH
ATTN: DIRECTOR OF RESEARCH

U.S. ARMY MEDICAL RESEARCH INSTITUTE OF CHEMICAL DEFENSE
ATTN: SGRD-UV-R

U.S. ARMY NUCLEAR AND CHEMICAL AGENCY
ATTN: MONA-NU

U.S. ARMY RESEARCH INSTITUTE OF ENVIRONMENTAL MEDICINE
ATTN: SGRD-UE-RPP

U.S. ARMY RESEARCH OFFICE
ATTN: BIOLOGICAL SCIENCES PROGRAM

WALTER REED ARMY INSTITUTE OF RESEARCH
ATTN: DIVISION OF EXPERIMENTAL THERAPEUTICS

DEPARTMENT OF THE NAVY

NAVAL AEROSPACE MEDICAL RESEARCH LABORATORY
ATTN: COMMANDING OFFICER

NAVAL MEDICAL COMMAND
ATTN: MEDCOM-21

NAVAL MEDICAL RESEARCH AND DEVELOPMENT COMMAND
ATTN: CODE 40C

NAVAL MEDICAL RESEARCH INSTITUTE
ATTN: LIBRARY

NAVAL RESEARCH LABORATORY
ATTN: LIBRARY

OFFICE OF NAVAL RESEARCH
ATTN: BIOLOGICAL SCIENCES DIVISION

DEPARTMENT OF THE AIR FORCE

BOLLING AIR FORCE BASE
ATTN: AFOSR

BROOKS AIR FORCE BASE
ATTN: AL/OEBSC
ATTN: USAFSAM/RZ
ATTN: OEHL/RZ

OFFICE OF AEROSPACE STUDIES
ATTN: OAS/XRS

SURGEON GENERAL OF THE AIR FORCE
ATTN: HQ USAF/SGPT
ATTN: HQ USAF/SGES

U.S. AIR FORCE ACADEMY
ATTN: HQ USAFA/DFBL

OTHER FEDERAL GOVERNMENT

ARGONNE NATIONAL LABORATORY
ATTN: ACQUISITIONS

BROOKHAVEN NATIONAL LABORATORY
ATTN: RESEARCH LIBRARY, REPORTS SECTION

CENTER FOR DEVICES AND RADIOLOGICAL HEALTH
ATTN: HFZ-110

GOVERNMENT PRINTING OFFICE
    ATTN: DEPOSITORY RECEIVING SECTION
    ATTN: CONSIGNED BRANCH

LIBRARY OF CONGRESS
    ATTN: UNIT X

LOS ALAMOS NATIONAL LABORATORY
    ATTN: REPORT LIBRARY/P364

NATIONAL AERONAUTICS AND SPACE ADMINISTRATION
    ATTN: RADLAB

NATIONAL AERONAUTICS AND SPACE ADMINISTRATION
GODDARD SPACE FLIGHT CENTER
    ATTN: LIBRARY

NATIONAL CANCER INSTITUTE
    ATTN: RADIATION RESEARCH PROGRAM

NATIONAL DEFENSE UNIVERSITY
    ATTN: LIBRARY

U.S. DEPARTMENT OF ENERGY
    ATTN: LIBRARY

U.S. FOOD AND DRUG ADMINISTRATION
    ATTN: WINCHESTER ENGINEERING AND
                ANALYTICAL CENTER

U.S. NUCLEAR REGULATORY COMMISSION
    ATTN: LIBRARY

RESEARCH AND OTHER ORGANIZATIONS

AUSTRALIAN DEFENCE FORCE
    ATTN: SURGEON GENERAL

BRITISH LIBRARY (SERIAL ACQUISITIONS)
    ATTN: DOCUMENT SUPPLY CENTRE

CENTRE DE RECHERCHES DU SERVICE DE SANTE DES ARMEES
    ATTN: DIRECTOR

INHALATION TOXICOLOGY RESEARCH INSTITUTE
    ATTN: LIBRARY

INSTITUTE OF RADIOBIOLOGY
ARMED FORCES MEDICAL ACADEMY
    ATTN: DIRECTOR

KAMAN SCIENCES CORPORATION
    ATTN: DASIAC

NBC DEFENSE RESEARCH AND DEVELOPMENT CENTER OF THE
FEDERAL ARMED FORCES
    ATTN: WWDBW ABC-SCHUTZ

NCTR-ASSOCIATED UNIVERSITIES
    ATTN: EXECUTIVE DIRECTOR

RUTGERS UNIVERSITY
    ATTN: LIBRARY OF SCIENCE AND MEDICINE

UNIVERSITY OF CALIFORNIA
    ATTN: LABORATORY FOR ENERGY-RELATED HEALTH
                RESEARCH
    ATTN: LAWRENCE BERKELEY LABORATORY

UNIVERSITY OF CINCINNATI
    ATTN: UNIVERSITY HOSPITAL, RADIOISOTOPE
                LABORATORY

XAVIER UNIVERSITY OF LOUISIANA
    ATTN: COLLEGE OF PHARMACY